



Universidad Pública de Navarra
Nafarroako Unibertsitate Publikoa

Department of Electrical, Electronic and Communications Engineering

Bachelor's Degree in
Telecommunications Engineering

BACHELOR'S THESIS

ALLSKY-CAMERA SYSTEM FOR MONITORING OF OPTICAL SATELLITE DOWNLINKS

Supervisor

Prof. Dr. Miguel A. G. Laso

Student

Iker Aldasoro Marculeta



DLR

**Deutsches Zentrum
für Luft- und Raumfahrt**

German Aerospace Center

The thesis work has been carried out at the German Aerospace Center (DLR), in the Institute of Communications and Navigation (IKN) with collaboration of the German Space Operations Center (GSOC), site Oberpfaffenhofen.



Supervisors

Dr. Dirk Giggenbach, IKN (Inst. of Communications and Navigation)

Dr. Marcus T. Knopp, RSC3 (Responsive Space Center)

Academic year 2023/2024

Acknowledgements

First of all, major thanks to my parents and family, for their upbringing and guiding me throughout my journey to adulthood, and for being there for me in the highs and lows. This could not have been possible without you.

I cannot fully express my gratitude to both my supervisors at the German Aerospace Center (DLR), Dr. Dirk Gigenbach and Dr. Marcus T. Knopp, for their guidance and support. I am immensely grateful for the time they dedicated to me, even outside of office hours, and giving the chance to experience this magnificent opportunity. A special thanks to Andrea for all her help with the measurements and for lending me a hand whenever I needed it.

I am also grateful to Dr. Miguel Angel Gomez Laso for his engaging lectures during my studies and his invaluable support and advice during my stay. I am also sorry for the timing of this work, which has not been optimal.

A big thanks to my friends from Pamplona, who helped me stay grounded and motivated during this long period away from home. We do not really value what we have, how close are we, although when being far apart. The longer and farther I am, the more I appreciate it.

Lastly, I would like to thank all the students from the Institute of Communications and Navigation: Chiara, Salvatore, Davide, Jan, Aurora, Matteo, Thomas, Luka, Raphael, Guillaume, Matti, Uri... Time has passed too quickly for us to realize it. You have all helped me grown up so much as a professional, but most importantly as a person, for which I am deeply thankful. I am sure you all have bright futures ahead of you—you are all wonderful people.

To whom it may concern: thank you, I am sorry, I love you.

Abstract

Satellites widely use the Radio Frequency (RF) band for communications. However, the rapid expansion of Low Earth Orbit (LEO) in the last decade, driven by reduce costs, has led to larger volumes of data to be transmitted from these satellites (the same problem appears in deep space communications). Optical communications offer a solution, providing higher throughputs with reduced equipment volume, lower power consumption, all while avoiding of the regulatory restrictions and tariffs associated with RF. The main problem of space-to-ground links is that the need to face multiple loss-effects primarily due to three main factors: pointing-error losses caused by the satellite's pointing precision; Free-Space Losses (FSL) resulting from the orbit geometry; and atmospheric effects and visibility problems such as atmospheric attenuation, scintillation, and obstruction. This could lead to miss the downlink, being difficult to assess exactly why did that happen.

We hypothesized that a validation tool could be developed as a proof of concept to evaluate the failure point of the operation. Based on an Indium Gallium Arsenide (InGaAs) camera, the system can locate the satellite and estimating its elevation, azimuth and the received intensity at the camera compared to the expected intensity based on the link budget, all without requiring mechanical tracking. This tool is a waterproof enclosure capable of being transported anywhere with any issue. The camera is fitted with a wide-angle lens, providing a 140 degrees field of view, capturing most of the relevant hemisphere. We tested the lens to estimate the Field of View FOV, while the intensity calibration was performed using a method involving a Coarse Wavelength Division Multiplexing (CWDM) and a radio tower equipped with a 1550 *nm* laser. The entire system is controlled by a Python project named "allsky4oleodl," composed of eight different scripts. Our findings indicate that the device successfully detected the satellite on occasions when the Optical Ground Station (OGS) did not, proving the proof-of-concept successful. If further developed and tested, this tool could become a critical standard component of Optical Low Earth Orbit Downlink (OLEODL) systems in the future.

Keywords: AllSky, Azimuth Angle, Beam Spot Size, Contour, CubeSat, CWDM, Deep Space Optical Communications, Elevation Angle, Exposure Time, Filter, GUI, InGaAs, Infrared Camera, Inter-satellite Links, Laser Signal Intensity, Laser Transmitter, Lens, Link Budget, NORSAT-TD, OLEODL – Optical Low Earth Orbit Downlinks, OGS - Optical Ground Station, Optical Satellite Terminal, Optical Space-ground Link, OSIRIS, Threshold.

Contents

Abstract	v
Abbreviations	xi
1 Introduction	1
2 Literature Review	3
2.1 Free Space Optical Communications	3
2.1.1 Free Space Optics vs. Fiber Optics Communications	4
2.2 Low Earth Orbit Satellites	4
2.2.1 History of Low Earth Orbit Satellites	5
2.2.2 Advantages and Disadvantages of Low Earth Orbit Satellites	5
2.3 Optical Ground Stations	6
2.3.1 Adaptive Optics	7
2.3.2 Point-ahead Angle and References for Uplink Pre-correction	7
2.3.3 Spatial Diversity for Turbulence Mitigation	8
2.3.4 Examples of Optical Ground Stations	9
2.4 Optical Low Earth Orbit Data DownLinks	10
2.4.1 Historical overview of Free Space Optics in space communications	11
2.4.2 Pointing, acquisition and tracking	11
2.4.3 Low Earth Orbit-Direct to Earth Geometry	13
2.4.4 Loss-Effects in Optical Space-Ground Links	13
2.4.5 Link Budget	19
2.5 Laser Transmitters for Optical Low Earth Orbit data DownLinks	21
2.5.1 OSIRISv1 Onboard Flying Laptop	21
2.5.2 OSIRIS4CubeSat Onboard Laser CubeSat	22
2.5.3 OSIRISv3 Onboard Titania	24
3 Materials and Methods	27
3.1 System Requirements	27
3.2 Component Selection	27
3.2.1 Indium Gallium Arsenide Camera	28
3.2.2 Wide Angle Lens	30
3.2.3 Dome	32
3.2.4 Enclosure	33
3.3 Final Overview of the AllSky-camera System	34
3.4 Controlling Software	34
3.4.1 Vmbpy Application Programming Interface	38
3.4.2 Image Processing	39
3.4.3 Elevation and Azimuth	46
3.4.4 Graphical User Interface	49
3.5 Testing	50
3.5.1 Calculation of the Link Budget for the Observed Satellites	50
3.5.2 Evaluation of the Lenses	52
3.5.3 Intensity Measurement with a Coarse Wavelength Division Multiplexing Transceiver	54
3.5.4 Camera Calibration and Intensity Assessing with the Radio Tower	57

4	Results & Discussion	63
4.1	OSIRIS4CubeSat Onboard Laser CubeSat Campaign	63
4.2	CubeCat Onboard NORSAT-TD Campaign	64
5	Conclusion	67
5.1	Summary	67
5.2	Future Work	67
	Bibliography	68
	Appendix A	A-1
A.1	Main.py	A-1
A.2	AllSkyCam4OLEODL Package	A-4
A.2.1	__init__.py	A-4
A.2.2	api.py	A-5
A.2.3	constants.py	A-25
A.2.4	gui.py	A-26
A.2.5	image_processing.py	A-30
A.2.6	input_checks.py	A-44
A.2.7	link_budget.py	A-45
A.2.8	printer.py	A-52

Abbreviations

4QD 4-Quadrant Diode. 23

API Application Programming Interface. 29, 35, 38

APK Absolute Pointing Knowledge. 25

ARTEMIS Advanced Relay and Technology MIssion Satellite. 11

CPA Coarse Pointing Assembly. 24, 25

CPF Consolidated Prediction Format. 64

CRL Communications Research Laboratory. 11

Cu Copper. 28

CubeL Laser CubeSat. 23, 24, 63, 64

CubeLCT CubeSat Laser Communication Transmitter. 23

CWDM Coarse Wavelength Division Multiplexing. v, 54

DLR Deutsches Zentrum für Luft- und Raumfahrt (German Aerospace Center). , 9–11, 16, 21, 22, 57, 68

DM Deformable Mirror. 6, 7

DPC Defect Pixel Correction. 30

DSOC Deep Space Optical Communications. 11

DTE Direct To Earth. 13, 15

EDFA Erbium-Doped Fiber Amplifier. 57

EDRS European Data Relay Satellite System. 11

ESA European Space Agency. 9, 11

ETS Engineering Test Satellite. 11

FEC Forward Error Correction. 6

FLP Flying LaPtop. 21, 22, 50, 63

FOC Fiber Optic Communication. 4

FOR Field Of Regard. 25

FOV Field Of View. v, 1, 21, 27–29, 31, 47, 48, 52, 53

FPA Fine Pointing Assembly. 23, 24

FSL Free-Space Losses. 13, 15

FSM Fine Steering Mirror. 23

FSO Free Space Optical. 25

FSOC Free Space Optical Communications. 1, 3, 4, 10–12, 14

FSOL Free Space Optical Links. 1, 3, 8

FWHM Full Width at Half Maximum. 12, 20, 55

GEO GEostationary Orbit. 8, 10, 11, 14

GOPEX Galileo Optical EXperiment. 11

GSO GeoSynchronous Orbit. 5, 9

GSOC German Space Operations Center. , 9, 58, 61, 64

GUI Graphical User Interface. 35, 49

HAP High-Altitude Platform. 11

IKN Institute of Communications and Navigation. , 9, 21, 51, 55, 57, 58, 61

InGaAs INdium GAllium ArSenide. v, 1, 28, 51, 67

IR InfraRed. 1, 10, 27, 31

IRT Index-of-Refractive Turbulence. 11, 13

ISI Intensity-Scintillation Index. 17

ISS International Space Station. 5

JAXA Japan Aerospace eXploration Agency. 11

KIODO KIrari’s Optical Downlink to Oberpfaffenhofen. 9

LADEE Lunar Atmosphere and Dust Environment Explorer. 11

LCRD Laser Communications Relay Demonstration. 11

LCT Laser Communication Terminal. 9

LEO Low Earth Orbit. v, 1, 3–5, 10, 11, 13–15, 27

LLCD Lunar Laser Communication Demonstration. 11

LOS Line Of Sight. 19

LUT Look-Up Tables. 30, 38, 39, 63

MDA Missile Defense Agency. 11

MFD Mode Field Diameter. 55

NASA National Aeronautics and Space Administration. 5, 11, 15

NASDA National Space Development Agency of Japan. 11

NICT National Institute of information and Communications Technology. 11

OGS Optical Ground Station. v, 1, 3, 6, 9, 11, 13, 14, 16–21, 23, 27, 49, 57, 58, 60, 63, 64, 67, 68

OGSOP Optical Ground Station in OberPfaffenhofen. 9, 10

OICETS Optical Inter-orbit Communications Engineering Test Satellite. 11

OLEODL Optical Low Earth Orbit data DownLinks. v, 1, 13, 15–17, 21, 60, 64, 65, 67

OP Oberpfaffenhofen. 16, 57, 58, 60, 63

OSIRIS Optical Space InfraRed downInk System. 21–25, 50, 63

OSIRIS4C Optical Space InfraRed downInk System for CubeSat. 23

OSL Optical Satellite Link. 6

PAA Point-Ahead Angle. 7

PAT Pointing, Acquisition and Tracking. 23

PCB Printed Circuit Board. 23

POE Power Over Ethernet. 34

PSI Power Scintillation Index. 17, 21

PTU Pan-Tilt-Unit. 53, 57, 58

QKD Quantum Key Distribution. 11

RF Radio Frequency. v, 3, 10–12, 14, 67

RSC3 Responsive Space Center.

SAR Synthetic Aperture Radar. 11

SILEX Semiconductor Inter satellite Link EXperiment. 11

SMF Single Mode Fiber. 54, 55

SOFA Optical Ground Station Focal Assembly. 57

SOTA Small Optical TrAnsponder. 11

SWIR Short-Wavelength InfraRed. 28–31

TAOGS Transportable Adaptive Optics Ground Station. 9

TLE Two-Line Elements. 64

TNO Dutch Organization for Applied Scientific Research. 64

TOGS Transportable Optical Ground Station. 9, 10

VIR Visual and InfraRed. 31

VIS Visible. 28, 31

VSWIR Visible to Short-Wavelength InfraRed. 28, 30

WFS WaveFront Sensor. 6

WOC Wireless Optical Communications. 3

1 Introduction

In recent years, wireless communications have developed at an unprecedented rate. From cellular networks to satellite links, every telecommunication branch has improved significantly. Free Space Optical Communications (FSOC) has emerged as a disruptive technology. Besides other major advantages discussed later, it unlocks the use of new technologies such as quantum communications or adaptive optics, and the use of smaller and lighter antennas, promising to revolutionize satellite communications.

All major space agencies have been testing Free Space Optical Links (FSOL) with Low Earth Orbit (LEO) satellites. One of the main challenges is diagnosing which element of the system is responsible for a failed link acquisition process, as the cause is often unknown. These failures can be due to misalignment, incorrect satellite's orbit data, or faulty equipment in the Optical Ground Station (OGS): The satellite itself could be the reason if its payload is malfunctioning. While visibility and atmospheric conditions significantly impact acquisition success, they are less critical, as a link is attempted only under favourable conditions. Correctly assessing the issue would enhance the understanding of data and lead to improvements in the entire process.

Our hypothesis was that a validation tool could assess the failure point of the entire operation. We propose a monitoring device based on an AllSky-Camera approach to verify the optical signal at the location of the optical ground station. Using an Indium Gallium Arsenide (InGaAs) Infrared (IR) camera operating at the same wavelength as the payload (typically 1550nm) should, if capable of observing most of the hemisphere: track, position and assess the quality of the satellite link throughout the whole acquisition without needing any tracking module. It must also acquire the necessary frames for the posterior analysis while excluding the background light effects. Everything must be built using standard hardware, keeping costs low.

Inspired by cloud coverage systems [1], [2], [3], this work presents a novel approach, offering a compact, portable and affordable solution capable of working as a secondary OGS. Although similar systems have been developed before, they are limited to tracking [4], [5], or narrow fields of view [6], [7]; none can measure the intensity and position of the satellite without a tracking module.

This thesis serves as a Proof of Concept to determine the feasibility of such a device, which has been developed from the ground up through the design, implementation, and evaluation phases. We went through several key phases: requirement analysis of the system sensitivity (link budget), Field Of View (FOV) and exposure times compared to the movement of the objects; component analysis and evaluation; software design and housing the components within a robust, autonomous mechanical setup controlled via Ethernet; testing, verification and analysis of Optical Low Earth Orbit data DownLinks (OLEODL); and documentation of the setup, experiments and their analysis.

The research is structured into five chapters, beginning with this introduction. The second chapter provides a review of the literature, primarily on OLEODL. The third chapter details the materials and methods used, including the system requirements, component selection, experiments and the controlling python software. The fourth chapter presents the results of the experiments. Finally in the fifth summarizes the thesis and offers an outlook for future work.

2 Literature Review

This chapter describes the nature of Free Space Optical Communications (FSOC) and its advantages and disadvantages compared to Radio Frequency (RF) communications. It also explores the use of Free Space Optical Links (FSOL) for Low Earth Orbit (LEO) satellite-to-ground communications, alongside the role of Optical Ground Stations (OGS).

This is an incredibly vast array of topics. Explaining them in its entirety would require a dedicated dissertation, which is beyond the scope of this work. Therefore, we will focus on the key aspects that directly influence this study.

2.1 Free Space Optical Communications

Free Space Optical Communications (FSOC), a branch of the Wireless Optical Communications (WOC), are classified into terrestrial and space systems, as shown by Fig. 2.1.

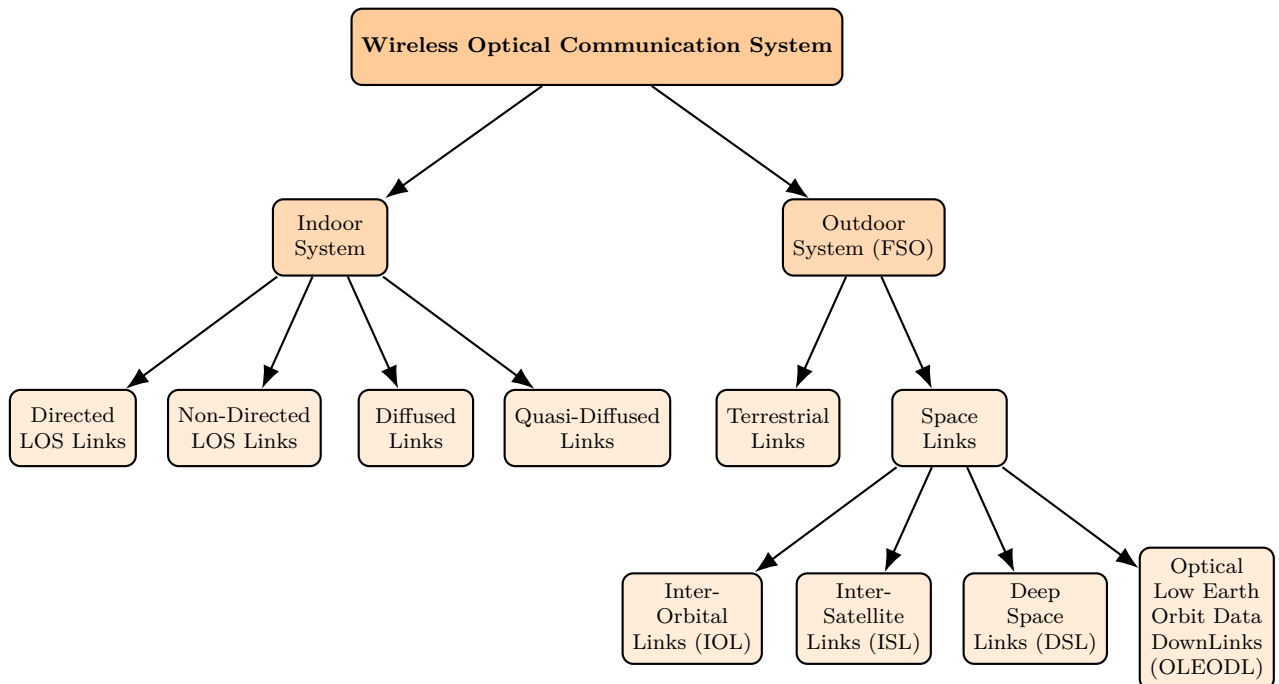


Figure 2.1: Classification of wireless optical communication systems. [8].

The concept of transmitting information through light can be traced back to ancient times, when humans used smoke signals for communication. Alexander Graham Bell, alongside his assistant Charles Sumner Tainter laid the groundwork for modern optical communication patenting the photophone in 1880 [9], predating Guglielmo Marconi's radio communication system [10]. The photophone transmitted sound by modulating light and then extracting the sound signal using materials sensitive to light [11].

Nowadays, a typical free space optical communication system consists of the following components: an

electronic data input; a small but powerful light source which can be modulated; emitter optics which shape the emitted beam into a highly directed beam; the atmosphere as the transmission medium; detector optics which receive the transmitted light and focus it onto a photodetector; and an electronic amplifier, as the data output. This setup is illustrated in Fig. 2.2.

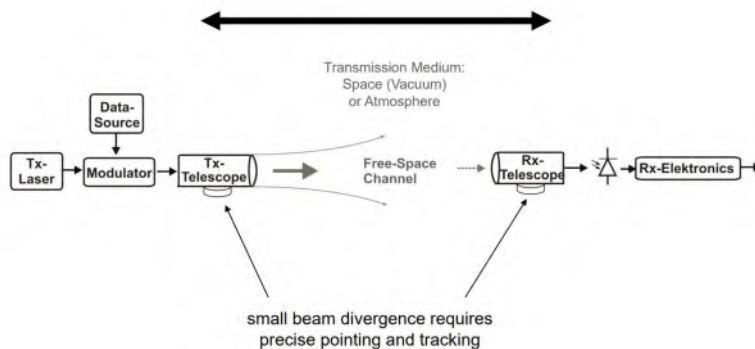


Figure 2.2: Directed Point-to-Point FSO Link by Modulated Laser Beams. Figure taken from [12].

2.1.1 Free Space Optics vs. Fiber Optics Communications

Both these communications methods rely on a light emitting diode or laser as a point source for data transmission. The main difference is that Fiber Optic Communication (FOC) guides an energy beam through an optical cable, while free space optic communication guides an energy beam through free space. FSO is particularly useful where physical connections via fiber optical cable are impractical or non-feasible, being a viable solution for "Last Mile Connectivity" [13]. However, it still has limitations.

FSO greatly suffers from weather conditions, line of sight requirement and range limitation. Weather dependence is particularly troublesome, as attenuation values can reach up to 300 dB/km under adverse conditions [14]. These disadvantages compared with fiber optics, have resulted in its limited adoption.

2.2 Low Earth Orbit Satellites

Almost 8000 active satellites are currently orbiting Earth [15]. This increase is primarily driven by the Low Earth Orbit (LEO) industry, which accounts for close to 90% of the total satellites. Technological advancements have made LEO satellites more cost-effective, easier to launch, and simpler to manage [16].

Low Earth orbit satellites are relatively low in altitude, typically orbiting between 350 and 2000 km above the Earth's surface [17]. They work in interconnected constellations, communicating with ground-based stations to transmit and receive data—enabling various applications such as global communications, Earth observation, and navigation.



Figure 2.3: Different satellite orbits classified by altitude. Figure taken from [18].

2.2.1 History of Low Earth Orbit Satellites

The Earth orbit is currently dominated by Low Earth orbit satellites, but this was not always the case. GeoSynchronous Orbit (GSO) satellites were the preferred method for observing the Earth until recently. The first GSO satellite, Syncom II launched in 1963 [19], was the world’s first geosynchronous communications satellite and set the standard for 30 years.

Sputnik I, the first LEO satellite was launched by the Soviet Union in 1957, marking the beginning of the Space Race against the United States [20]. Sadly, low Earth orbit technology stagnated until the early 1990s, with its resurgence by the launch of the IRIDIUM system, a constellation of satellites aimed to provide global communication [21]. However, many LEO missions struggled to meet demands due to their high costs. This would be solved in the 2000s with the development of the CubeSats: a class of nanosatellites using a standard size and form factor. Originally developed in 1999 by California Polytechnic State University and Stanford University [22], The National Aeronautics and Space Administration (NASA) Ames launched its first CubeSat, GeneSat, in December 2006 [23]. The 2010s saw a shift with the rise of commercial companies like SpaceX, and its Starlink project [24]. The increase in LEO satellite deployments has raised concerns about space traffic management and orbital debris, potentially leading into what is known as the "Kessler syndrome", rendering the entire Low Earth Orbit unusable [25], [26].

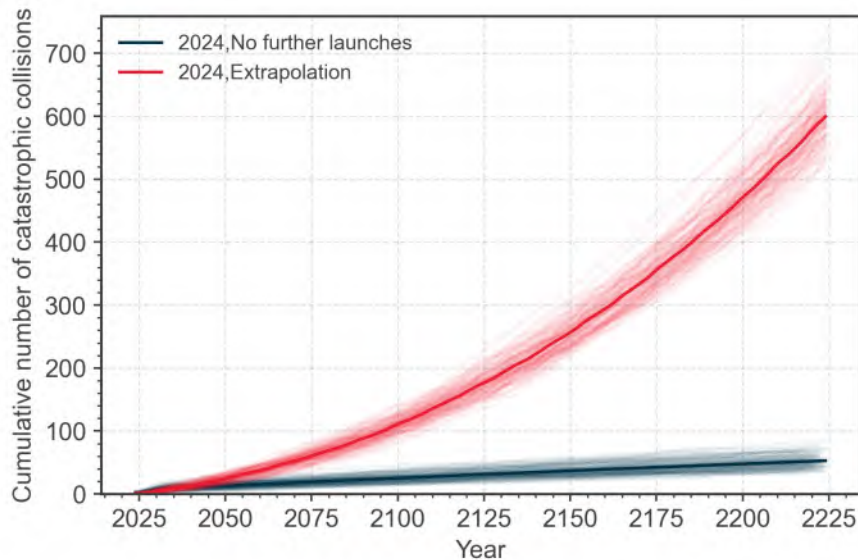


Figure 2.4: The future number catastrophic collisions in Earth orbit. Figure taken from [27].

2.2.2 Advantages and Disadvantages of Low Earth Orbit Satellites

Being closer to the Earth’s surface offers different advantages compared to satellites in higher orbits: lower latency and higher bandwidth; enhanced image resolution; faster orbiting speeds (traveling at 7.8 km/s it takes just over 90 minutes to complete an orbit, which means circling around Earth approximately 16 times per day); greater path flexibility, as tilting the orbital plane relative to the Equator allows for more route options; and reduced energy requirements for reaching the final orbit, which is why the International Space Station (ISS)—scheduled for deorbit in 2030 [28]—is positioned at 415 km altitude, enabling quicker and more cost-effective access for spacecrafts.

The main problem of the low Earth orbit is the overcrowding of space debris as the number of launches increases. This problem is aggravated by the fact that LEO satellites, due to their lower altitudes, suffer from a higher rate of atmospheric drag, requiring more power and limiting their lifespan to 7-10 years. Additionally, LEO satellites cannot function effectively alone for communication purposes as they are hard to track, requiring full constellations.

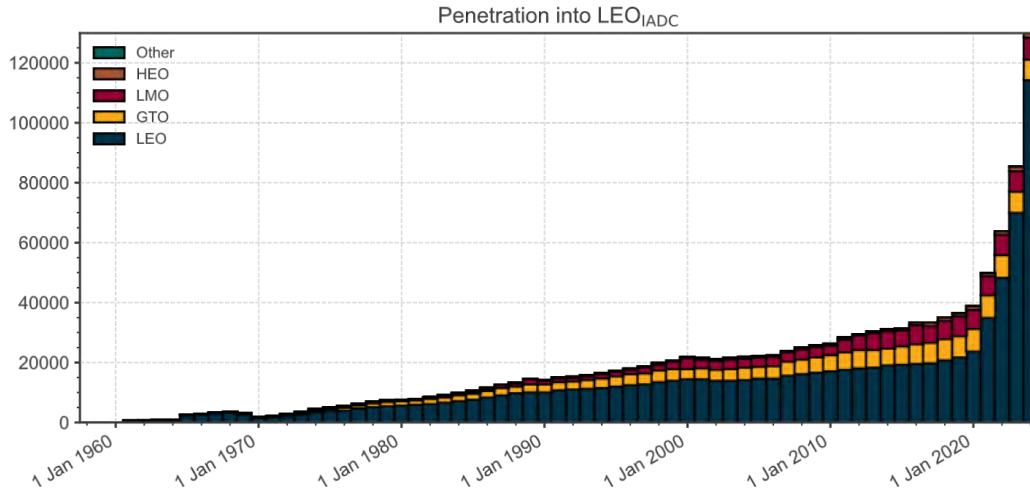


Figure 2.5: Evolution of absolute area residing in or penetrating LEO_{IADC} . Figure taken from [27].

2.3 Optical Ground Stations

To establish an Optical Satellite Link (OSL), an Optical Ground Station (OGS) is required to communicate with the optical terminal. Fig. 2.6 illustrates the main components of the ground segment for a very-high throughput communication system.

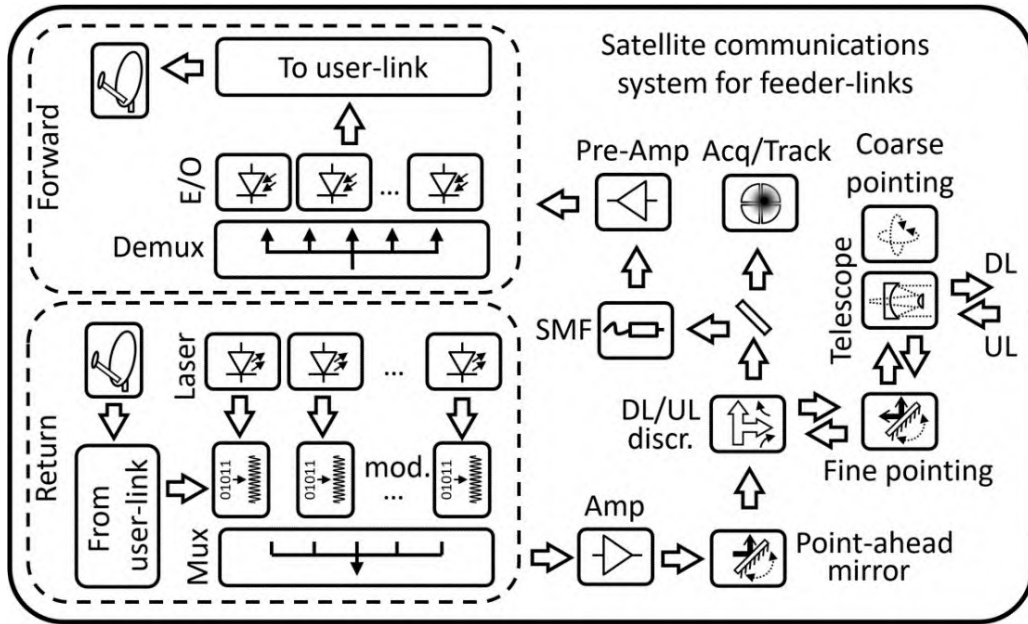


Figure 2.6: Main components of the space terminal of a very-high throughput communications satellite based on optical feeder link. Figure taken from [29].

The telescope transmits and receives data to and from the satellite. The coarse-pointing system points towards the satellite, maintaining a small pointing error to compensate for the signal’s angle-of-arrival. The WaveFront Sensor (WFS) and Deformable Mirror (DM), components of the adaptive optics system, compensate phase distortions caused by atmospheric turbulence. Both the adaptive optics and pointing systems are employed in both link directions: in the downlink for fiber coupling and in the uplink for pre-compensation of beam wander and phase distortions.

In the downlink process, the light is coupled into a single-mode fiber, pre-amplified, demultiplexed, and converted to the electrical domain for Forward Error Correction (FEC) and data processing before sending it to the network. Using a large telescope benefits the link budget, as the receiver gain increases

with the diameter of the receiver.

For the uplink, data from the network is converted into the optical feeder-link format, modulated onto each laser carrier, multiplexed, amplified, and after compensating for the point-ahead angle, coupled into the telescope system to be transmitted towards the satellite. The transmitter size is constrained by atmospheric turbulence and pointing accuracy, which is limited by the beam wander.

Certain systems are required at ground stations to ensure reliable and stable satellite-to-ground communications. Given their complexity, we will provide only a brief overview of these systems.

2.3.1 Adaptive Optics

To utilize components such as low-noise amplifiers or multiplexers, the light collected by the telescope must be coupled into a single-mode optical fiber. This coupling efficiency is compromised due to wavefront distortions caused by atmospheric turbulence. These phase distortions increase with the telescope's diameter, as larger apertures capture more phase aberrations—amount defined by the ratio between the aperture's diameter and the fried parameter D/r_o . This is a key constraint in increasing telescope diameter [30].

Adaptive optics systems can partially correct for these phase distortions. A typical adaptive optics setup includes a tip-tilt mirror, which compensates for angle-of-arrival fluctuations caused by atmospheric turbulence and tracking errors; a deformable mirror, composed of a set of actuators, which receives the beam and compensates its phase distortion; and a wavefront sensor, which estimates the phase of the received wavefront and computes the signals to drive the DM.

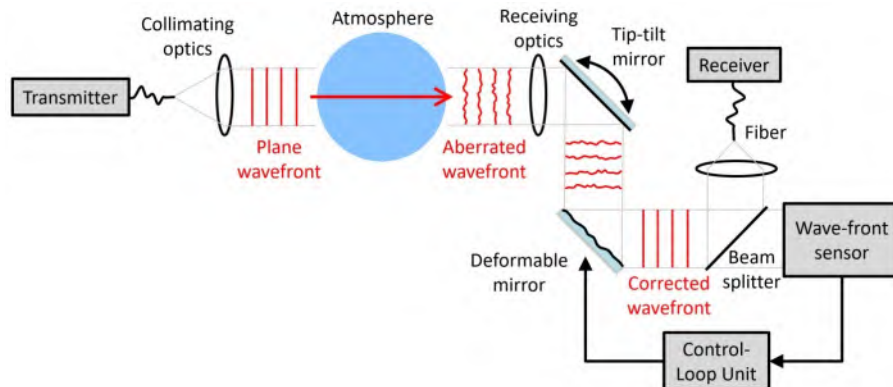


Figure 2.7: Block diagram of an ideal adaptive-optics system. Figure taken from [29].

2.3.2 Point-ahead Angle and References for Uplink Pre-correction

As previously discussed, the tip-tilt mirror is necessary to compensate for angle-of-arrival fluctuations caused by atmospheric turbulence. In the meantime, the finite speed of light delays the uplink signal reaching the satellite, resulting in an angular separation between the uplink and downlink directions. This separation is referred to as the Point-Ahead Angle (PAA), as shown in Fig. 2.8.

This angle Φ can be calculated using equation (2.1), where v_t is the tangential velocity of the satellite and c denotes the speed of light.

$$\Phi = \frac{2v_t}{c} \quad (2.1)$$

The pointing direction of the uplink will fluctuate due to atmospheric turbulence generating intensity fluctuations; this phenomenon is known as beam wander. Ideally, the uplink could be compensated for beam wander using the same measurements from the tip-tilt mirror as a form of pre-compensation. A key challenge is that atmospheric effects are correlated within a certain cone, known as the isoplanatic

angle [31] (as illustrated in Fig. 2.8). If the point-ahead angle exceeds the isoplanatic angle, the system will move outside this cone. Exiting the coherent cone leads to increased decorrelation between both paths, resulting in greater beam wander and, ultimately, more significant intensity fluctuations at the satellite.

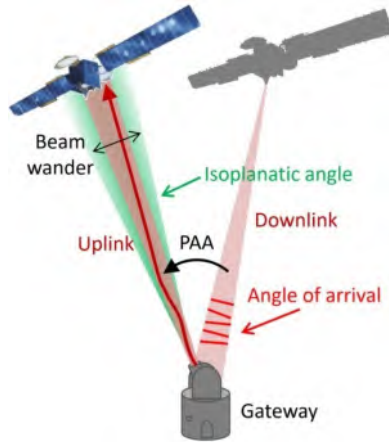


Figure 2.8: Block diagram of an ideal adaptive-optics system. Figure taken from [29].

The most straightforward solution to reduce beam wander is to increase the divergence. The main drawback is the reduction in mean power received at the satellite. Other solutions are possible, such as laser guide stars based on Rayleigh scattering or adaptive optics, exist but they will not be covered in this discussion.

2.3.3 Spatial Diversity for Turbulence Mitigation

Atmospheric turbulence can cause a significant performance degradation in Free Space Optical Links (FSOL). Spatial diversity is applied on both the transmitter and receiver, alongside adaptive optics, to minimize its impact.

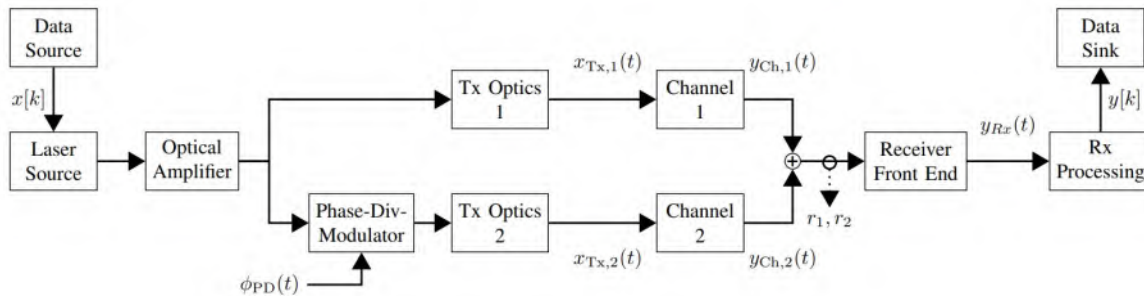


Figure 2.9: Block diagram of transmitter diversity system with Phase-Division in Bit-Time for two transmitters and a single receiver. Figure taken from [32].

At the transmitter, size N uncorrelated beams are transmitted to reduce the scintillation at the receiver side by an equal factor [33], limiting power fluctuation. N independent sources might be used to obtain these N beams, although this can be circumvented using on-off keying data modulation [34]. Each beam is located at a certain distance respect to the others, to ensure that the turbulence crossed by each one is mutually uncorrelated—as the atmospheric paths are assumed to be uncorrelated when they are half a meter apart. The more beams we can use, the lower the scintillation will become; however, this technique is mostly used for Geostationary Orbit (GEO) satellite links. Experimental results can be found in [35], [36].

Data can be modulated on the laser carrier, but careful consideration is required, as partial bandwidth overlap can result in strong interference. Techniques like polarization or wavelength separation can

mitigate this, although new methods, such as employing multiple signal sidebands, are currently being researched [37].

At the receiver, diversity can be achieved using an array of telescopes, beneficial in avoiding monolithic mirrors in deep space scenarios while achieving similar performance.

2.3.4 Examples of Optical Ground Stations

There are over 30 OGSs operated by various international organizations worldwide, with more planned for the future. The European Space Agency (ESA)-OGS, located at the *Observatorio del Teide* in Tenerife, Canary Islands (Spain) [38], was built in 2001 to support ground-to-GeoSynchronous Orbit (GSO) satellite links as part of the SILEX project [39].

The Transportable Adaptive Optics Station (TAOGS), developed by the Deutsches Zentrum für Luft- und Raumfahrt (DLR) and Tesat Spacecom, was designed to support Tesat’s spaceborne Laser Communication Terminals (LCTs). The key features of this OGS are its adaptive optics system and its portability, with all equipment housed within a container [40].

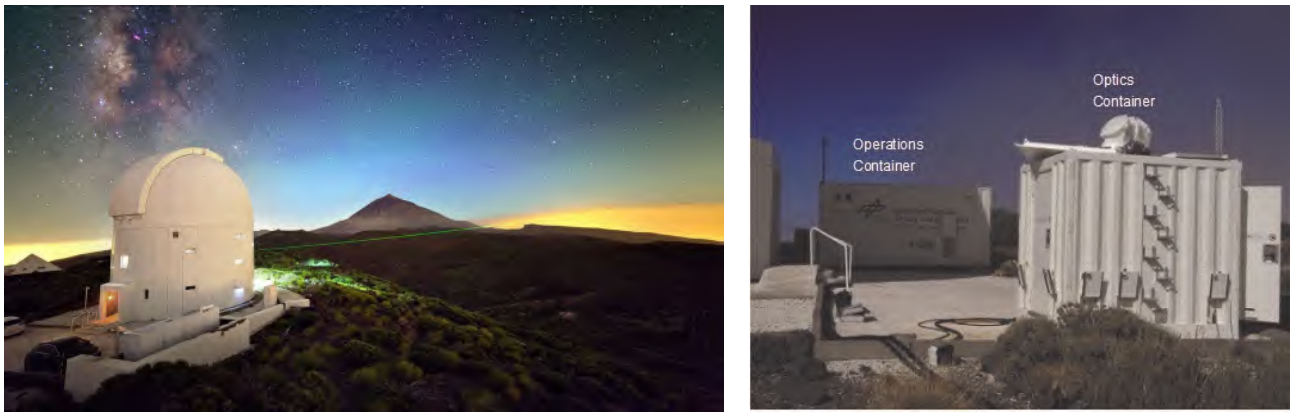


Figure 2.10: ESA Optical Ground Station in Tenerife, Canary Islands (left). Figure taken from [41]. Photograph of the TAOGS (right). Figure taken from [42].

The DLR Optical Ground Station in OberPfaffenhofen (OGSOP), originally implemented for the KIrari’s Optical Downlink to Oberpfaffenhofen (KIODO) experiment in 2006 [43], equipped with a 40-cm Ritchey–Chrétien telescope, a similar version of this telescope is now used at the German Space Operations Center (GSOC). In 2021, this telescope was replaced with an 80-cm telescope featuring a Coudé path [44].

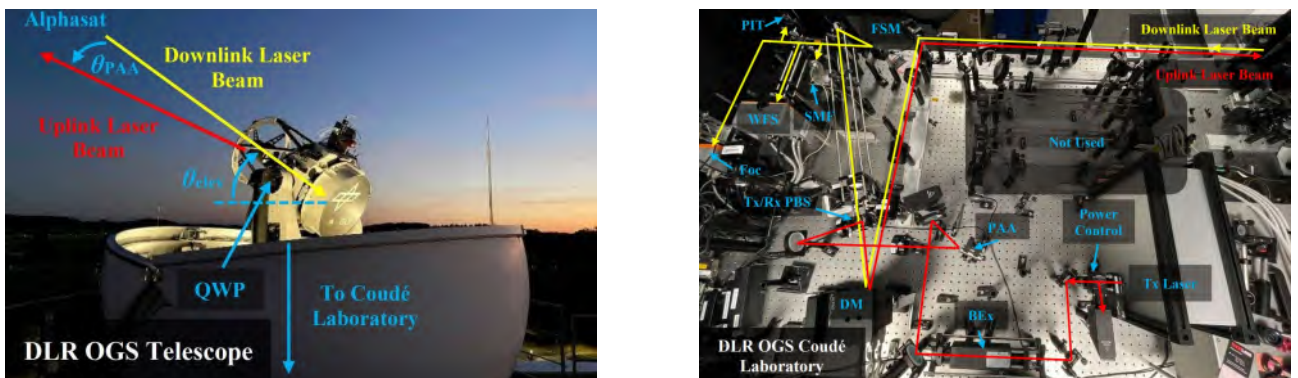


Figure 2.11: DLR Oberpfaffenhofen OGS’s 80-cm telescope (left). Pre-distortion Adaptive Optics experimental setup (right). Figure taken from [45].

In addition to the OGSOP, the the Institute of Communications and Navigation (IKN) at DLR developed the Transportable Optical Ground Station (TOGS) in 2010, shown in Fig. 2.12. The TOGS is a versatile and modular OGS designed for experimental optical uplink and downlink scenarios, as

well as for measuring the atmospheric optical channel. Equipped with a 60cm Ritchie-Chrétien, it was intended for rapid deployment and determination of position and attitude, as required for alignment with a known target.



Figure 2.12: DLR Transportable Optical Ground Station. Figure taken from DLR Media.

Both the OGSOP and the TOGS transmit and receive through different apertures (The OGSOP can also use the same for transmission and reception). As a result, beam wander cannot be minimized, forcing to increase divergence to ensure that the uplink reaches the satellite most of the time despite the increased beam wander, as shown in equation (2.2). The root-mean-squared value of the beam wander from GEO links are in the order of tens of microradians, however for LEO satellite links decreases to a few microradians, making the impact of beam wander due to turbulence negligible in that case.

$$\sqrt{\sigma_{\text{pointing}}^2} = 0.73 \left(\frac{\sqrt{2}\lambda}{D_T} \right) \left(\frac{D_T}{\sqrt{2}r_0} \right)^{5/6} \quad (2.2)$$

2.4 Optical Low Earth Orbit Data DownLinks

As the amount of data we gather and transmit to Earth increases, we need solutions to accommodate this need. Free Space Optical Communications (FSOC) have found their niche in satellite to ground, inter-satellite and deep space communications, addressing the limitations of Radio Frequency (RF) communications.

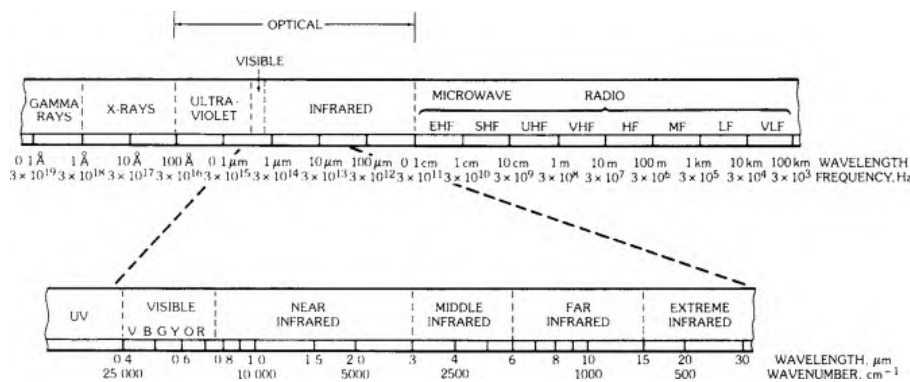


Figure 2.13: The electromagnetic spectrum. Figure taken from [46].

Although compatible [47], FSOC is establishing itself as an alternative over RF in many application scenarios due to its reduced weight and volume of the transmitter and receiver equipment (up to 50% less), lower power consumption (25% less power), and avoidance of the tariffs or regulatory restrictions associated with RF usage. The InfraRed (IR) light packs data into tighter waves, allowing ground stations to receive more data at once. While laser communications do not always provide higher throughput, that is the goal as more data can be transmitted in one downlink, increasing bandwidth

by 10 to 100 times compared with radio frequency systems (Data rates up to Terabit/s are possible).

Main challenges such as link blocking by clouds and fog, signal scintillation by Index-of-Refraction Turbulence (IRT) and precise pointing and tracking for the link acquisition, will remain.

2.4.1 Historical overview of Free Space Optics in space communications

Using free space optical communications for space communication is not new. Developed in 1965 by the United States for deep space exploration, it would take until 1975 to complete an inter-satellite communication system. Despite this progress, FSOC development stalled for two decades due to atmospheric effects with optical signals.

In 1992, the National Aeronautics and Space Administration (NASA) performed the Galileo Optical EXperiment (GOPEX)—they emitted megawatts power, 532nm pulses from Earth, detecting them with a camera onboard Galileo probe, up to 6 million km away [48]. In 1994, the Communications Research Laboratory (CRL) carried out the first laser-based ground-to-space downlink communication using the Japanese Engineering Test Satellite VI (ETS-VI), launched by the National Space Development Agency of Japan (NASDA) [49]. The 21st century is witnessing a series of significant milestones: the first inter-satellite link between the French SPOT4 Low Earth Orbit (LEO) satellite and the European Space Agency (ESA) Advanced Relay and TEchnology MISsion (ARTEMIS) GEostationary Orbit satellite (GEO), was achieved by the Semiconductor Inter satellite Link EXperiment (SILEX) experiment in 2001 [50]; the first optical Gbit/s High-Altitude Platform (HAP) to ground downlink by the Deutsches Zentrum für Luft- und Raumfahrt (DLR) in 2005 [51]; the first LEO-to-ground optical communication link—between the "Kirari" Optical Inter-orbit Communications Engineering Test Satellite (OICETS) and the Optical Ground Station (OGS) developed by the National Institute of Information and Communications Technology (NICT)—was performed in collaboration with the Japan Aerospace Exploration Agency (JAXA) in 2006 [52]; the first LEO-to-LEO link between the US Missile Defense Agency (MDA) experimental satellite and TerraSAR-X, a German commercial Synthetic Aperture Radar (SAR) satellite—utilizing a secondary laser communication payload built by Tesat-Spacecom—in 2007 [53]; the first duplex laser communication between a satellite in lunar orbit, the Lunar Atmosphere and Dust Environment Explorer (LADEE), and ground stations on the Earth, performed by NASA as the Lunar Laser Communication Demonstration (LLCD) in 2013 [54]; the first LEO-to-ground optical communications using a Small Optical TrAnsponder (SOTA) and Quantum Key Distribution (QKD) by NICT in 2014 [55]; the first optical communications link through the atmosphere with a throughput over 1 Tbit/s under a realistic turbulence environment by DLR in 2016 [56]; the first long distance quantum-entanglement distribution experiment using the Chinese quantum science experiments LEO satellite, Micius, in 2017 [57]; the first system to provide data relay services to the LEO satellites from GEO orbit by means of optical and RF bands in real-time and at a rate of 1.8 Gbit/s, European Data Relay Satellite System (EDRS), developed, manufactured and tested by OHB System AG in 2019 [58]; the inclusion of the Laser Communications Relay Demonstration (LCRD) in the previously discussed LLCD to prove that optical communications can meet needs for higher data rates, by NASA in 2022 [59] and the first mission using the Deep Space Optical Communications (DSOC) system, PSYCHE, by NASA in 2023 [60].

2.4.2 Pointing, acquisition and tracking

The fundamental parameters involved in the pointing of a lasercom system are the spot size and the divergence: the former estimates how well the system can focus the received laser signal, the latter estimates how narrowly can it transmit a laser beam. Both can be studied through the concept of the diffraction limit, given by the equation (2.3).

$$\frac{I(\theta)}{I(0)} = \left[2 \frac{J_1\left(\frac{\pi D}{\lambda} \sin(\theta)\right)}{\frac{\pi D}{\lambda} \sin(\theta)} \right]^2 \quad (2.3)$$

Here, the angular variation of the intensity of the radiation $\frac{I(\theta)}{I(0)}$ depends on: the aperture's diameter D ;

the wavelength λ ; and the Bessel function of the first kind of x , $J_1(x)$. By applying the first-minimum criterion and the approximation $\sin(\theta) \approx \theta$, the diffraction limit of a telescope θ can be approximated by equation (2.4). The graph shown in Fig. 2.14 deviates from the practical application, as we can only detect intensity levels down to -10/-15 dB—one will not detect much more than the Full Width at Half Maximum (FWHM) as the sidelobes are too faint.

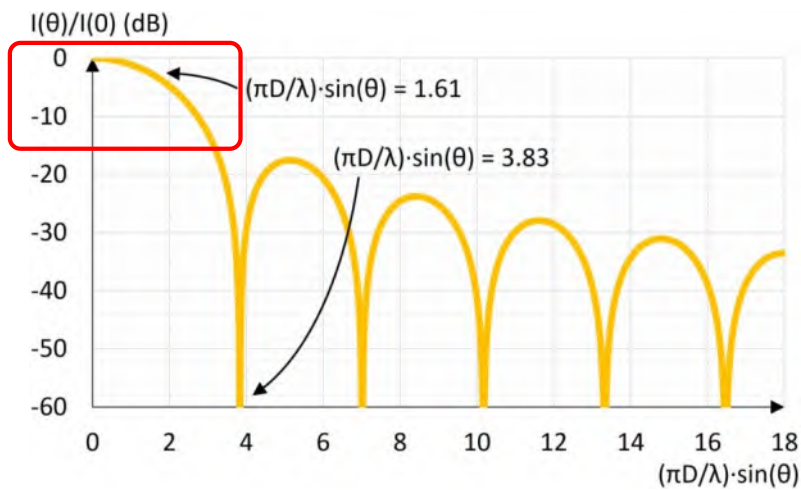


Figure 2.14: Intensity of radiation as a function of the wavelength λ , the aperture diameter D and the angular width θ . The detectable part is marked in red. [29].

$$\theta = 1.22 \frac{\lambda}{D} \quad (2.4)$$

From the transmitter perspective, equation (2.4) demonstrates that shorter wavelengths produce narrower, minimal divergence beams: One of the main advantages of FSOC over RF. Low divergence is crucial for long distances as it enhances directivity, but it also demands higher pointing accuracy—in radio frequency communications pointing accuracy is in the order of milliradians, whereas deep-space laser communications need sub-microradian precision.

To keep a stable line, the satellite requires a reference point: celestial bodies in deep space or a laser beacon transmitted from the ground if the satellite is near Earth. As discussed in subsection 2.3.2, the beacon emits a signal with a divergence matching the uncertainty zone where the satellite is predicted to be. The satellite tracks this beacon and starts the downlink at a different wavelength or polarization. The complete process is illustrated in Fig. 2.15.

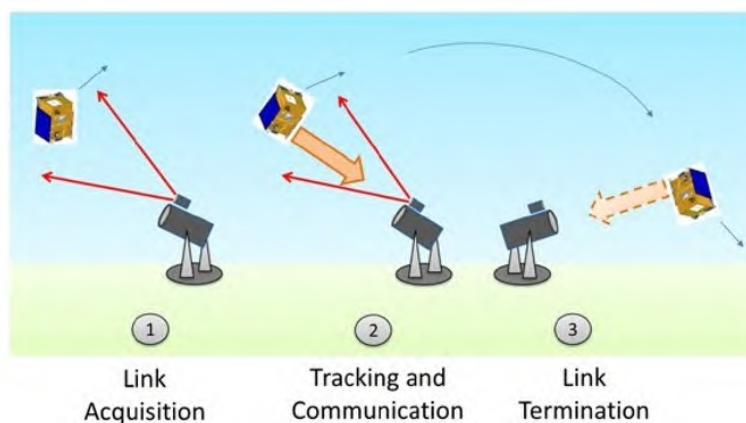


Figure 2.15: Schematic representation of the 3 phases in optical downlink. Figure taken from [61].

2.4.3 Low Earth Orbit-Direct to Earth Geometry

Link duration, range, and angular slew rate (rate at which a satellite changes its orientation, measured in degrees per second) for optical LEO-Direct to Earth (DTE) links are well-established from conventional LEO-satellite studies. A minimum elevation angle of 5° is assumed for the start of signal acquisition, with 10° or higher required for secure data transmission

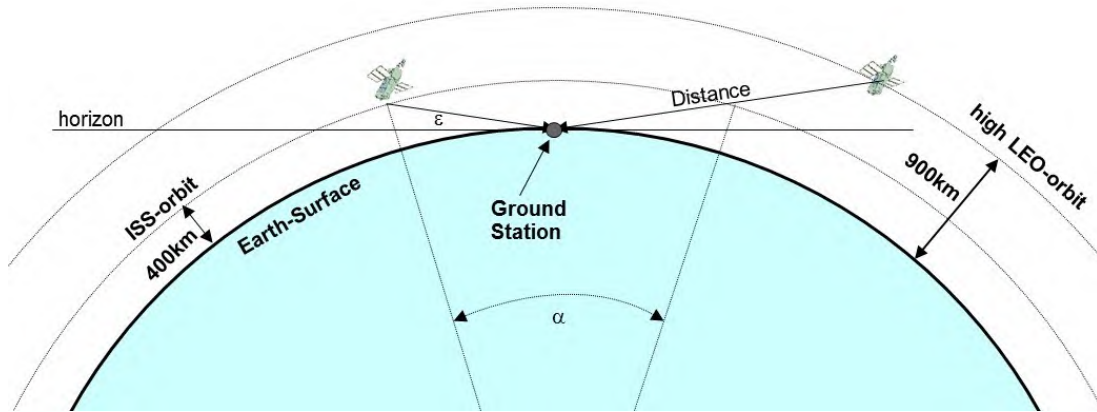


Figure 2.16: Link geometry of typical LEO satellite downlinks with circular orbits. Figure taken from [62].

Low elevations must be carefully considered, as the satellite spends nearly 80% of the time between 0° and 20° , as illustrated in Fig. 2.17.

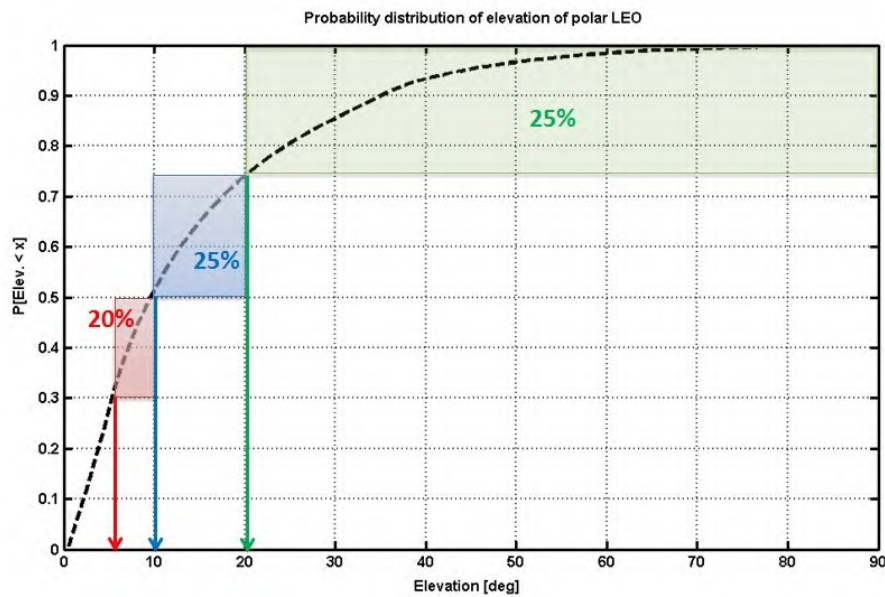


Figure 2.17: Typical distribution of the average viewing elevation for a polar LEO satellite (500 km orbit height). This relative distribution is qualitatively similar for any optical ground station (OGS) location on earth, although of course the absolute overall visibility changes depending on orbit and OGS latitude. Figure taken from [62] [63].

2.4.4 Loss-Effects in Optical Space-Ground Links

The losses in Optical Low Earth Orbit data DownLinks (OLEODL) are primarily due to three main factors: pointing-error losses caused by the satellite's pointing precision; Free-Space Losses (FSL) resulting from the orbit geometry; and atmospheric effects such as atmospheric attenuation, scintillation due to IRT, and obstruction. These factors are illustrated in Fig. 2.18.

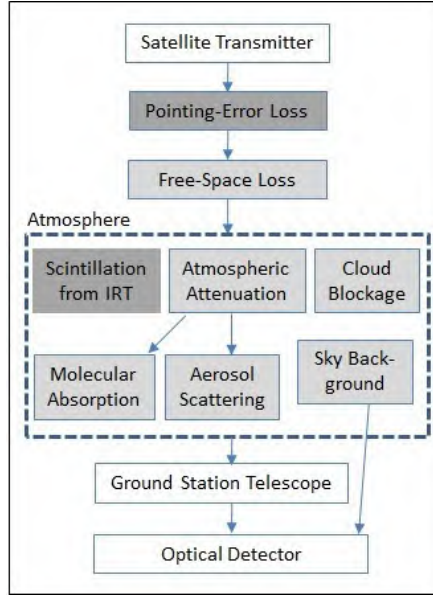


Figure 2.18: Link-parameters affecting the optical downlink quality. Effects in darker boxes change faster during downlink, values in blank boxes are static. Figure taken from [64].

Pointing-error losses are defined as the ratio between the actual received power at the OGS and the ideal received power [65]. It is crucial to address this issue as FSO links have smaller divergence compared to RF links, risking missing the OGS entirely. This is one of the key aspects which we want to assess in this thesis, identifying how much did the satellite pointing deviated from its ideal value. For GEO satellites, the uplink uses the information of the downlink’s angle-of-arrival (tilt component of the phase) to point towards the satellite and pre-correct for pointing fluctuations: This is achievable as both uplink and downlink paths are assumed the same for GEO links. For LEO satellites, the presence of the point-ahead angle causes the uplink and downlink paths to be uncorrelated, making this approach unsuitable.

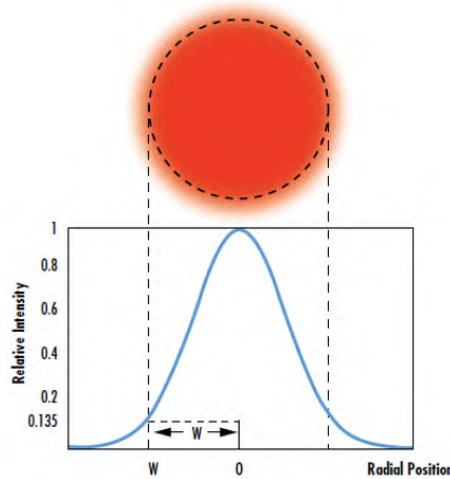


Figure 2.19: The waist of a Gaussian beam is defined as the location where the irradiance is $1/e^2$ (13.5%) of its maximum value. Figure taken from [66].

The impact of the residual pointing jitter can be estimated by normalizing the beam wander variance, $\sigma_{\text{pointing}}^2$ (presented on equation 2.2) by the beam divergence. The beam divergence is defined as the radius of the Gaussian wave where the intensity decays to $1/e^2$, also known as Half Angle Beam Divergence $\vartheta_{\text{beam}} = \lambda/\pi w_0$, where w_0 represents the beam waist radius, illustrated in Fig. 2.19. The impact factor in the pointing is defined by equation (2.5), and its relation with the beam waist radius can be appreciated in Fig. 2.20.

$$\beta_{\text{pointing}} = \frac{\sqrt{\sigma_{\text{pointing}}^2}}{\vartheta_{\text{beam}}} \quad (2.5)$$

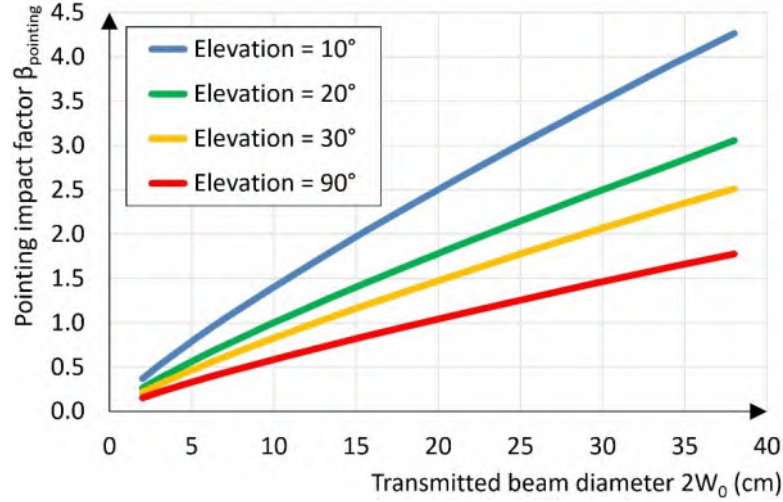


Figure 2.20: Pointing impact factor β_{pointing} vs transmitted beam diameter for several link elevation angles. Figure taken from [29].

Free-space losses decrease with both distance and wavelength, as shown in Fig. 2.21, where the satellite approaches zenith (closer to Earth). Shorter wavelengths should also minimize these losses, but this is not entirely the case, as larger scintillation is generated when passing through the atmosphere. This is one of the reasons—though not the primary one—why 1550 nm is typically used for LEO-DTE links, while 1064 nm is preferred for inter-satellite links (eye safety can be ignored in this scenario). The main reason of the dominance of the 1550 nm wavelength is the superior availability of components, to the extent that organizations like NASA are beginning to adopt this wavelength even for inter-satellite links.

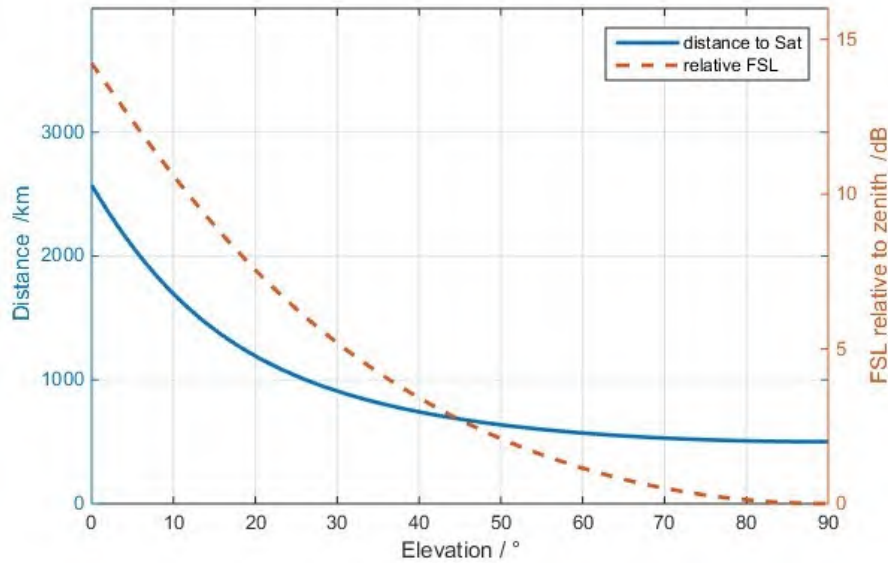


Figure 2.21: Distance and relative FSL for 500km orbit height. Figure taken from [64].

OLEODL systems deal with three major atmospheric effects: absorption, scattering, and scintillation. Absorption occurs when photons in the beam collide with particles suspended in the atmosphere—water vapor, volcanic ash, and aerosols—the latter being particularly problematic. This effect can be

minimized by optimizing the location of the optical ground station. The three main communication wavelengths used in OLEODL occupy absorption-free windows, as shown in Fig. 2.22. In these cases, absorption can be considered negligible at zenith, however it still need to be regarded in lower elevation due to the larger presence of molecular and aerosol particles as appreciated in Fig. 2.23 and Fig. 2.24, respectively.

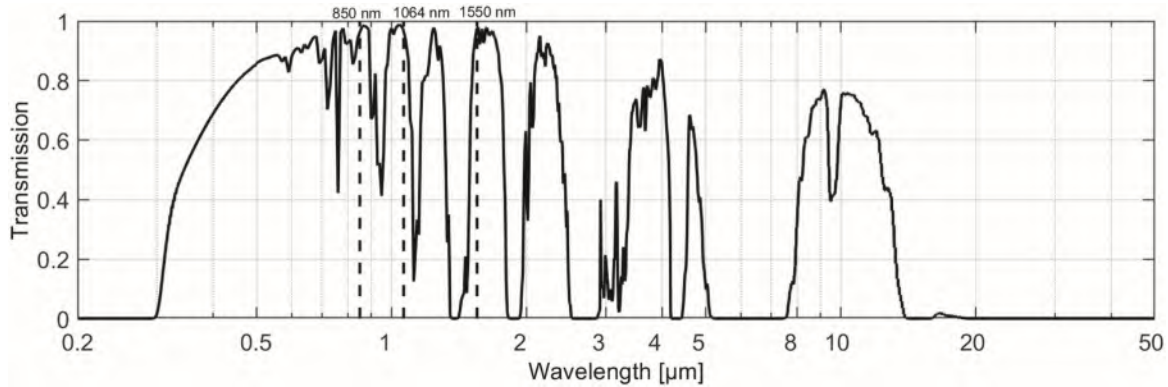


Figure 2.22: Atmospheric (clear-sky) transmission window for absorption only. 850nm, 1064nm and 1550nm windows are shown. Figure taken from [67].

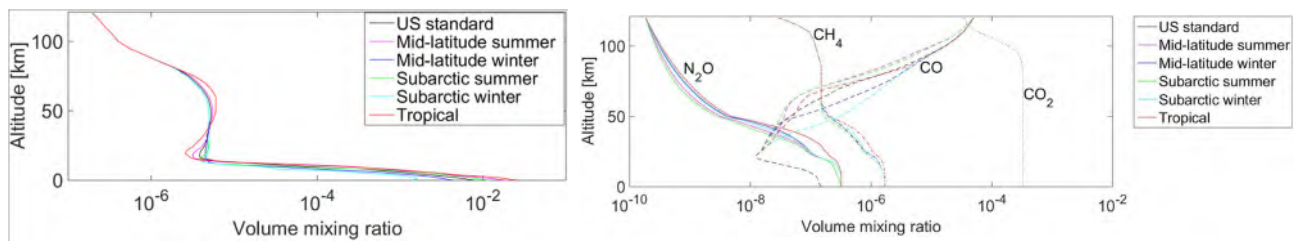


Figure 2.23: Volume mixing ratio of H_2O molecules with respect to altitude, for different atmospheric models (left). Volume mixing ratio of N_2O , CH_4 , CO , and CO_2 with respect to altitude for different atmospheric models (right). Figure taken from [67].

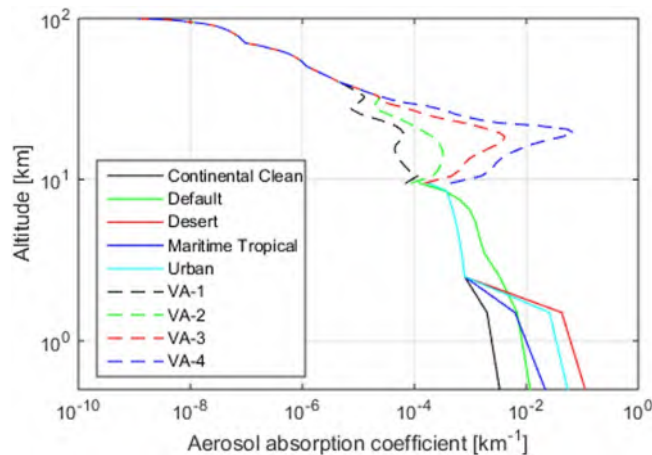


Figure 2.24: Aerosol absorption coefficients for different atmospheric models and volcanic activity (VA) levels (4 being the maximum) at 1550 nm. Figure taken from [67].

Scattering refers to the dispersal of the beam by suspended particles in the atmosphere. Aerosols particles are larger than the wavelength of the incident beam, and variate depending on the height: this known as Mie Scattering. Calculating its losses using simple equations is complex. For the OGS-OP of DLR, a flat-Earth approximation model already exists [64], which confirms that 1550 nm is the best choice. Scattering due to smaller particles than the wavelength, also known as Rayleigh scattering, is

negligible for near-infrared or longer wavelengths [68].

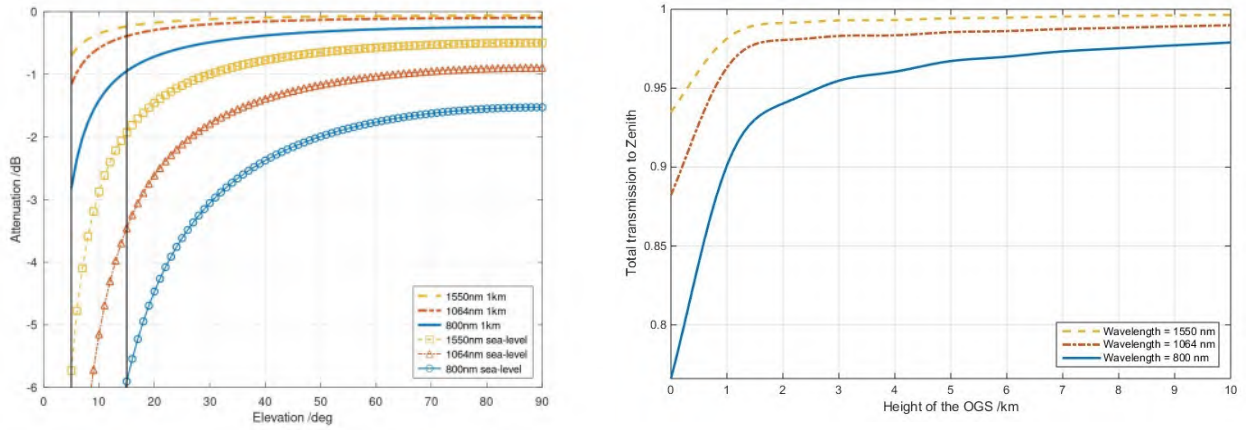


Figure 2.25: Atmos. attenuation over elevation at different wavelengths, air qualities, and OGS-altitudes, using flat-Earth modelling. The minimum (5°) and typical medium (15°) elevation for OLEODL are labeled as vertical lines (left). Zenith transmission vs OGS altitude, acc. to models (right). Figure taken from [64].

Scintillation, defined as the variance of the signal normalized to its squared mean, characterizes the temporal or spatial fluctuations of the received signal, this causes "speckle-patterns" in intensity through self-interference (the cause why we observe stars twinkle). The Power Scintillation Index (PSI) is used to describe this effect on the optical wave at a single point, like a receiver—if we quantify it with the normalized variance of the intensity, we obtain the Intensity-Scintillation Index (ISI), σ_I^2 . When the aperture of the receiver increases beyond the correlation length of the intensity fluctuations, the scintillation decreases as a bigger receiver can collect multiple correlation lengths, averaging signal fluctuations. This is so-called aperture averaging.

As discussed in subsection 2.3.4, different apertures are often used for reception and transmission in satellite communications. For the downlink, the receiver aperture is larger than the intensity correlation length, applying aperture averaging and reducing scintillation. For the uplink, the turbulence is closer to the transmitter, causing the intensity correlation length to extend up to several hundred of meters, much larger than the transmitter aperture. The (ISI), for both paths can be estimated as follows (equations 2.6 and 2.7):

$$\sigma_{I,downlink}^2 = \exp \left[\frac{0.49\sigma_{B_d}^2}{\left(1 + 1.11\sigma_{B_d}^{12/5}\right)^{7/6}} + \frac{0.51\sigma_{B_d}^2}{\left(1 + 0.69\sigma_{B_d}^{12/5}\right)^{5/6}} \right] - 1 \quad (2.6)$$

$$\sigma_{I,uplink}^2 = \exp \left[\frac{0.49\sigma_{B_u}^2}{\left(1 + 0.56\sigma_{B_u}^{12/5}\right)^{7/6}} + \frac{0.51\sigma_{B_u}^2}{\left(1 + 0.69\sigma_{B_u}^{12/5}\right)^{5/6}} \right] - 1 \quad (2.7)$$

where:

$$\sigma_{B_d}^2 = 2.25k^{7/6} \sec(\zeta)^{11/6} \int_{h_0}^H C_n^2(h) (h - h_0)^{5/6} dh \quad (2.8)$$

$$\sigma_{B_u}^2 = 2.25k^{7/6}L^{5/6} \int_{h_0}^H C_n^2(h) \left(1 - \frac{h-h_0}{H-h_0}\right)^{5/6} \left(\frac{h-h_0}{H-h_0}\right)^{5/6} dh \quad (2.9)$$

Both equations give an estimation of the maximum expected scintillation. The wave number is represented by $k = 2\pi/\lambda$, with λ as the wavelength; the link distance by L ; the zenith angle of the link path is ζ ; the height of the OGS is h_0 ; and the height of the satellite is indicated by H .

After aperture averaging, scintillation values can be estimated using equation (2.10). This approximation is valid only under weak turbulence conditions, which applies until 30° .

$$\sigma_{I,av}^2 = 8.70k^{7/6}(H-h_0)^{5/6} \sec(\zeta)^{11/6} \Re \left\{ \int_{h_0}^H C_n^2(h) \left[\left(\frac{kD^2}{16L} + i \frac{h-h_0}{H-h_0} \right)^{5/6} - \left(\frac{kD^2}{16L} \right)^{5/6} \right] dh \right\} \quad (2.10)$$

The refractive index structure parameter or index-of-refraction, denoted as C_n^2 [69], describes the turbulence strength along the transmission path by a certain profile. One of the most used models is the Hufnagel-Valley profile [70], shown in equation (2.11).

$$C_n^2(h) = Ae^{-h/100} + 2.7 \times 10^{-16}e^{-h/1500} + 0.00594 \left(\frac{\nu}{27}\right)^2 (10^{-5}h)^{10}e^{-h/1000} \quad (2.11)$$

This parameter depends on the height on the altitude above ground h ; the turbulence at ground level, defined by the structure parameter at zero height $A = C_n^2(0)$; and the mean cross-wind velocity v . Based on these factors, the structure parameter can be optimized or even ignored depending on the location of the OGS [64], as shown in Fig. 2.26.

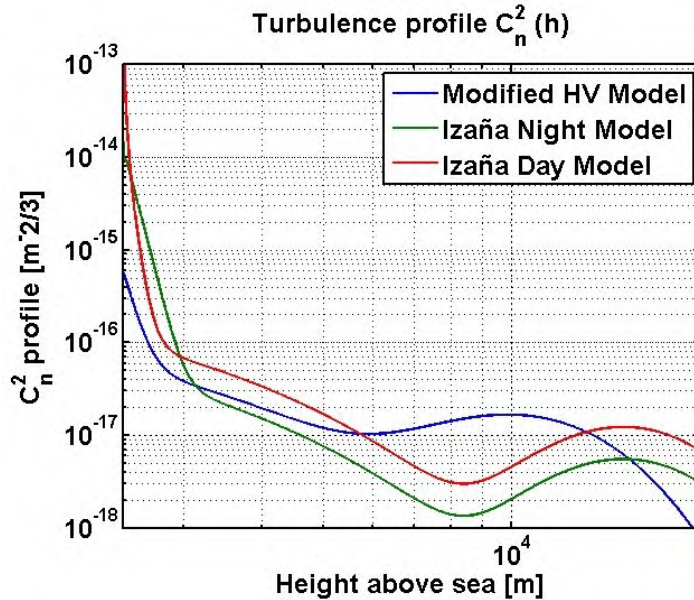


Figure 2.26: Sample turbulence profiles. High C_n^2 values mean strong atmospheric turbulence near to the surface. Figure taken from [33].

It is important for our application to discuss the relationship between scintillation and integration time. When using a monitoring device, such as an infrared camera, we can increase the exposure time to integrate the spatial fluctuations of the received signal. This is typically achieved from 100 ms onwards, as illustrated in Fig. 2.27.

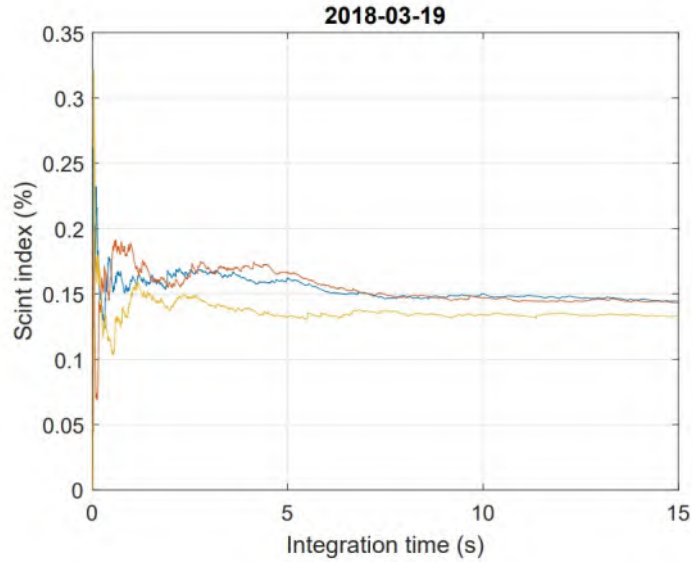


Figure 2.27: Scintillation index as a function of the integration time for 3 different data sets. The horizontal axis is limited to the range [0–15]s. Figure taken from [71].

The final atmospheric effect to consider is obstruction. Establishing an optical link requires a clear Line Of Sight (LOS) between the satellite and the OGS. The primary source of obstruction is cloud coverage. As demonstrated in [72], cloud attenuation cannot be significantly mitigated by selecting different wavelengths within the visible to near-infrared range. The most logical approach is to avoid these conditions when attempting to establish a link. One promising strategy, as suggested in [73], involves developing a network of OGSs to provide alternative communication pathways when cloud cover impacts the primary LOS [73].

2.4.5 Link Budget

The link budget is key for determining the performance of a lasercom system under various operating conditions. The total mean received power regarding all gains and losses can be calculated as the sum of all link budget components in dB [64]:

$$p_{Rx} = p_{Tx} + a_{Tx} + g_{Tx} + a_{BW} + a_{FSL} + a_{Atm} + a_{Sci} + g_{Rx} + a_{Rx} \quad (2.12)$$

p_{Tx}	average transmit optical source power	[dBm]
a_{Tx}	optical power loss inside the transmitter terminal	[dB]
g_{Tx}	transmitter antenna (telescope) gain	[dB]
a_{BW}	average loss by dynamic beam miss-pointing and beam wander	[dB]
a_{FSL}	free-space loss by link distance	[dB]
a_{Atm}	sum of atmospheric attenuation effects	[dB]
a_{Sci}	losses through atmospheric scintillation	[dB]
g_{Rx}	receiver antenna gain	[dB]
a_{Rx}	optical losses inside receiver terminal (attenuation and splitting)	[dB]
p_{Rx}	received power on detector	[dBm]

Gains (g) are positive values, while attenuations (a) are negative. The logarithmic calculation of the link budget simplifies the representation of complex propagation effects. The linear representation are G (values greater than 1 for gain) and A (with values ranging from 0 to 1 for attenuation).

- Tx-Antenna Gain [dB]:

$$g_{Tx} = 10 \log_{10} \left(\frac{4\sqrt{\ln 2}}{\theta_{FWHM}} \right)^2 = 10 \log_{10} \left(\frac{3.33}{\theta_{FWHM}} \right)^2 \quad (2.13)$$

Let θ_{FWHM} represents the Full Width at Half Maximum (FWHM) = $\sqrt{\frac{\ln 2}{2}} \theta_{e-2}$. Where θ_{e-2} denotes the full divergence angle = $2 \frac{\lambda}{\pi \cdot \omega_0(0)}$, with λ being the wavelength and $\omega_0(0)$ the waist radius at the beam's narrowest point.

- Pointing-error loss [dB]:

$$a_{BW} = 10 \log_{10} \frac{\beta}{\beta + 1} \quad (2.14)$$

Where $\beta = \frac{1}{2} \left(\frac{\theta_{e-2}/2}{\sigma_{BW}} \right)^2 = \frac{\theta_{FWHM}^2}{4 \ln 2 \cdot \sigma_{BW}^2} = \left(\frac{0.85 \cdot \theta_{FWHM}}{2 \sigma_{BW}} \right)^2$ is a special case of the beta-distribution.

- Free-Space loss [dB]:

$$a_{FSL} = 10 \log_{10} \left(\frac{\lambda}{4\pi L} \right)^2 \quad (2.15)$$

Where λ is the wavelength [m], and the link distance L [m] is computed as:

$$L = \sqrt{(R_E + H_{GS})^2 [\sin \varepsilon]^2 + 2(H_O - H_{GS})(R_E + H_{GS}) + (H_O - H_{GS})^2} - (R_E + H_{GS}) \sin \varepsilon \quad (2.16)$$

R_E	Earth radius	$[6370 \times 10^3 m]$
H_{GS}	height of the OGS over sea-level	$[DLR - OP = 650 m]$
H_O	height of the circular orbit above Earth	$[m]$
ε	link elevation angle	$[^\circ]$

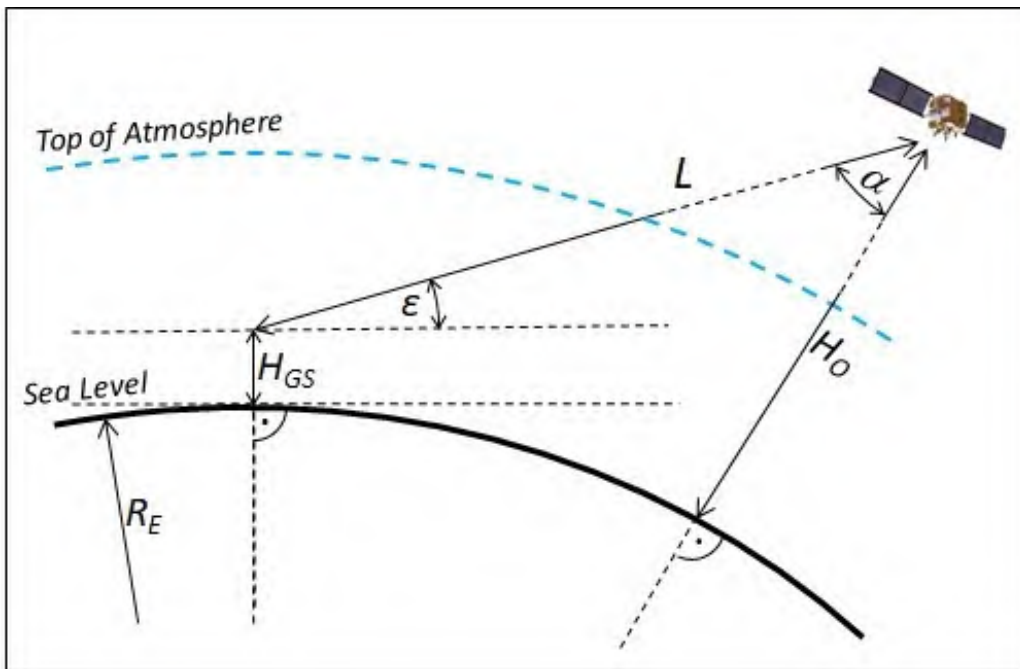


Figure 2.28: Angles and distances in the general triangle Sat-OGS-Earth. Figure taken from [64].

- Atmospheric effects loss [dB]:

$$a_{Atm} = 10 \log_{10} T_Z^{1/\sin(\epsilon)} \quad (2.17)$$

As previously said in subsection 2.4.4, only aerosol absorption and scattering need to be considered. The zenith transmission value, T_Z , is computed assuming a flat-Earth model, as detailed [67]. Different values of T_Z will be used based on atmospheric conditions; for example $T_Z = 0.891$ for 1550nm under poor conditions [64].

- Scintillation loss [dB] [74]:

$$a_{sci} = 4.343 \left\{ \text{erf}^{-1}(2p_{\text{thr}} - 1) \cdot [2 \ln(\sigma_p^2 + 1)]^{1/2} - \frac{1}{2} \ln(\sigma_p^2 + 1) \right\}. \quad (2.18)$$

Where σ_p^2 , the Power Scintillation Index (PSI), is defined as $\frac{\langle P_{Rx}^2 \rangle - \langle P_{Rx} \rangle^2}{\langle P_{Rx} \rangle^2}$, representing the variance of the received optical power P_{Rx} [W] [75]. The power threshold p_{thr} indicates the allowed fractional time during which the received power is above this threshold.

- Rx-Antenna Gain [dB]:

$$g_{Rx} = 10 \log_{10} \left(\frac{4\pi A_{Rx}}{\lambda^2} \right) \quad (2.19)$$

Where A_{Rx} is the aperture area of the receiver, assumed to be smaller than the spot size. is assumed smaller than the spot size. When calculating the area of a Cassegrain-type telescope, we need to subtract the area of the inner obscuration, which is the area blocked by the secondary mirror.

The parameters p_{Tx} and a_{Tx} depend on the laser terminal, while a_{Rx} depends on the receiver telescope and is typically measured for each link.

2.5 Laser Transmitters for Optical Low Earth Orbit data DownLinks

Different types of laser terminals are employed for Optical Low Earth Orbit data DownLinks (OLEODL). These transmitters can be categorized into three distinct groups: No tracking systems, relying on full body-pointing through satellite's attitude knowledge from star-camera sensors; Dynamic coarse body-pointing by the satellite during Optical Ground Station (OGS)-overflight, with fine-pointing achieved through beacon tracking by the optical terminal; and Terminals equipped with a coarse-pointing assembly for a hemispherical Field Of View (FOV), which actively track a ground-based beacon.

2.5.1 OSIRISv1 Onboard Flying Laptop

The small satellite "Flying Laptop" (FLP), launched in 2017, was developed and built by students at the University of Stuttgart. It has a mass of 110 kg and is equipped with the first version of the Optical Space InfraRed downlink System (OSIRIS) [76], built by the Institute of Communications and Navigation (IKN) at the Deutsches Zentrum für Luft- und Raumfahrt (DLR). The satellite employs an open-loop body pointing mode, avoiding dedicated optomechanical pointing assemblies. Instead, the satellite relies on its entire rotation, controlled by onboard star cameras, to point towards the ground station without feedback from the instrument [77].

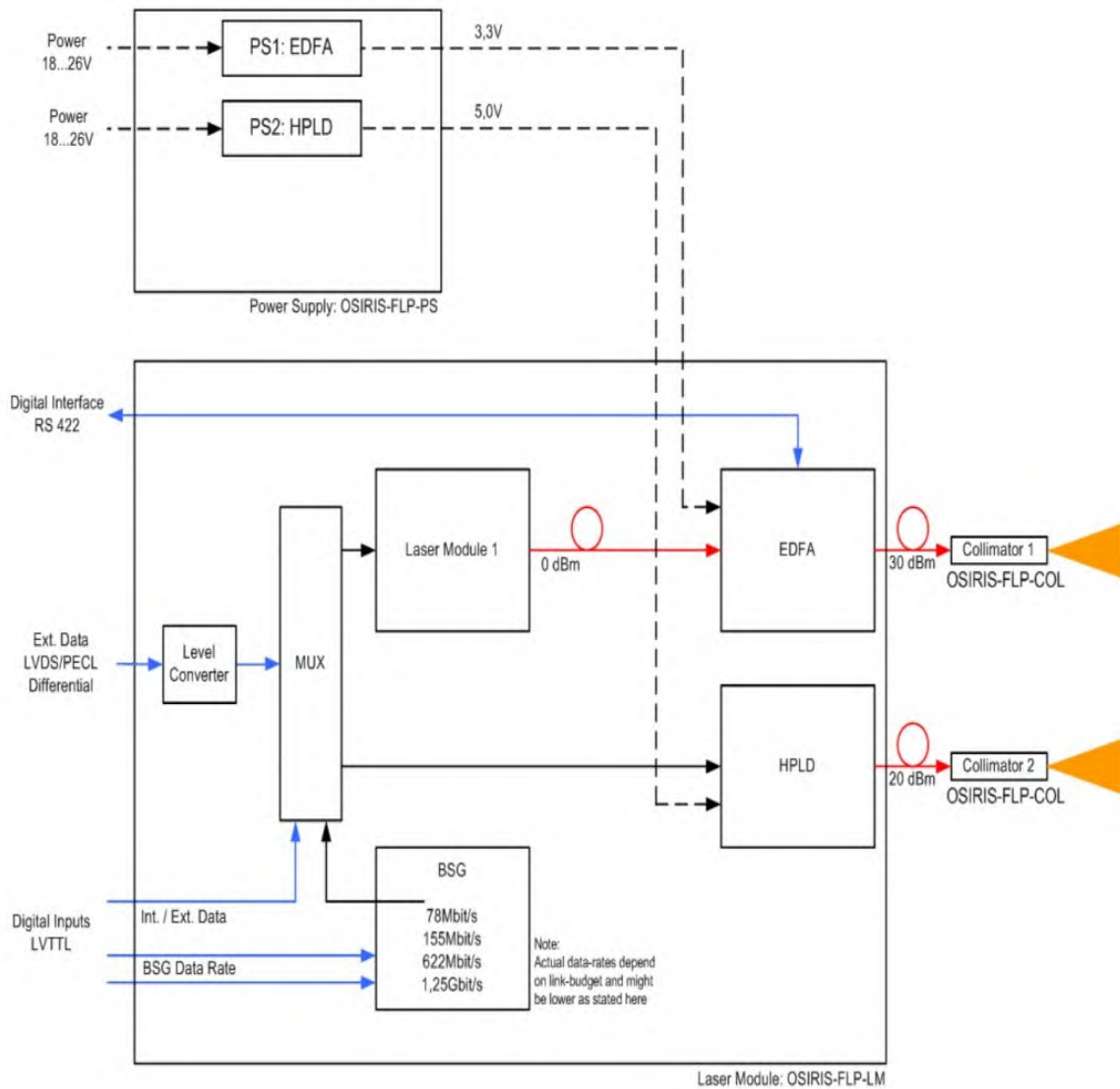


Figure 2.29: OSIRISv1 setup, as located onboard FLP. Figure taken from [78].

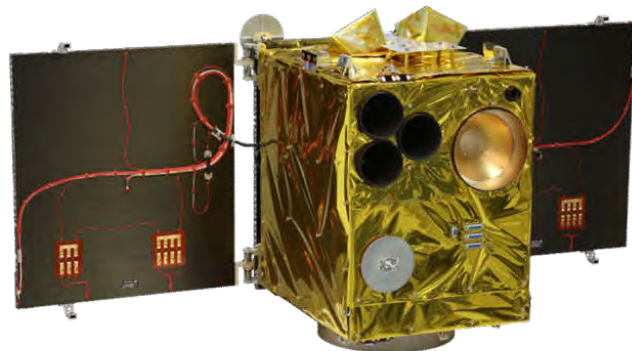


Figure 2.30: "Flying Laptop" satellite. Figure taken from [79].

2.5.2 OSIRIS4CubeSat Onboard Laser CubeSat

In contrast to the other OSIRIS payloads that focus on increasing data rates, OSIRIS4CubeSat aims to achieve a highly compact system design that enables the use of optical communication even on small satellites like CubeSats. Developed by the Deutsches Zentrum für Luft- und Raumfahrt (DLR) on behalf of Tesat Spacecom, the OSIRIS4CubeSat terminal, also known as CubeSat Laser Communication

Transmitter (CubeLCT), has established itself as the smallest laser communication terminal in the world.

The first demonstration of complete end-to-end transmission took place as part of the PIXL-1 mission [80]. On January 24, 2021, the CubeL satellite carrying the CubeLCT terminal was launched into space.

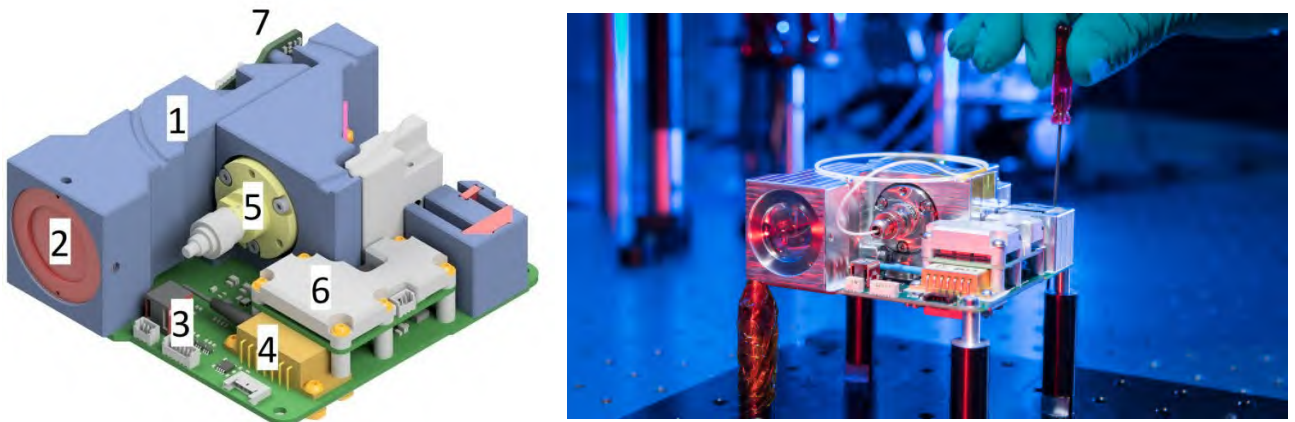


Figure 2.31: 3D model of OSIRIS4CubeSat Payload (left). Figure taken from [81]. OSIRIS4C - Flight model of the laser terminal OSIRIS4CubeSat (right). Figure taken from [82].

As shown in Fig. 2.31, the optomechanics, shown in blue (1), consist of the mechanical mounts and housings for the optical elements, highlighted in light red (2) while the electronics mainboard is depicted in green (3). The transmission system consists of the laser source in orange (4), and the transmit collimator, shown in yellow (5). The driver electronics are mounted on the green Printed Circuit Board (PCB) below a passive cooling element in gray (6). The receiver sensor is located on a separate PCB at the back of the terminal (7).

The OSIRIS4C system combines body pointing with closed-loop tracking. To establish a connection, the terminal uses the Pointing Acquisition and Tracking (PAT) system. A relatively broad beacon signal is sent from an OGS to illuminate the satellite. This beacon is acquired by a 4-Quadrant Diode (4QD), functioning as a tracking sensor within the satellite. The 4QD measures the angular error, and a Fine Steering Mirror (FSM) then corrects it. Throughout the transmission, the satellite must maintain a pointing accuracy of better than 1° towards the OGS. To ensure that the transmission beam accurately reaches the OGS, it is coupled into the same optical path as the incoming beacon.

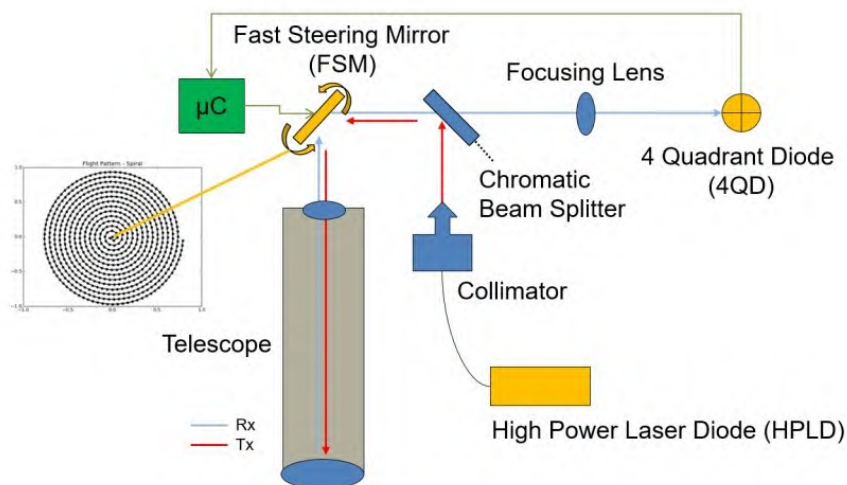


Figure 2.32: Block diagram of Fine Pointing Assembly (FPA) inside OSIRIS4C. Figure taken from [80].

The primary objective of the PIXL-1 mission was to integrate a high-power laser terminal into a 3U

CubeSat, such as the Laser CubeSat (CubeL), extending CubeSats' data transmission rates up to 100 Mbit/s.

SYSTEM OVERVIEW

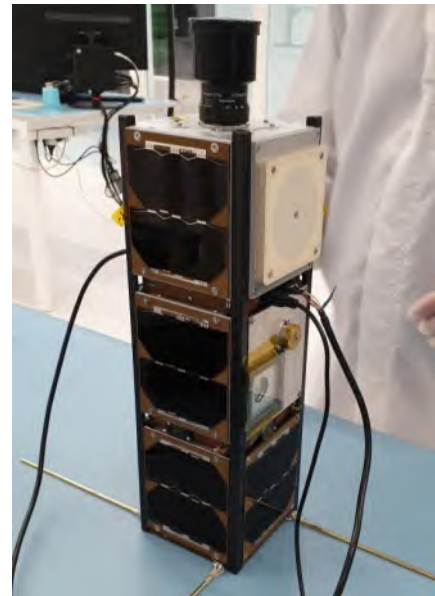
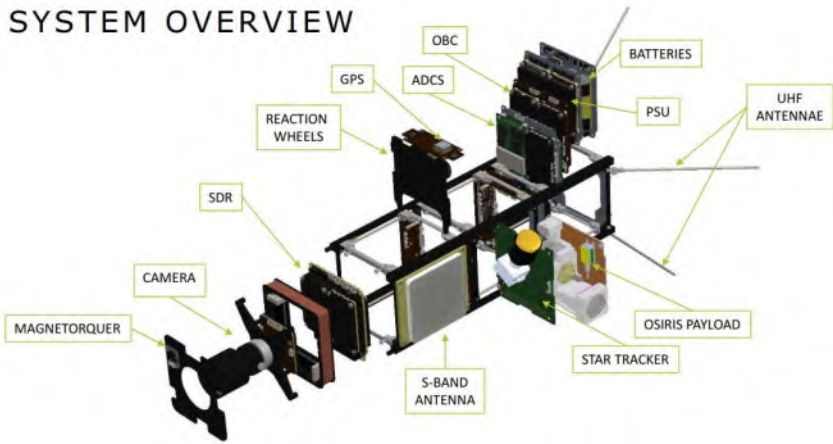


Figure 2.33: System overview of CubeL (left). Integrated CubeL (right). Figure taken from [81].

2.5.3 OSIRISv3 Onboard Titania

The next stage in the development of the OSIRIS program, OSIRISv3, aims to achieve higher data rates, up to 10 Gbit/s. With a smaller divergence, OSIRISv3 relies on a new dedicated alignment unit. This so-called Coarse Pointing Assembly (CPA) enables hemispheric movement, decoupling the laser beam from the satellite's position. The transmitter is also equipped with a FPA and a point ahead assembly for improved accuracy and performance.

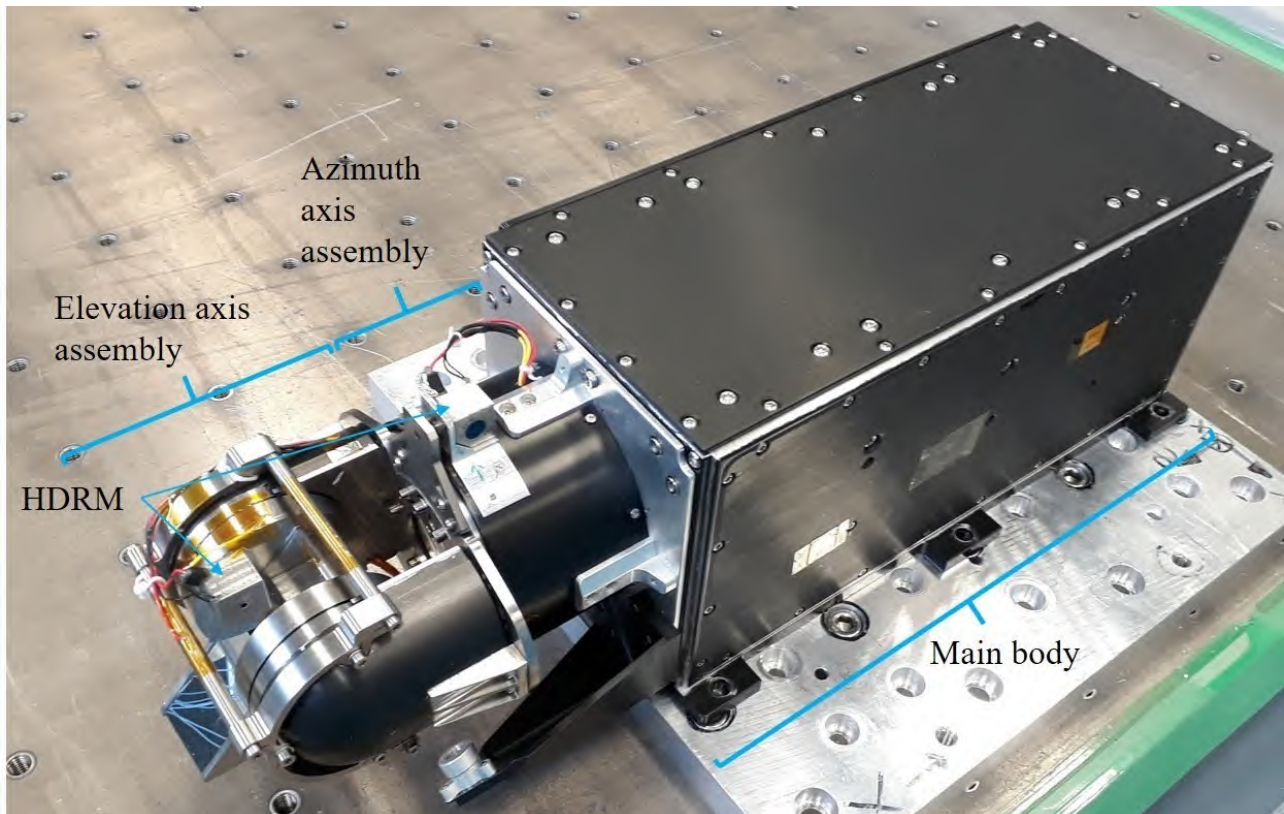


Figure 2.34: OSIRISv3 laser communication Terminal including CPA. Figure taken from [83].

The OSIRISv3 system provides a hemispherical Field Of Regard (FOR), which is the total area that can be observed by the movable sensor. This FOR is achieved through two axes of movement—elevation and azimuth—while maintaining an optical aperture of 30 mm. One key aspect of this system is the Absolute Pointing Knowledge (APK) in both axes, which measures the satellite’s ability to accurately determine its orientation in space. The position data is transmitted to the motor controller unit, which manages the motor movements along the elevation and azimuth axes. For a Free-Space Optical (FSO) link to an optical ground station, the OSIRISv3 CPA steers the beam during the full overflight.

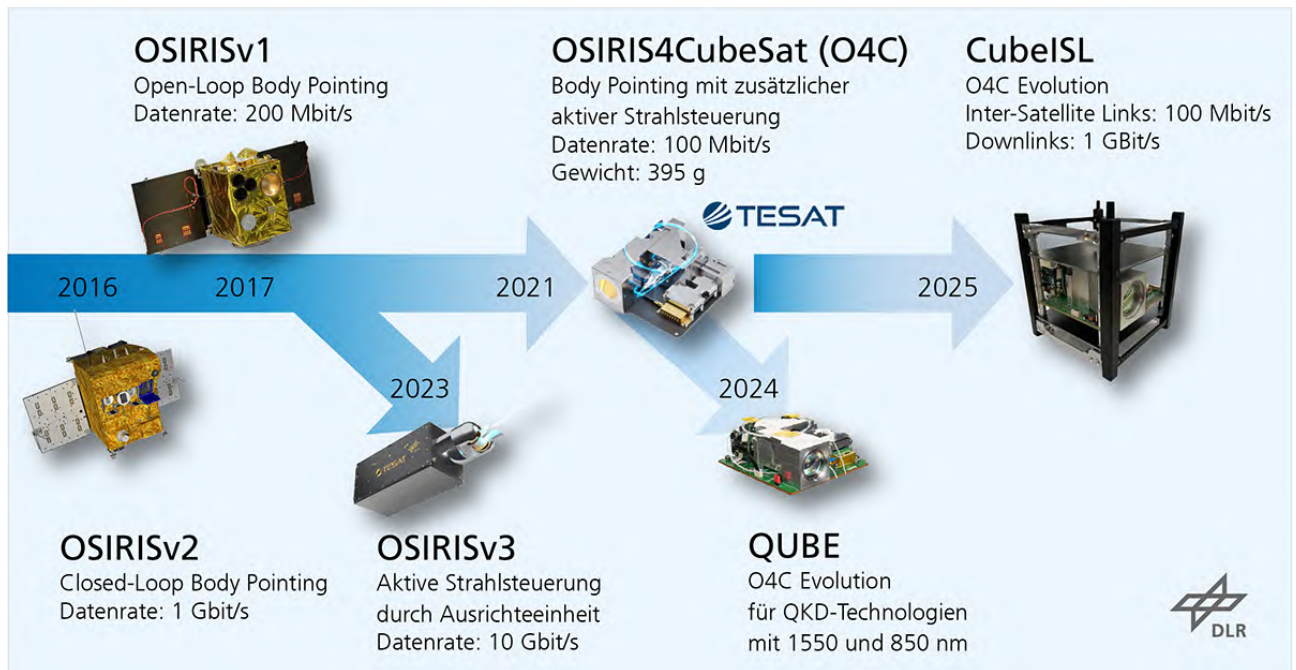


Figure 2.35: OSIRIS-Program Road map. Figure taken from [84].

3 Materials and Methods

In this chapter we will discuss the design, implementation, and testing of the AllSky-camera system, including its constraints and reasons behind the multiple decisions made throughout the process.

3.1 System Requirements

The proposed system was designed as a compact, portable, and self-sufficient device for use during Low Earth Orbit (LEO) satellite downlinks. Based on an Infrared (IR) camera equipped with a wide Field of View (FOV) lens, it covers the entire hemisphere without the need for satellite orbit information or pointing. This approach allows continuous observation of satellite passes, providing real-time assessment of elevation, azimuth, and intensity as detected by the camera with minimal user intervention. The system could be remotely operated or even fixed as a permanent installation in the future, serving dual purposes: evaluating the satellite’s pointing accuracy, and acting as a validation tool for the Optical Ground Station (OGS) by verifying the correlation of results.

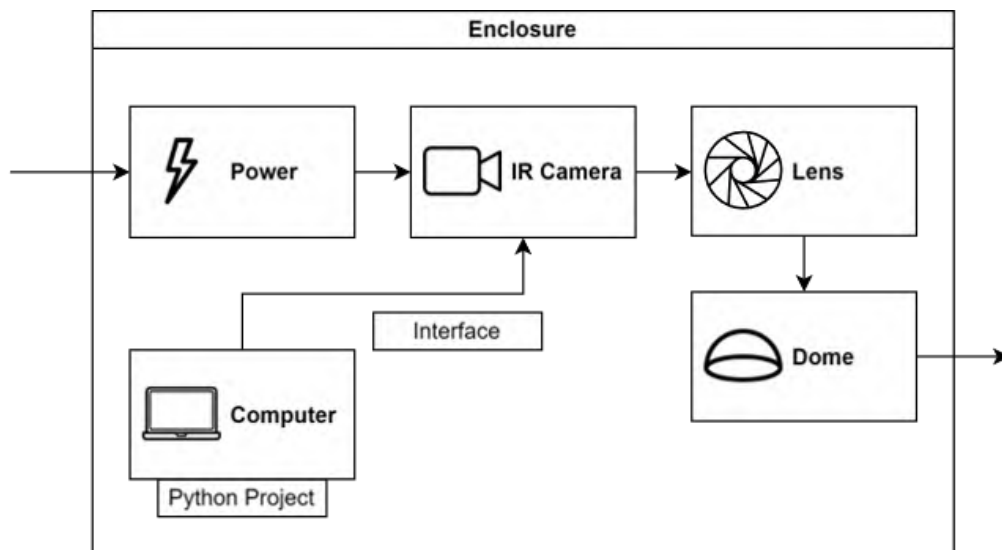


Figure 3.1: Initial diagram of the AllSky-camera system.

Given the system’s operational conditions, waterproofing, ventilation, and internet connectivity must be regarded. Meeting those requirements was challenging, as we will discuss later.

3.2 Component Selection

The first step after defining the goals and requirements of the project, was to decide which components were the most suitable for our application. The key elements are the camera, the lens, the dome and the enclosure.

3.2.1 Indium Gallium Arsenide Camera

The camera serves as the primary component of our system. The satellites under observation are equipped with a 1550nm laser terminal. Indium Gallium Arsenide (InGaAs) is the most appropriate material for working at this wavelength.

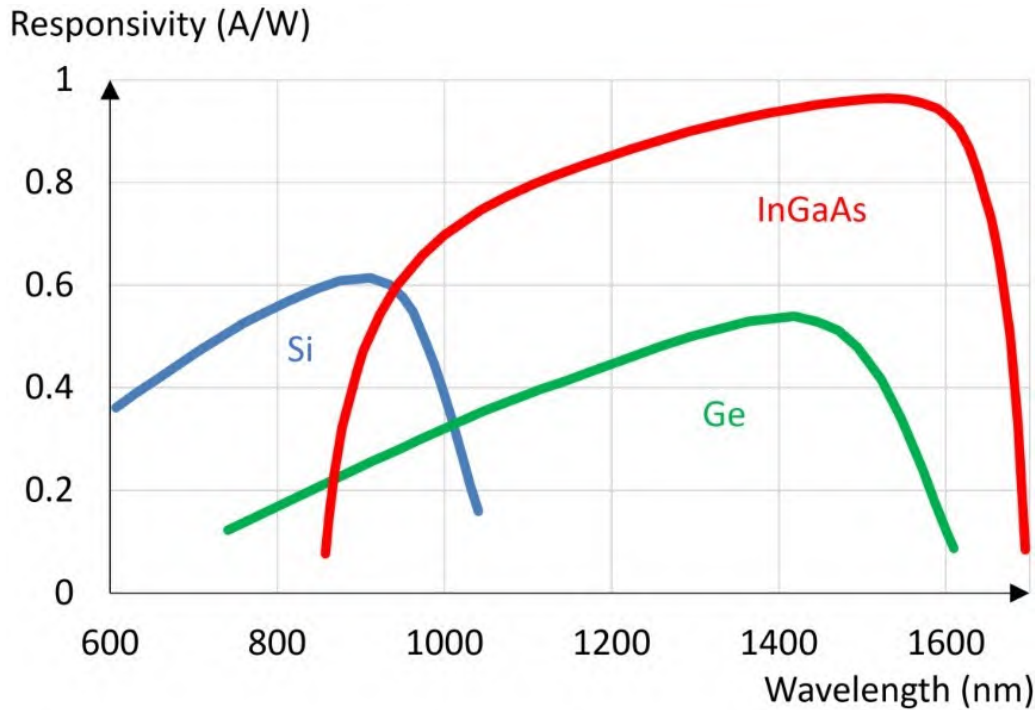


Figure 3.2: Typical responsivity vs wavelength for silicon, InGaAs, and germanium. Figure taken from [29]

Initially, the plan was to utilize the newly developed SONY Short-Wavelength InfraRed (SWIR) Image Sensor Technology, known as SenSWIR. This technology integrates InGaAs photodiodes with silicon readout circuits via Copper (Cu)-Copper bonding, resulting in a wide-band and highly sensitive SWIR image sensor. SenSWIR allows imaging across a broad spectrum of wavelengths, ranging from 0.4 μm to 1.7 μm . A single camera can now capture both the visible (VIS) light and the SWIR spectrum, which previously required separate cameras. These cameras are called Visible to Short-Wavelength InfraRed (VSWIR) cameras.

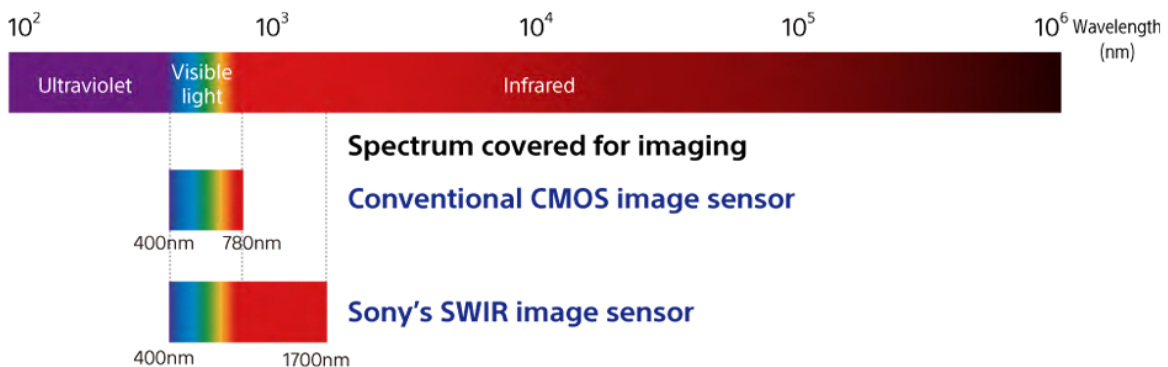


Figure 3.3: Operational Range SONY'S SWIR Sensor. Figure taken from [85]

There are two versions of the chip: The General-purpose SWIR Image Sensor (IMX990/IMX991) and the High-resolution, High-performance SWIR Image Sensor (IMX992/IMX993). The general-purpose chips feature 5 μm pixels, whereas the high-performance variants feature 3.45 μm pixels. The main problem of these sensors is that the IMX992 and IMX993 are not yet available for purchase until Q4 2024, and using the IMX990 or IMX991 would compromise the Field Of View (FOV) of our final

system. The FOV of an imaging system depends on the focal length of the lens and the dimensions of the sensor of the camera, as we will later discuss in subsection 3.2.2.

The dimensions of a camera's sensor are calculated as follows, where the result can then be approximated to match one of the standard sensor sizes, as shown in Fig. 3.4:

$$V_{sensor\ size} [mm] = V_{resolution} [pixels] \cdot P_{size} [\mu m] \quad (3.1)$$

$$H_{sensor\ size} [mm] = H_{resolution} [pixels] \cdot P_{size} [\mu m] \quad (3.2)$$

$$D_{sensor\ size} [mm] = \sqrt{(H_{sensor\ size} [mm])^2 + (V_{sensor\ size} [mm])^2} \quad (3.3)$$

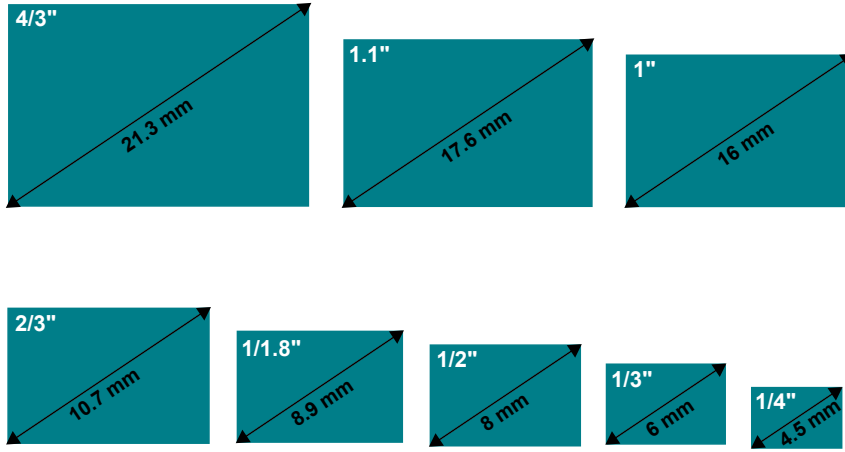


Figure 3.4: Common sensor formats and their diagonal dimensions. Figure taken from [86].

Device structure

Thermoelectric cooling element included model	IMX990-AABA	IMX991-AABA	IMX992-AABA	IMX993-AABA
Thermoelectric cooling element not included model	IMX990-AABJ	IMX991-AABJ	IMX992-AABJ	IMX993-AABJ
Image size	8.2 mm diagonal (Type 1/2)	4.1 mm diagonal (Type 1/4)	11.4 mm diagonal (Type 1/1.4)	8.9 mm diagonal (Type 1/1.8)
Effective pixels	1296 (H) × 1032 (V) approx. 1.34 megapixels	656 (H) × 520 (V) approx. 0.34 megapixels	2592 (H) × 2056 (V) approx. 5.32 megapixels	2080 (H) × 1544 (V) approx. 3.21 megapixels
Unit cell size	5 μm (H) × 5 μm (V)		3.45 μm (H) × 3.45 μm (V)	
Optical black	Horizontal direction	Front 0 pixels, rear 96 pixels		Front 96 pixels, rear 0 pixels
	Vertical direction	front 20 pixels, rear 0 pixels		front 24 pixels, rear 0 pixels
Input drive frequency	37.125 MHz/74.25 MHz/54 MHz		37.125 MHz/74.25 MHz/54 MHz	
Power supply	1.2 V, 1.8 V, 2.2 V, 3.3 V, 1.2 V (Pixel), 2.2 V (Pixel)		1.2 V, 1.8 V, 2.2 V, 3.3 V, 2.2 V (Pixel)	
Shutter mode	Global shutter		Global shutter (rolling shutter when DRRS on)	
Output interface	SLVS (2 ch/4 ch)		SLVS (2 ch/4 ch/8 ch) / MIPI (2 lane/4 lane)	
Package	Thermoelectric cooling element included: 30.0 mm (H) × 30.0 mm (V) Thermoelectric cooling element not included: 20.0 mm (H) × 16.8 mm (V)		Thermoelectric cooling element included: 30.0 mm (H) × 30.0 mm (V) Thermoelectric cooling element not included: 21.0 mm (H) × 20.0 mm (V)	

Figure 3.5: Specifications of the SONY SWIR image sensors. Figure taken from [85].

After careful evaluation, we decided to disregard the SenSWIR sensors and instead prioritized selecting the camera with the largest possible sensor, we chose the Goldeye G-008 TEC1 [87]. The selection of this specific camera was mainly backed by its software and Application Programming Interface (API) as specifications are consistent across all considered cameras.

The C-mount camera records in 320×256 pixels at 344 frames per second. Users can select between 8-bit, 12-bit, 12-bit packed, or 14-bit monochrome pixel format. The camera also features advanced image processing capabilities, such as background correction, Defect Pixel Correction (DPC), and Look-Up Tables (LUTs). Designed for durability, the camera operates within a temperature range of -20°C to $+55^{\circ}\text{C}$, making it suitable for extended use in harsh environments. Additionally, the camera exhibits a quantum efficiency of approximately 78% at 1550 nm , as illustrated in Fig. 3.6.

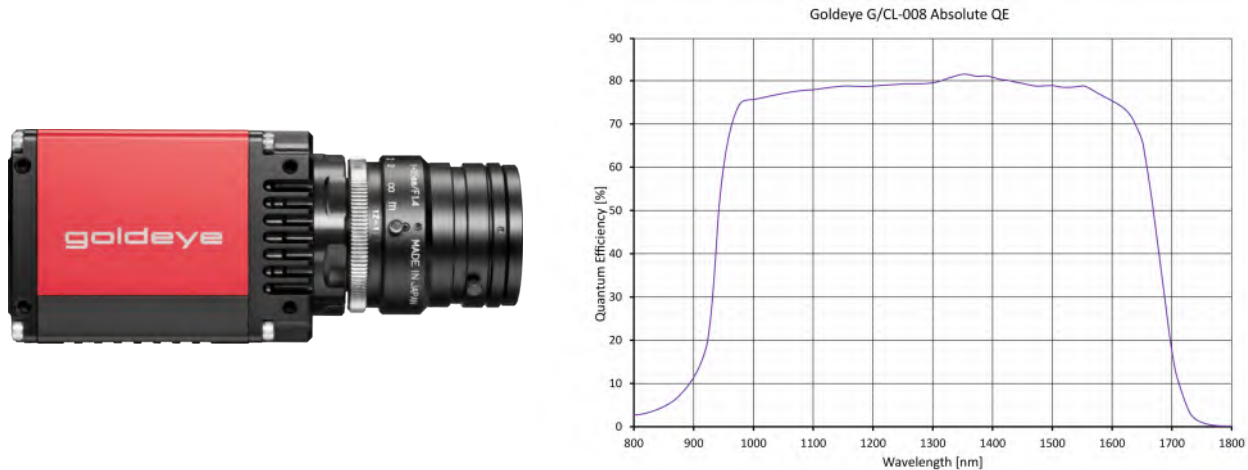


Figure 3.6: Goldeye G-008 TEC1 camera. (left). Quantum efficiency. (right). Figure taken from [87].

Table 3.1: Comparison of different cameras.

Specification	Goldeye TEC1 [88]	G-130	Goldeye TEC1 [87]	G-008	Xenics Bobcat 320 CL 400 [89]
Interface	Power over Ethernet		Power over Ethernet		CameraLink
Spectral range [nm]	400 - 1700		900 - 1700		900 - 1700
Resolution [$H \times V$ px.]	1280×1024		320×256		320×256
Pixel size [$H \times V$ μm]	5×5		30×30		20×20
Sensor	Sony IMX990 Type 1/2" VSWIR		Type 2/3" SWIR		Type 1/2" SWIR
Lens mount	C-Mount		C-Mount		C-Mount
Max. frames per second	94		344		400
Bit depth	8-bit to 12-bit		8-bit to 14-bit		8-bit to 16-bit
Power consumption [W]	<12.95		<12.95		2.8
Operating temperature [$^{\circ}\text{C}$]	-20 to +55		-20 to +55		-40 to +70
Body dimensions*					
[$L \times W \times H$ mm]	$78 \times 55 \times 55$		$78 \times 55 \times 55$		$72 \times 55 \times 55$
Mass* [g]	340		340		285

*Lens not included.

3.2.2 Wide Angle Lens

Once an appropriate InGaAs camera is selected, the next challenge is finding a suitable C-Mount lens that meets our requirements. The primary concern is achieving the largest possible field of view, ideally close to 180 degrees. Fulfilling this requirement is challenging due to the limitations of the C-Mount

standard, which being relatively small, makes it difficult to accommodate the larger lenses providing a wide FOV. Additionally, the requirement for InfraRed (IR) operation adds further complexity to the selection process.

We considered two different approaches, the first used a specialized SWIR lens. The main problem of these kind of lenses, besides being expensive (around €2000), is their limited FOV—there are no lenses with a wide enough FOV for our application, as the materials required to construct them also make the lenses tedious to miniaturize, creating optics that are too large for a C-Mount (lenses like this can be custom-made, they are just not available in the market as they go in a different direction to the intended).

The second option featured a Visual and InfraRed (VIR) lens. Visible light lenses are more affordable and offer wider FOVs. While these lenses can operate in the infrared spectrum, their transmittance is reduced, leading to potential chromatic aberrations. This occurs when the lens fails to focus all wavelengths to the same convergence point or image plane, resulting in color distortion and reduced image quality.

Table 3.2: Comparison of different lenses.

Specification	NAVITAR SWIR 8 [90]	KOWA LM100JC1MS [91]	THOR- LABS MVL4WA [92]	FUJINON FE185C057HA- 1 [93]
Spectral range [nm]	700 - 1900 (SWIR)	380 - 1400 (VIR)	380 - 1400 (VIR)	380 - 780 (VIS)
Transitivity at 1550 nm [%]	81.6*	65**	56.8***	42****
Focal length [mm]	8	100	3.5	1.8
F-Number [$f/\#$]	1.4 - 16	2.8 - 32	1.4 - 16	1.4 - 16
Focus control	Manual	Manual	Manual	Fixed
Max. Aperture diameter [mm]	5.7	35.7	2.5	1.3
Diagonal Field of View [°]				
2/3" sensor size	92.4	6.3	140*****	185
1/2" sensor size	70.7	4.6	132.1	185
Operating temperature [°C]	-10 to +45	-10 to +50	-10 to +45	-10 to +50
Mass* [g]	205	145	70	135

*Transitivity at 1500 nm - Confidential Document.

**Transitivity at 1400 nm [94].

***Transitivity at 1400 nm [95].

****Transitivity at 1000 nm - Confidential Document.

*****In theory not compatible with 2/3" sensor size.

As we can see in Tab. 3.2, the narrow fields of view render the Navitar and Kowa lenses unusable. When comparing the Thorlabs and Fujinon lenses, a compromise must be made: the MVL4WA offers a narrower field of view with higher transmittance, while the FE185C057HA-1 provides a wider field of view at the expense of lower transmittance. The Thorlabs lens is also incompatible with 2/3" sensors, which could lead to potential issues such as distortion, vignetting, or cropping of the field of view.

Given the difficulty of deciding based just on this data, we tested both lenses to determine which one would be more suitable for our specific application. The results of these tests will be discussed in subsection 3.5.2.



Figure 3.7: Fujinon FE185C057HA-1. (left). Figure taken from [93]. Thorlabs MVL4WA. (right). Figure taken from [96].

3.2.3 Dome

The lens will be protected from the exterior by a dome. We explored multiple options to ensure high transmittance at 1550 nm . We inquired multiple companies, such as TTV and RÖHM, about the transitivity of their Plexiglas/acrylic sheets that might meet our requirements. While the performance of the materials was adequate, shaping them into a dome proved to be complex and impractical. As an alternative, we considered crystal domes made from 1550 nm compatible materials.

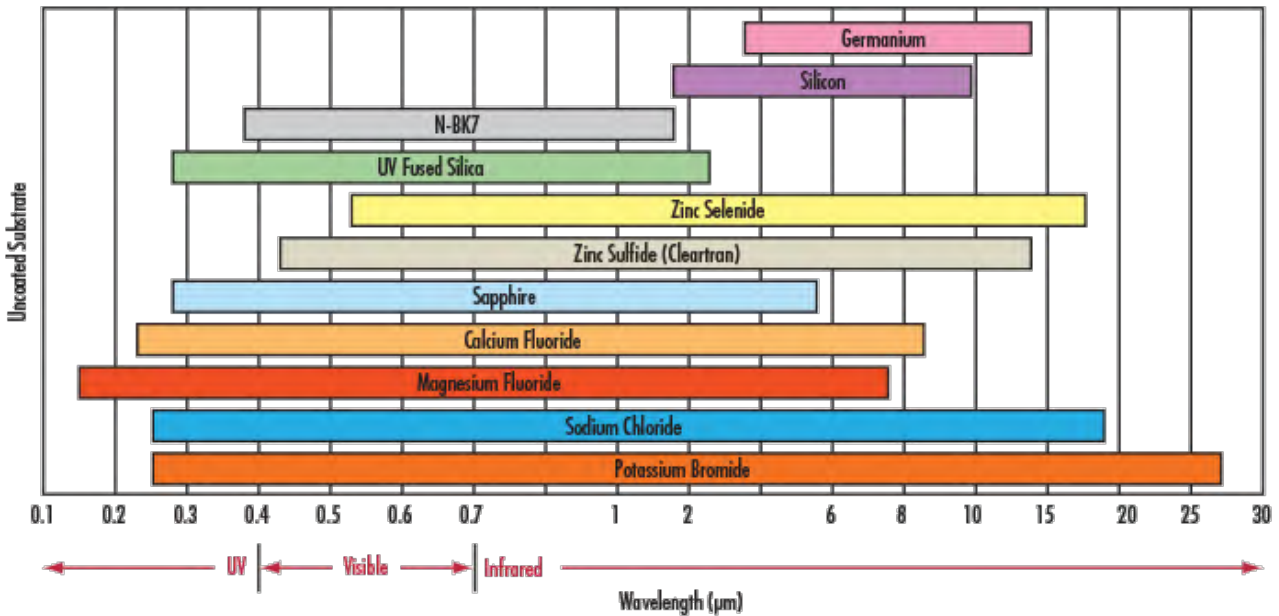


Figure 3.8: Infrared Substrate Comparison (Wavelength Range for N-BK7 is Representative for the Majority of Substrates Used for Visible Wavelengths Such as B270, N-SF11, BOROFLOAT®, etc.). Figure taken from [97]

N-BK7, fused silica, and sapphire exhibited excellent transmittance, but their cost was too much for what they provided. Ultimately, we opted for a plexiglas dome that we already had in our possession, as its performance in our tests was acceptable.



Figure 3.9: Final plexiglass dome.

3.2.4 Enclosure

All components must be enclosed in a box for transport and operation. This enclosure must meet specific requirements to withstand harsh conditions: waterproofing; dustproofing; and sturdiness, to ensure the components are fixed and can be moved without risk. The inclusion of a laptop for operating the camera forces us to increase the dimensions of the box.



Figure 3.10: Max Koffer MAX540H245 box closed. (left). Max Koffer MAX540H245 box opened. (right). Figures taken from [98].

The enclosure displayed in Fig. 3.10 has an IP67 rating, meaning it is dustproof, airtight, and waterproof, even if temporarily submerged. With internal dimensions of $53.8 \times 40.5 \times 19.5$ [$L \times W \times H$ cm], weight of 7.7 kg, and operating temperature range from -30°C to $+90^{\circ}\text{C}$, the box is more than sufficient to house all the required components and protect them from external conditions.

3.3 Final Overview of the AllSky-camera System

The final device will be controlled by a laptop housed inside the enclosure. This laptop will be connected to a switch, linking the laptop and the camera and providing an option for internet connectivity. The camera needs to go through a Power Over Ethernet (POE) injector before the switch to be granted power, this could be ignored if POE switch was available, but is not the case.

A four-outlet power strip will supply power to the system: one outlet for the laptop charger, one for the switch, one for the POE injector, and an additional outlet for a potential future dust filter. The power cable of the power strip will exit the left side of the enclosure through a cable gland, maintaining the system's waterproof integrity.

The camera will be mounted on the left side of the lid, opposite the laptop. A hole will be made in the lid for the camera lens, which will be protected from the exterior by the dome. The assembly of the dome is key to prevent condensation and ensure the box remains waterproof.

One challenge with this device is that when the laptop needs to be pulled out for operation, the Ethernet cable connected to the switch gets pinched between the lid and the box—not being able to close properly—the solution was to install a double Ethernet socket on the right of the box. Both internal connectors of the socket will be connected to the switch, this way if the laptop is inside of the box, the internet cable will be connected to one of the external socket connectors, leaving the second one free. If the laptop is outside the box, the internet cable will remain connected to one socket connector while the laptop will be connected to the second connector, keeping connection to the switch. The final iteration of the device can be shown in Fig. 3.11.

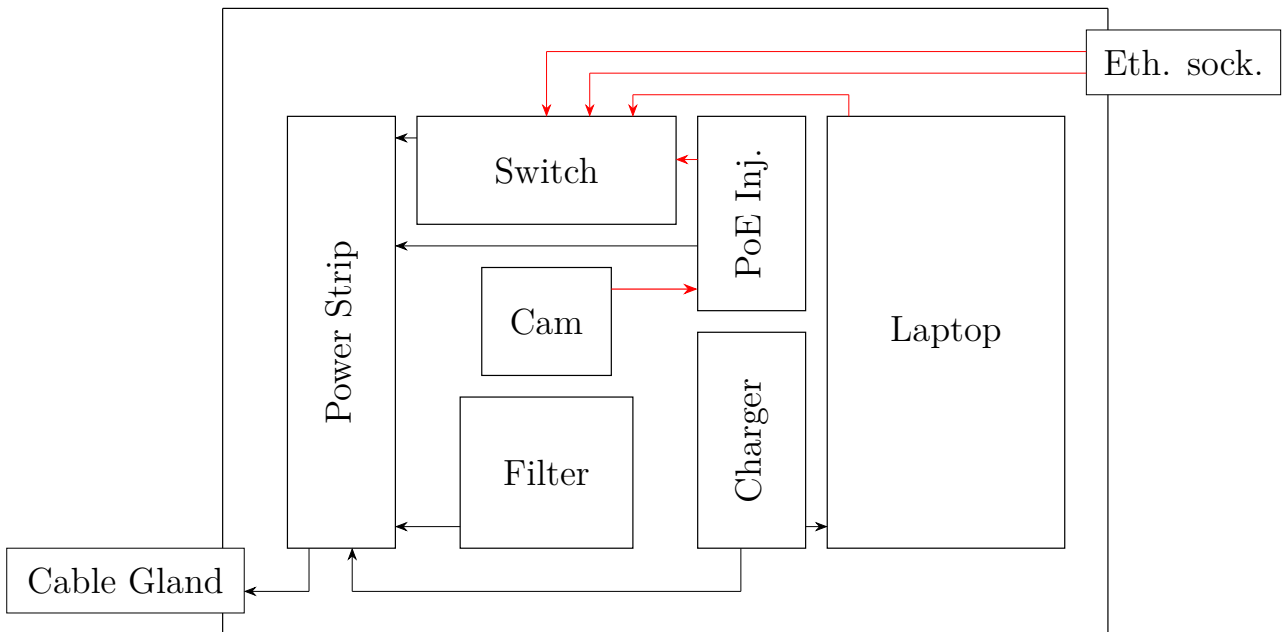


Figure 3.11: Final diagram of the proposed AllSkyCam4OLEODL system. Ethernet cables in red, power cables in black.

3.4 Controlling Software

We developed software capable of managing the camera operations and processing the images to obtain the required measurements. We will briefly explain the functionality of the code, rather than its construction, as detailed documentation has been written for that purpose [99]. The source code is included both in the documentation and in Appendix A.

Python was chosen as the programming language because the Application Programming Interface (API) is available only in C or Python [100], with Python being faster for creating an initial iteration of the software. In the future, the software could be ported to C if performance becomes a critical factor, but the image processing would be challenging.

The program installation files and process can be found in the GitHub repository [101]. Both Git and Python (version 3.7.4 or higher) need to be previously installed.

1. Install the PyPI package:

```
1 pip install allskycam4oleodl
```

2. Clone the AllSkyCam4OLEODL Git repository:

```
1 git clone https://github.com/Ikerald/AllSkyCam4OLEODL.git
```

3. Navigate to the AllSkyCam4OLEODL directory:

```
1 cd AllSkyCam4OLEODL/
```

4. Manually install the VmbPy API:

```
1 pip install './data/vmbpy-1.0.4-py3-none-any.whl [numpy,opencv]'
```

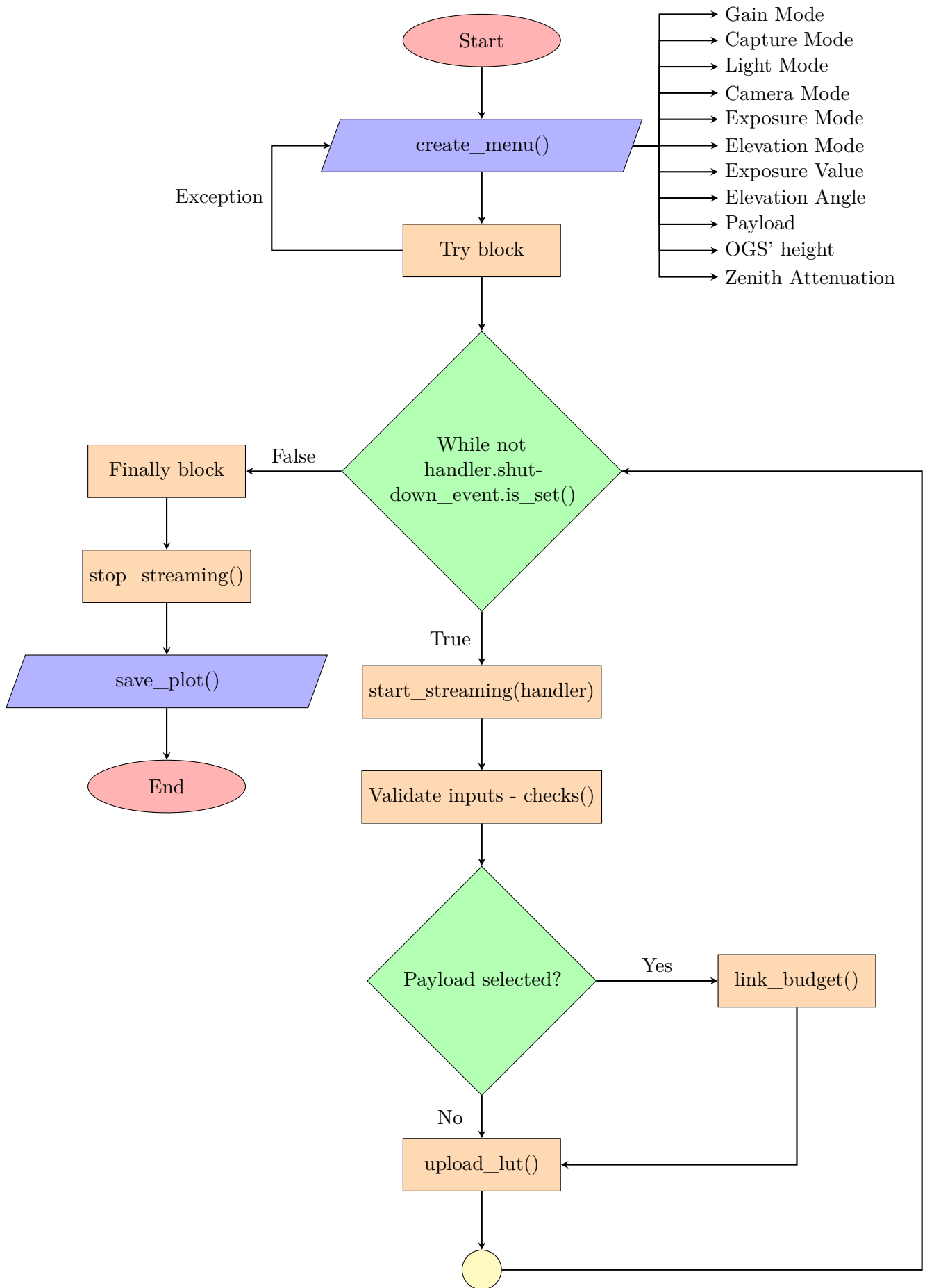
5. Execute the program:

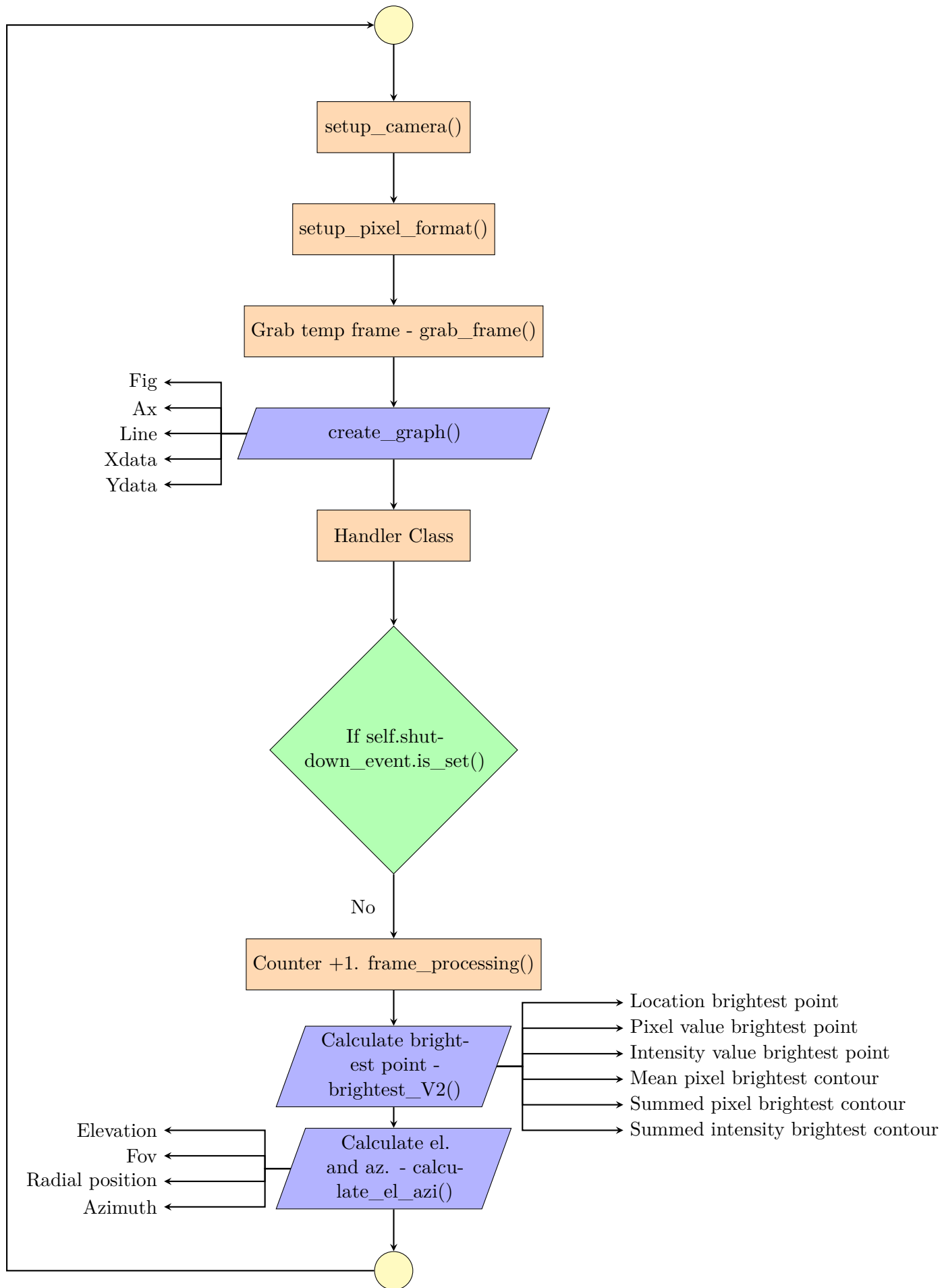
```
1 python main.py
```

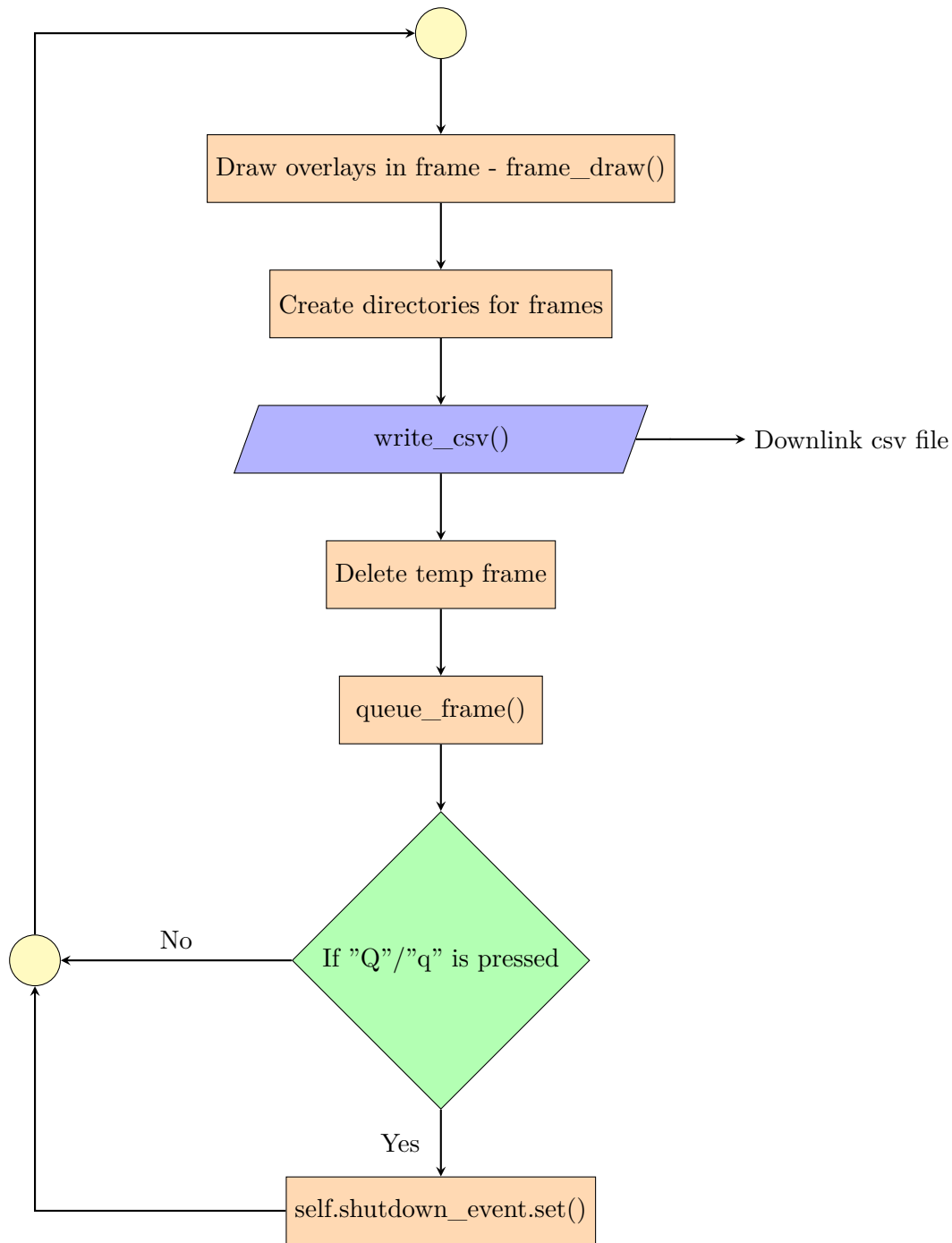
The program is executed from the *main.py* file, which imports all necessary functions from the AllSkyCam4OLEODL package. This package consists of seven different scripts:

- *api.py*: Manages the API for camera control.
- *constants.py*: Stores all necessary constant values.
- *gui.py*: Handles the Graphical User Interface (GUI).
- *image_processing.py*: Processes the frames.
- *input_checks.py*: Grabs and validates input values.
- *link_budget.py*: Calculates and prints the link budget.
- *printer.py*: Prints the preambles.

The program operates as indicated in the following flow chart. This is a simplified diagram, as to accurately represent every aspect of the code, we would need an individual diagram for each function.







3.4.1 Vmbpy Application Programming Interface

The Allied Vision’s python API, Vmbpy [102], gives us control over most of the camera’s settings directly from the code, allowing us to expand its functionalities.

One of the most important functions is `setup_camera()` in `api.py`. This function allows us to configure the exposure mode, which can be set either in manual or automatic, and the gain mode, which is chosen between gain 0 (0 dB), or gain 1 (18 dB)—the latter is preferred, as it enhances the visibility of the satellite. In `setup_pixel_format()` the pixel format is set to 8-bit. Although our camera is a 14-bit camera, this format is incompatible with the main processing tools like OpenCV or Pillow, forcing us to use the inferior mode.

The `upload_lut()` function is responsible for uploading the Look-Up Table (LUT) to the camera according to the selected mode. The goal is to correct the slight non-linearity in the camera output, as can be seen in Fig. 3.12, 3.13 and 3.14.

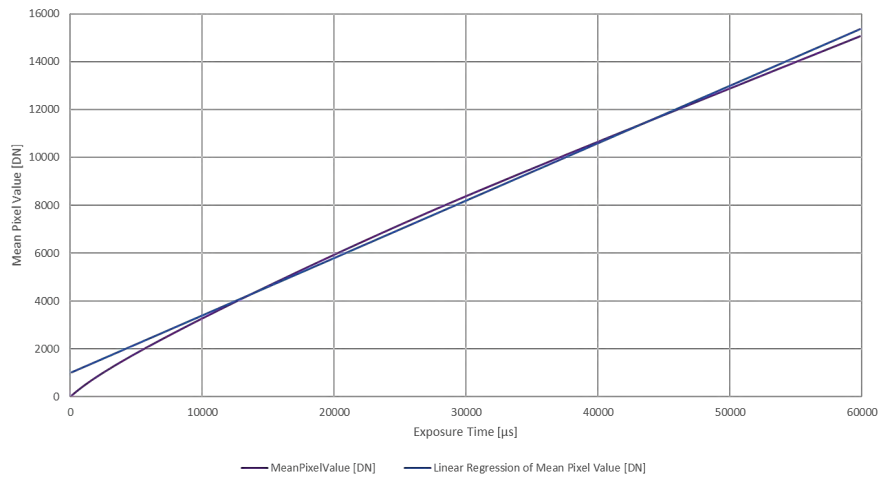


Figure 3.12: Mean pixel value of the camera with no LUT uploaded. Figure taken from [103]

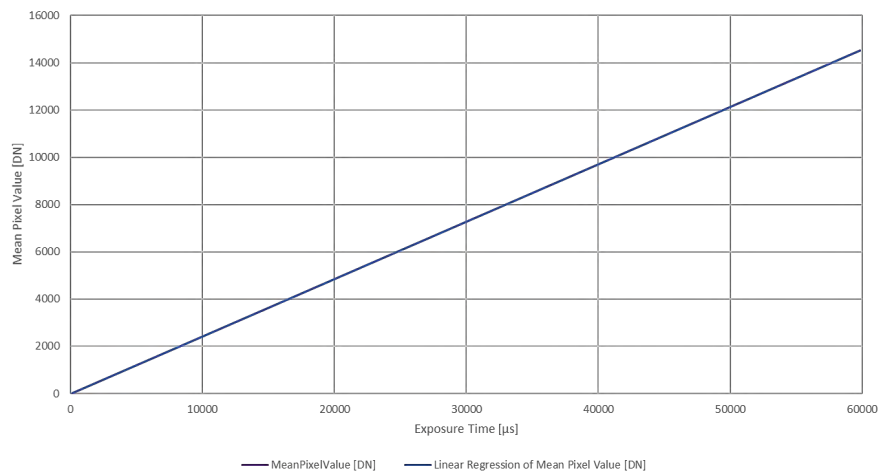


Figure 3.13: Mean pixel value of camera with LUT uploaded. Figure taken from [103]

Camera	Gain	Linearity Error LE [%]
G-008	Gain0	3.74
	Gain1	0.17

Figure 3.14: Percentage of linearity error of both modes. Figure taken from [103]

3.4.2 Image Processing

The main goal of the software is to process all captured images in real time and tracking the satellite while assessing its intensity, elevation and azimuth angle. This posed a challenge, as we had to balance what we wanted to do with the computational resources needed to do so.

The process goes as follows: first, the taken frame from the camera is duplicated. If we want to assess the intensity based on the pixel values of the image, the original must remain unaltered, or the values will change. Depending on the selected camera mode, different processing algorithms are applied.

- Hot-pixel removal:

We captured a set of images with exposure times ranging from 20000 μs to 300000 μs with the lid on (lower exposure times were not considered, as hot pixels are not present at those levels). These images, which feature only the hot pixels of the camera, are stored in the following directory:

We do not need to process anything as the camera handles it all. However, the problem with the exposure times remains, besides the intensity values are now more difficult to obtain, as we do not know the subtracted value.

- Normal operation:

Nothing is removed from the frame under normal operation. We recommend using both this method and the hot-pixel removal technique, as they are the most consistent. While background subtraction is useful in specific scenarios, the normal mode is expected to be used most of the time.

Now that the camera mode has been selected, the next step is tracking the satellite. We chose to avoid inputting the satellite orbit information because we wanted to be able to track any satellite without prior knowledge, discarding local thresholding. Therefore, the most effective approach was to track the brightest point in the image, filtering by minimum and maximum spot size.

We developed two different modes based on lightning conditions. The daytime mode involves applying a bilateral filter followed by an Otsu's thresholding. Bilateral filtering smooths images while preserving their edges as each pixel is replaced by a weighted average of its neighbours. The weighting is dictated by a spatial component that penalizes distant pixels and a range component that penalizes pixels with a different intensity. This combination ensures that only nearby similar pixels contribute to the result. This method is ideal for our application, as we will apply contour detection, where maintaining the edges around the satellite is crucial for distinguishing it from the rest of the image.

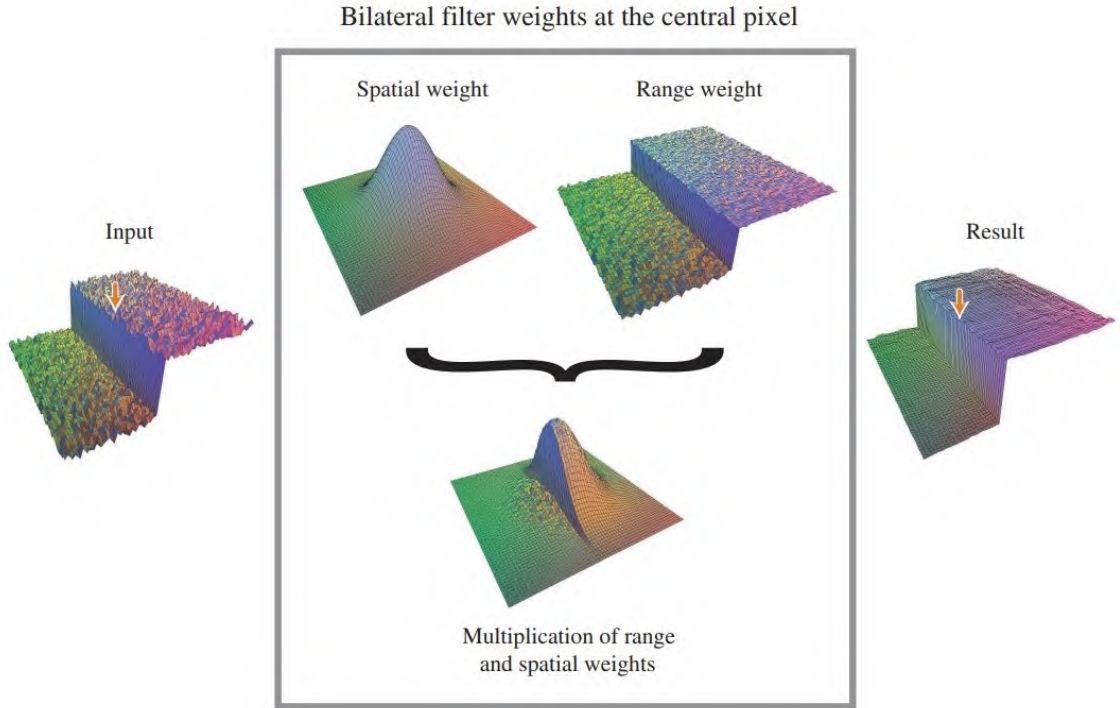


Figure 3.16: Bilateral filter weights. Figure taken from [104], reproduced from [105]

The key idea of the bilateral filter is that for a pixel to influence another pixel, it should not only occupy a nearby location but also have a similar value. Denoted by $BF[\cdot]$, the bilateral filter is defined by equation (3.4) [105]:

$$BF[I]_{\mathbf{p}} = \frac{1}{W_{\mathbf{p}}} \sum_{\mathbf{q} \in S} G_{\sigma_s}(\|\mathbf{p} - \mathbf{q}\|) G_{\sigma_r}(|I_{\mathbf{p}} - I_{\mathbf{q}}|) I_{\mathbf{q}} \quad (3.4)$$

Here, $G_{\sigma_s}(\|\mathbf{p} - \mathbf{q}\|)$ represents the spatial weight, a Gaussian function that decreases the influence of distant pixels. $G_{\sigma_r}(|I_{\mathbf{p}} - I_{\mathbf{q}}|)$ represents the range weight, a Gaussian function that reduces the influence of pixels \mathbf{q} when their intensity values differ from $I_{\mathbf{p}}$. $W_{\mathbf{p}}$ represents the normalization factor, ensuring pixel weights sum to 1:

$$W_{\mathbf{p}} = \sum_{\mathbf{q} \in S} G_{\sigma_s}(\|\mathbf{p} - \mathbf{q}\|) G_{\sigma_r}(|I_{\mathbf{p}} - I_{\mathbf{q}}|) \quad (3.5)$$

Fig. 3.16 shows how the weights are computed for a pixel near an edge. Fig. 3.17 compares different proposed blurring techniques, with the bilateral filter configured with a diameter of pixel neighborhood of 3 and a σ value of 200 for both the color and coordinate space, performing the best.

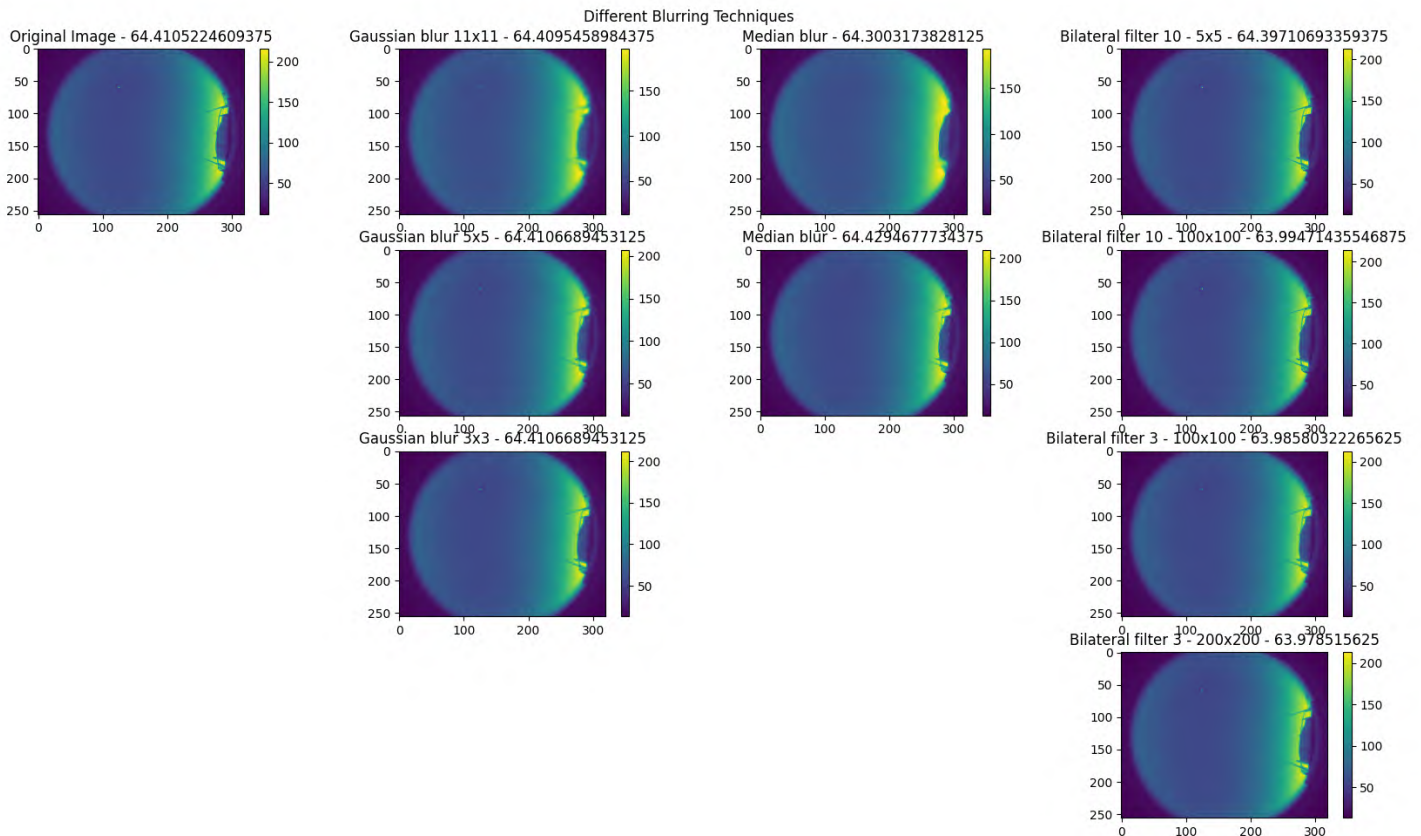


Figure 3.17: Different blurring techniques.

The Otsu’s thresholding method, also known as the Otsu’s method, was the solution for the changing exposure. When exposure times vary, the mean pixel values also change, which makes standard thresholding techniques unreliable, as they may segment the satellite. We first thought of an adaptive thresholding technique; however, as shown in Fig. 3.18, their performance was suboptimal. The Otsu’s method automatically determines the threshold that separates pixels into two classes—foreground and background—as explained in [106].

Fig. 3.18 demonstrates that only the Otsu’s thresholding method correctly localizes the satellite under daylight conditions. Fig. 3.19 illustrates the effectiveness of combining the Otsu’s thresholding with the previously discussed filters. We apply a filter prior to thresholding because, as shown in the lower left image of Fig. 3.19, using Otsu’s thresholding by itself results in the removal of pixels with lower values that are still illuminated by the satellite. By blurring, we average those pixels with the ones with higher values, capturing the full area of the satellite in the image. Among all the filters tested, the bilateral 3 200 × 200 performs best.

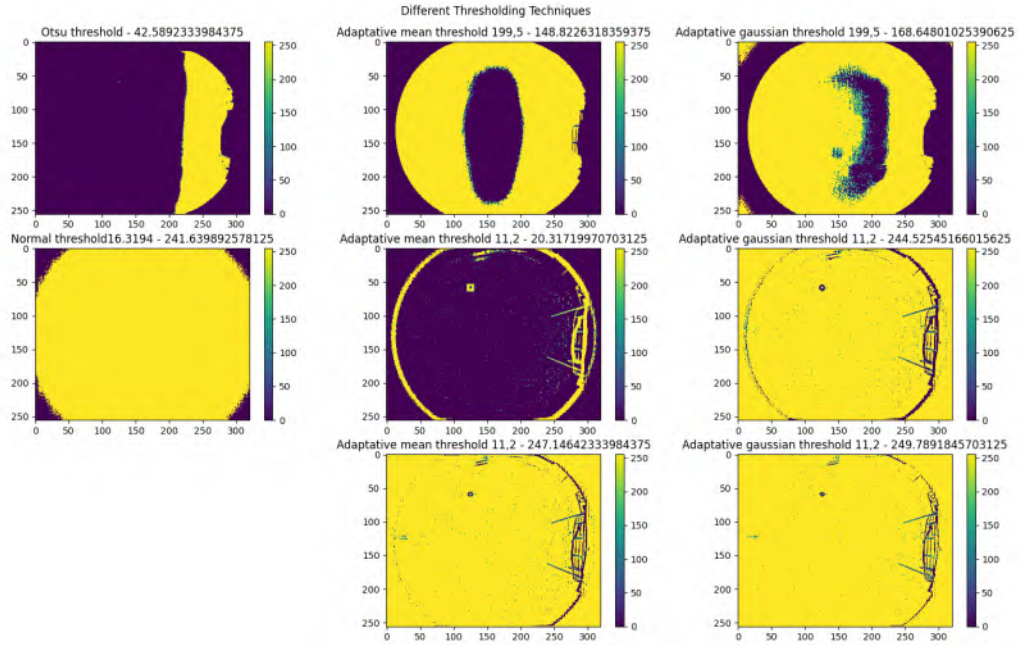


Figure 3.18: Different blurring techniques.

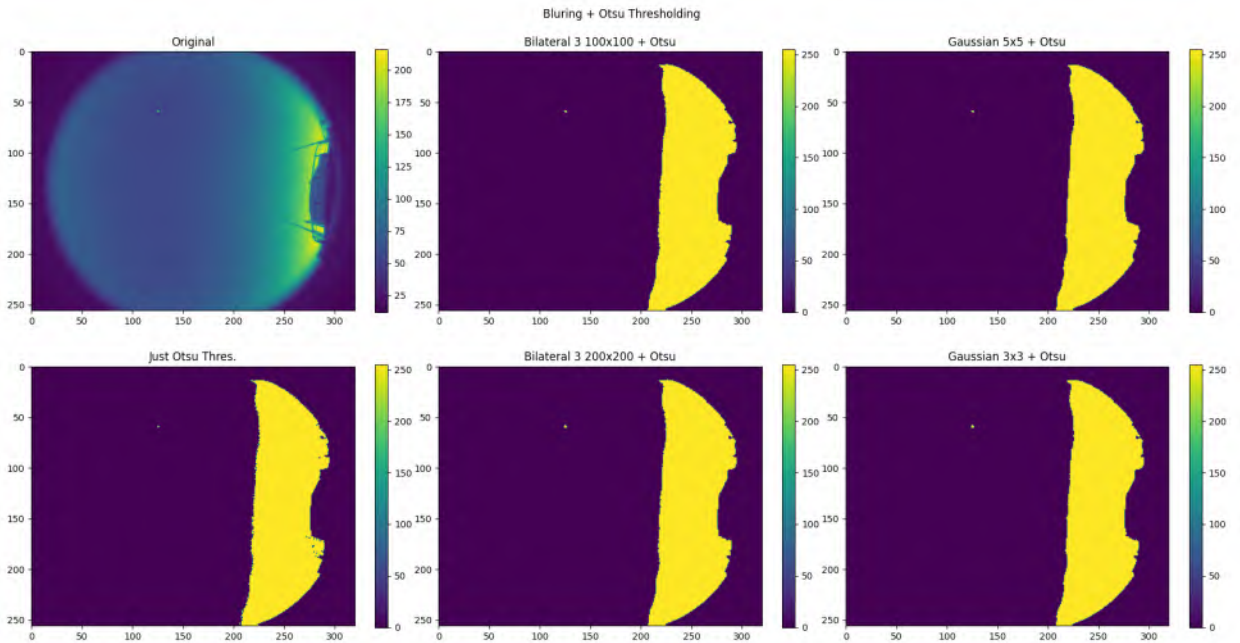


Figure 3.19: Otsu thresholding plus different blurring techniques.

After applying the appropriate threshold, we will obtain the contours of the mask, as shown in Fig. 3.20. These contours will then be filtered by the selected maximum and minimum spot size, based on equations (3.6) and (3.7): obtaining the contour with the maximum total pixel value, as illustrated in Fig. 3.21:

$$\text{height of contour} \times \text{width of the contour} \geq \text{minimum spot size value} \quad (3.6)$$

$$\text{height of contour} \times \text{width of the contour} \leq \text{maximum spot size value} \quad (3.7)$$

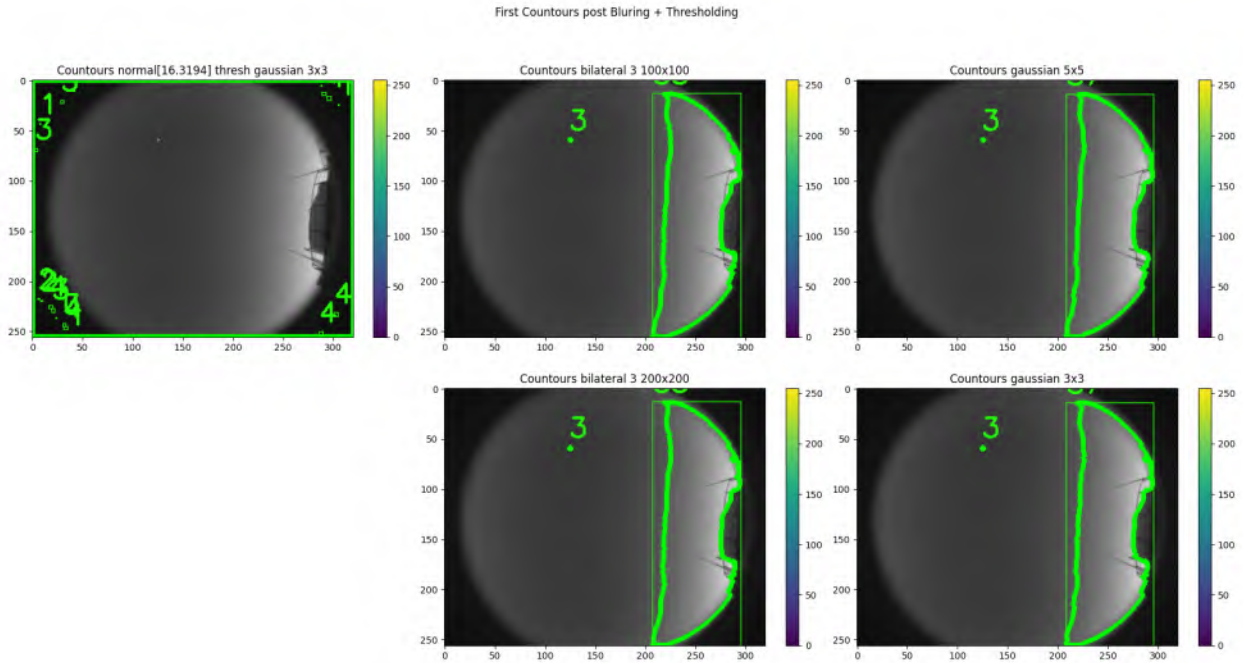


Figure 3.20: Contours of the image obtained by different techniques.

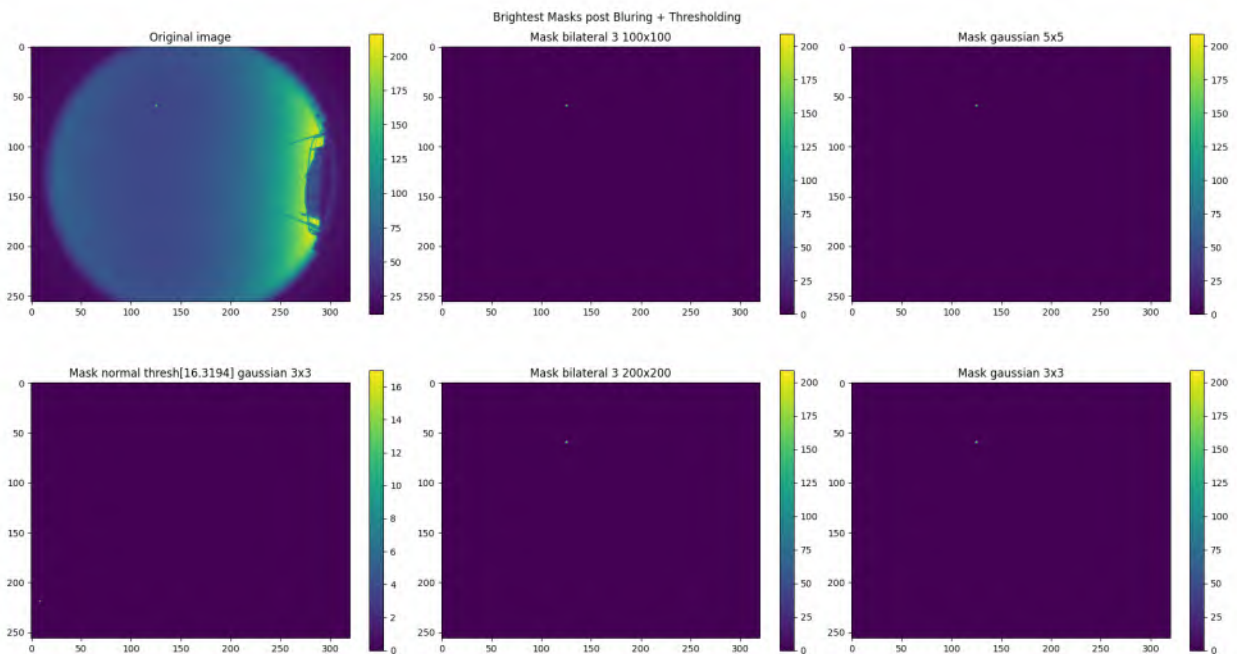


Figure 3.21: Brightest contour of the image by different techniques filtered by spot size value.

From the mask, we extract the location of the brightest contour, which is then overlaid onto the original image, as illustrated in Fig. 3.22. We extract the final values applying this location to the original image: the value of the brightest pixel and the mean and summed pixel value of the entire brightest contour. All these values along with the current date and time, exposure value, minimum and maximum spot size, elevation, azimuth, and the cardinal coordinates, will be overlaid onto the original image.”

The process of obtaining the intensity values involves applying a correction factor, the selection

of which will be explained in subsection 3.5.4.

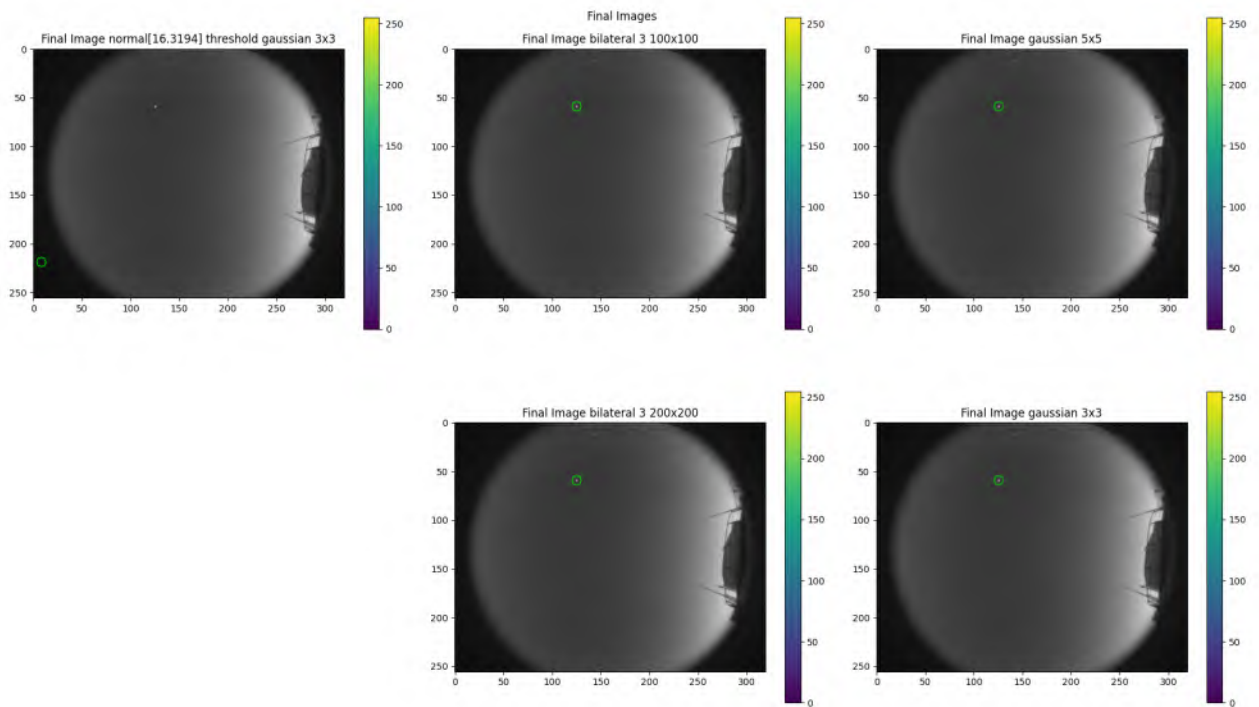


Figure 3.22: Final brightest point of the image by different techniques filtered by spot size value.

When using the night-time mode, the procedure remains same as in daytime, with two differences: the bilateral filter is replaced by a Gaussian 3×3 filter, and the Otsu's thresholding method is substituted with a binary threshold determined by the background noise curve of the camera. At night-time, the mean pixel value is lower, therefore the difference with the satellite is higher, which allows us to threshold the image based on the camera's background noise. To obtain the noise curve, we captured frames with exposure times ranging from $10 \mu s$ to $256000 \mu s$, as illustrated in Fig. 3.23

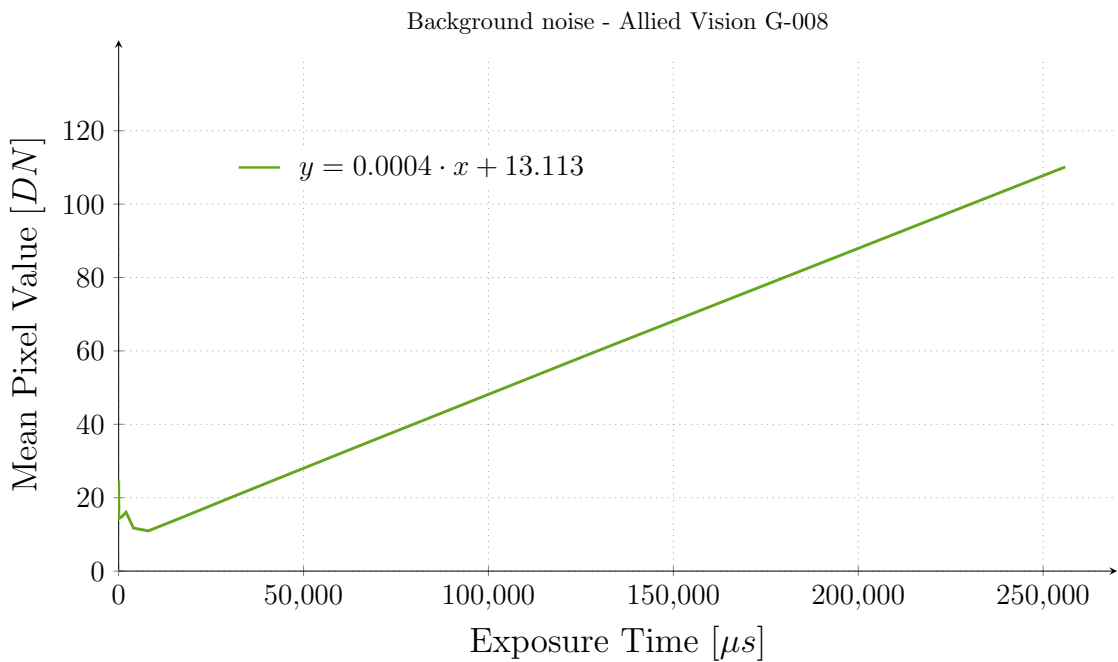


Figure 3.23: Camera's background noise curve of gain1 mode.

Both processed and unprocessed frames will be saved in the following directory with an specific name depending on the date, time, exposure mode and time, camera mode, gain mode and payload:

1 AllSkyCam40LEODL/data/tracking_images

A CSV file containing all the relevant parameters will be saved in the same directory as the processed frames. This file is crucial, as it all the values necessary to assess the performance of the link. The Intensity received - expected [dB] parameter will indicate us how far were we from the estimated value from the link budget:

- Frame Number
- Gain Mode
- Time [CEST]
- Exposure [μs]
- Location [x, y]
- Elevation [°]
- Azimuth [°]
- FOV
- R
- Brightest Pixel Value [DN]
- Intensity Brightest Pixel [$\mu W/m^2$]
- Mean Pixel Value of the Frame [DN]
- Summed Brightest Contour Pixel Value [DN]
- Summed Brightest Contour Intensity [$\mu W/m^2$]
- Payload
- Payload Intensity [$\mu W/m^2$]
- Intensity received - expected [$\mu W/m^2$]
- Intensity received - expected [dB]

A graph of the entire recording is also saved in the same directory as the recorded frames. An example of the graph is provided in Fig. 3.24.

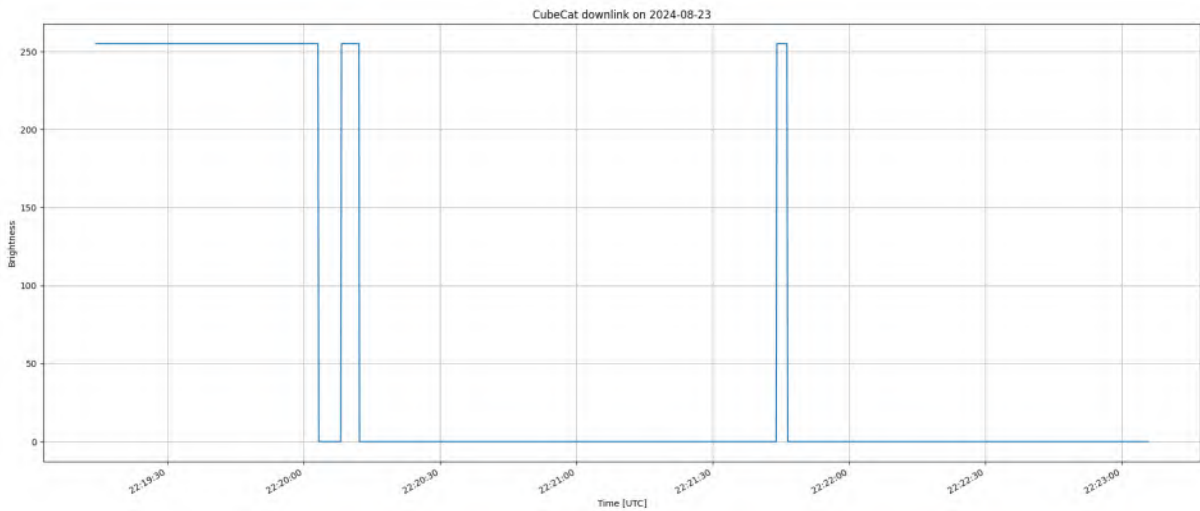


Figure 3.24: Graph of a failed CubeCat downlink.

The y-axis represents the pixel value from the camera, as the intensity is not yet properly calibrated; once calibrated, intensity will be the variable used. The title of the graph is automatically generated based on the payload and current date.

3.4.3 Elevation and Azimuth

Elevation and azimuth are angular measurements to identify the position of a satellite relative to an observer location. Measured both in degrees, they start from 0 degrees: azimuth starts from the north

and covers 360 degrees clockwise, being 90° east, 180° south and 270° east; elevation goes from horizon (0°) until zenith at 90°. To accurately calculate these angles, it is necessary to know the focal length of the lens, its mapping projection and the center coordinates of the capture image.

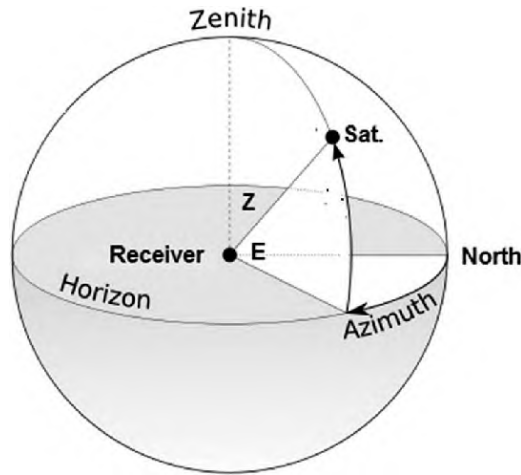


Figure 3.25: Diagram of the elevation and azimuth of an object. Figure taken from [107]

In this work, we use wide angle or fisheye lenses, this type of lenses provide a very wide FOV by distorting the image. This distortion is achieved through an specific mapping function, referred as a projection. There are several projection as illustrated in Fig. 3.26, but we will focus in the most used, the equisolid projection.

projection	math
equidistant fisheye	$R = f \cdot \theta$
stereographic	$R = 2f \cdot \tan\left(\frac{\theta}{2}\right)$
orthographic	$R = f \cdot \sin(\theta)$
equisolid (equal-area fisheye)	$R = 2f \cdot \sin\left(\frac{\theta}{2}\right)$
Thoby fisheye	$R = k_1 \cdot f \cdot \sin(k_2 \cdot \theta)$ with $k_1 = 1.47$ and $k_2 = 0.713$
PTGui 11 fisheye	$R = \begin{cases} \frac{f}{k} \cdot \tan(k \cdot \theta) & \text{for } 0 < k \leq 1 \\ f \cdot \theta & \text{for } k = 0 \\ \frac{f}{k} \cdot \sin(k \cdot \theta) & \text{for } -1 \leq k < 0 \end{cases}$

Figure 3.26: Different types of fish-eye lens mapping functions. Figure taken from [108]

Let θ represent the angle in radians between a point in the real world and the real axis, f denotes the focal length of the lens, and R is the radial distance in the image (the distance from the center to an specific point). In a circular lens, θ can be interpreted as the field of view of the lens. For any point within a given frame, all points at the same radius with respect of the center will share the same

θ . Thus, θ can be considered as the FOV that allows observation of that specific circle, defined by equation (3.8).

$$\theta = 2 \arcsin \left(\frac{R \cdot P_{size}}{2f} \right) \quad (3.8)$$

Where P_{size} is the pixel size in $mm/pixel$ and the radial distance R is calculated as $R = \sqrt{(x - x_c)^2 + (y - y_c)^2}$ [pixels].

Our final field of view and elevation angle will be defined by equations (3.9) and (3.10), respectively.

$$\theta_{deg} = 2\theta \cdot \left(\frac{180}{\pi} \right) \quad (3.9)$$

$$elevation = \frac{(180 - \theta_{deg})}{2} \quad (3.10)$$

To calculate the azimuth angle, we will define θ as the angle measured in the clockwise direction from the origin of the north line A , to the object B , as illustrated in Fig. 3.27.

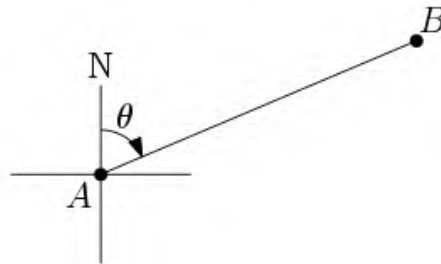


Figure 3.27: Azimuth diagram of an object. [109]

Then the coordinates of point B can be described by equation (3.11):

$$(b_1, b_2) = (a_1 + r \sin \theta, a_2 + r \cos \theta) \quad (3.11)$$

Where r is the length of the line segment AB . θ is therefore defined by equation (3.12):

$$\theta = \arctan \left(\frac{b_1 - a_1}{b_2 - a_2} \right) \quad (3.12)$$

The frame is divided into three quadrants: one for the bottom section of the image and two dividing the upper section in half. It is important to note that the origin is at the upper left corner of the image. Additionally, the images captured by the camera are mirrored, the left side of the image corresponds to the west side, and vice versa. This is clearly illustrated in Fig. 3.28.

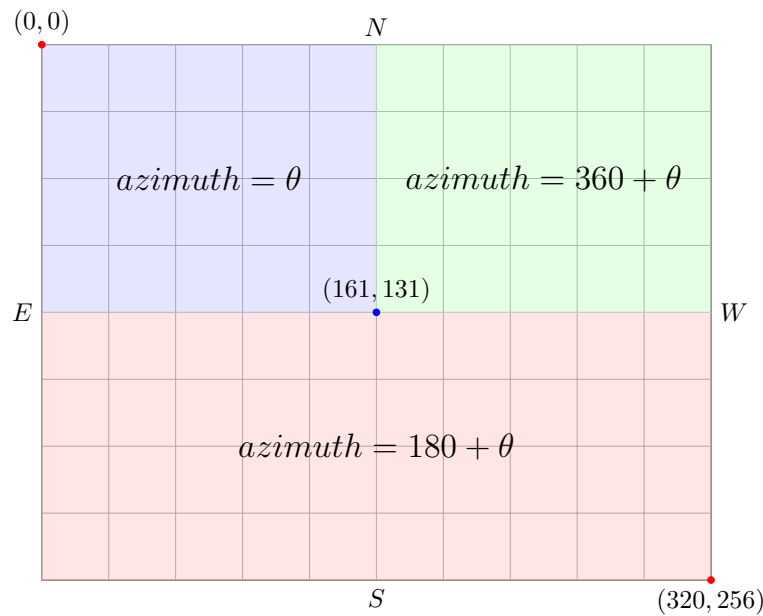


Figure 3.28: Diagram of the calculation of the azimuth for the different quadrants of a picture.

3.4.4 Graphical User Interface

When executed, the program displays a Graphical User Interface (GUI) menu, allowing the user to choose the settings for both the camera and link budget. The camera settings include the gain mode, capture mode, lightning mode, camera mode, exposure mode and exposure time. For the link budget, the user can adjust the payload, the height of the Optical Ground Station (OGS), the zenith attenuation, the elevation mode and the elevation angle.

When capturing is initiated, three new windows appear on screen. The one on the bottom right is tasked with controlling the exposure time, and the minimum and maximum spot size value—the sliders use a logarithmic scale, making it easier to select lower values. The window on the bottom left, displays a live graph, similar to the one shown in Fig. 3.24, which plots time against the mean pixel value in real-time. The final window on the top left, shows both the processed and unprocessed frames from the camera. An image of an actual operation of the system is displayed in Fig. 3.29.

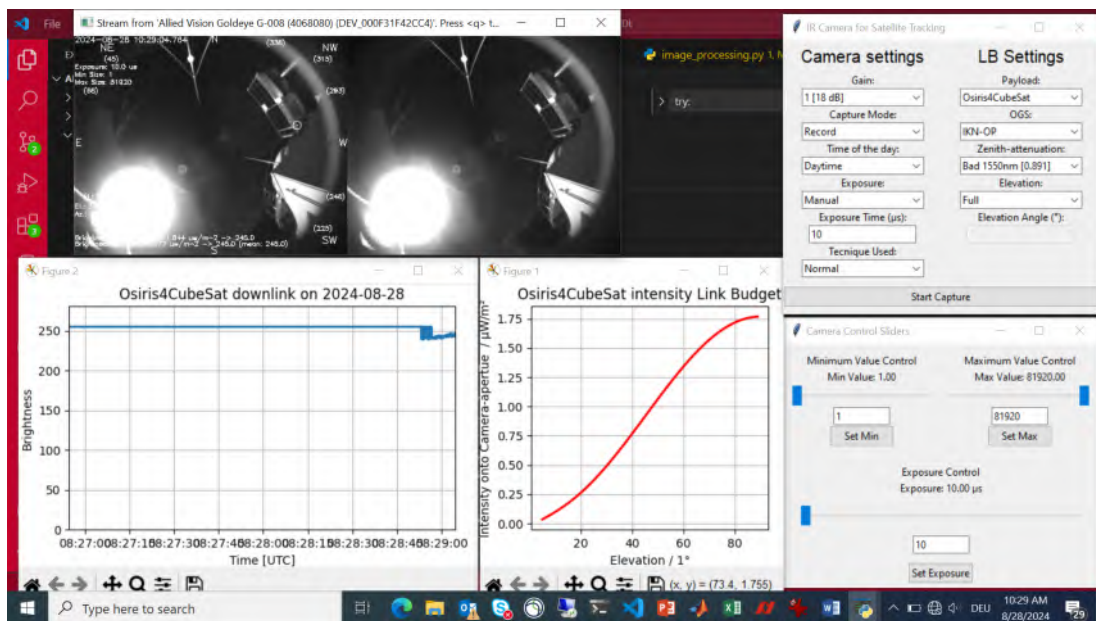


Figure 3.29: Real time system operation.

3.5 Testing

In this section we will go over all the executed tests to ensure that we meet all the necessary requirements of the final system.

3.5.1 Calculation of the Link Budget for the Observed Satellites

The first challenge we faced was the complexity of the satellite's visibility. We required an intensity value to determine whether the camera could detect satellite. We chose the OSIRISv1 onboard Flying Laptop (FLP), described in subsection 2.5.1, because it is one of the dimmest satellites that we will test with the AllSky camera system.

Using the procedure outlined in subsection 2.4.5, we will perform the link budget analysis for the laser terminal. Since we are using a camera, few exceptions need to be considered: The optical losses inside the receiver terminal, a_{Rx} , are disregarded as we want to measure the intensity before it goes through the camera; beam wander losses, or the average loss due to dynamic beam miss-pointing, a_{BW} are also ignored, as our camera is able to see the whole hemisphere, ensuring that the satellite will be within the field of view of the receiver, regardless of pointing accuracy; finally, scintillation losses a_{Sci} will be negligible. As explained in subsection 2.4.4, using a long exposure time (around 100000 μs) will average the scintillation index over time.

For our calculations, we will use 15° as the minimum elevation angle visible:

Table 3.3: Link Budget from the observed satellites.

Parameter (formula)	OSIRISv1 on Flying Laptop [64]: <i>595km polar orbit, 1.0 mrad FWHM Tx-div., 1W Tx-power of $\lambda = 1545$ nm into the 2.5mm \varnothing effective aperture of the InGaAs on the IKN</i>		OSIRIS4CubeSat on CubeL [80]: <i>560km polar orbit, 120 μrad FWHM Tx-div., 85mW Tx-power of $\lambda = 1550$ nm into the 2.5mm \varnothing effective aperture of the InGaAs on the IKN</i>		CubeCat on NORSAT-TD: <i>455km polar orbit, 104 μrad FWHM Tx-div., 300mW Tx-power of $\lambda = 1545$ nm into the 2.5mm \varnothing effective aperture of the InGaAs on the IKN</i>	
	15° elevation	zenith	15° elevation	zenith	15° elevation	zenith
Mean source power p_{Tx}	+30 dBm	+30 dBm	+19.29 dBm	+19.29 dBm	+24.77 dBm	+24.77 dBm
Tx internal losses a_{Tx}	-1 dB	-1 dB	NA	NA	NA	NA
Tx antenna gain g_{Tx} (2.13)	+70.4 dB	+70.4 dB	+88.9 dB	+88.9 dB	+90.1 dB	+90.1 dB
Pointing loss a_{BW} (2.14)	NA	NA	NA	NA	NA	NA
Distance L (2.16)	1613 km	594 km	1538 km	559 km	1303 km	454 km
Freespace loss a_{FSL} (2.15)	-262.4 dB	-253.7 dB	-261.9 dB	-253.1 dB	-260.5 dB	-251.4 dB
Atmos. attenuation a_{Atm} (2.17)	-1.94 dB	-0.50 dB	-1.94 dB	-0.50 dB	-1.94 dB	-0.50 dB
Scintillation loss a_{Sci}	NA	NA	NA	NA	NA	NA
Rx antenna gain g_{Rx} (2.19)	+74.1 dB	+74.1 dB	+74.1 dB	+74.1 dB	+74.1 dB	+74.1 dB
Power into camera's aperture p_{Rx}	-90.7 dBm	-80.6 dBm	-81.6 dBm	-71.4 dBm	-73.4 dBm	-62.9 dBm
Rx-internal losses and signal splitting for tracking a_{Rx}	NA	NA	NA	NA	NA	NA
Intensity into camera's aperture	0.1723 $\mu W/m^2$	1.7679 $\mu W/m^2$	1.407 $\mu W/m^2$	14.819 $\mu W/m^2$	9.228 $\mu W/m^2$	105.64 $\mu W/m^2$
Link margin for communication	-31.7 dB	-21.6 dB	-22.6 dB	-12.4 dB	-14.4 dB	-3.8 dB

To obtain the Intensity into the camera's aperture [W/m^2], we transformed the Power into camera's aperture p_{Rx} (in dBm) and divided the resulting value by the effective area of the camera's aperture as shown in equation (3.13):

$$\frac{10^{\frac{p_{Rx}}{10}} \cdot 10^{-3}}{area_{Rx}} \quad (3.13)$$

Where the effective area of the camera $area_{rx}$ is given by the area of a circle:

$$area_{Rx} = \pi \cdot \left(\frac{\varnothing_{ap}}{2}\right)^2 \quad (3.14)$$

Being \varnothing_{ap} the diameter of the effective aperture of the camera, $2.5 \cdot 10^{-3} m$, in our case.

The intensity requirements are strict—the link margin does not affect us, as we do not want to establish any communication. Our goal is to visualize the satellite and assess weather observed intensity is comparable to the value calculated under "Intensity into camera's aperture" in the link budget. After recording, we will calculate the difference in decibels at each elevation angle of the satellite.

3.5.2 Evaluation of the Lenses

As explained in subsection 3.2.2, the two major factors to consider for the lenses are the Field Of View (FOV) and transmittance at the desired wavelength of $1550 nm$. The transmittance is already suboptimal: it is below 45 % for the Fujinon lens at $1000 nm$, and around 60 % for the Thorlabs lens at $1400 nm$. The field of view values are better: the FE185C057HA-1 maintains its 185° FOV, as it is compatible with our $2/3''$ sensor; on the contrary, the MVL4WA is only compatible with sensors up to a $1/2''$ size (we should obtain around 140° FOV with a $2/3''$ sensor based on our calculations). The purchase of the Thorlabs MVL4WA was risky because using a lens not suitable for a certain sensor could lead to the presence of vignetting, unexpected distortions or even a reduction in the camera's field of view. We tested the lens to verify its correct functionality.

We took two pictures to estimate the field of view: one with the subject positioned at the center of the frame, and the other with the subject at the edge of the field of view, illustrated in Fig. 3.30. The used setup is shown in Fig. 3.31.

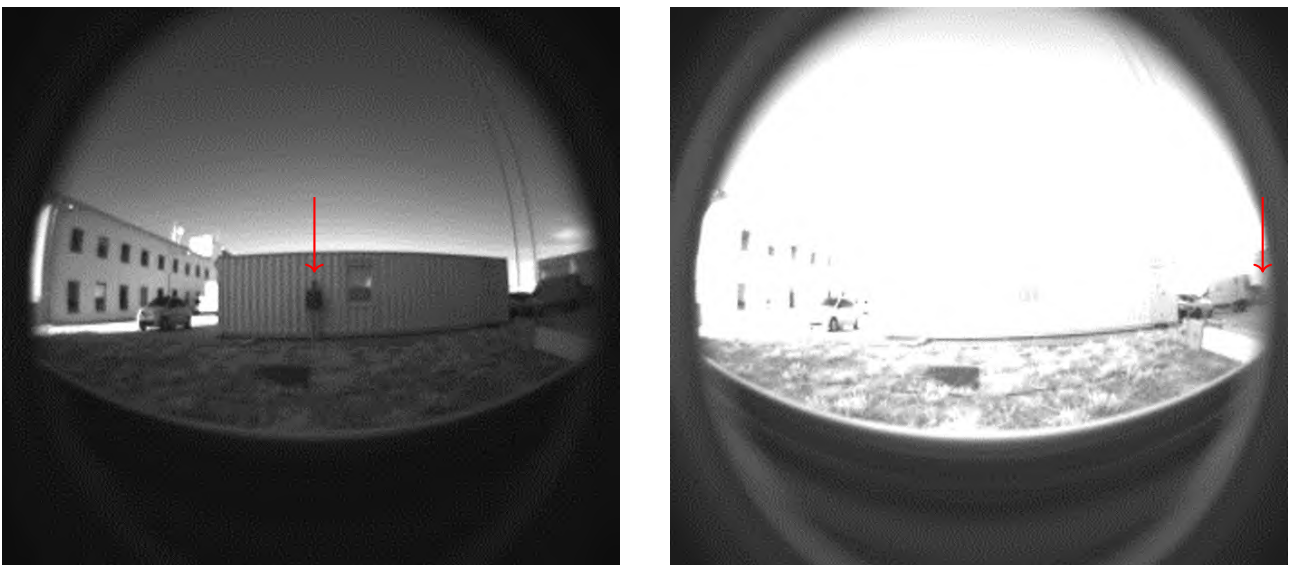


Figure 3.30: Subject in the middle of the frame. (left). Subject on the right edge of the frame. (right)

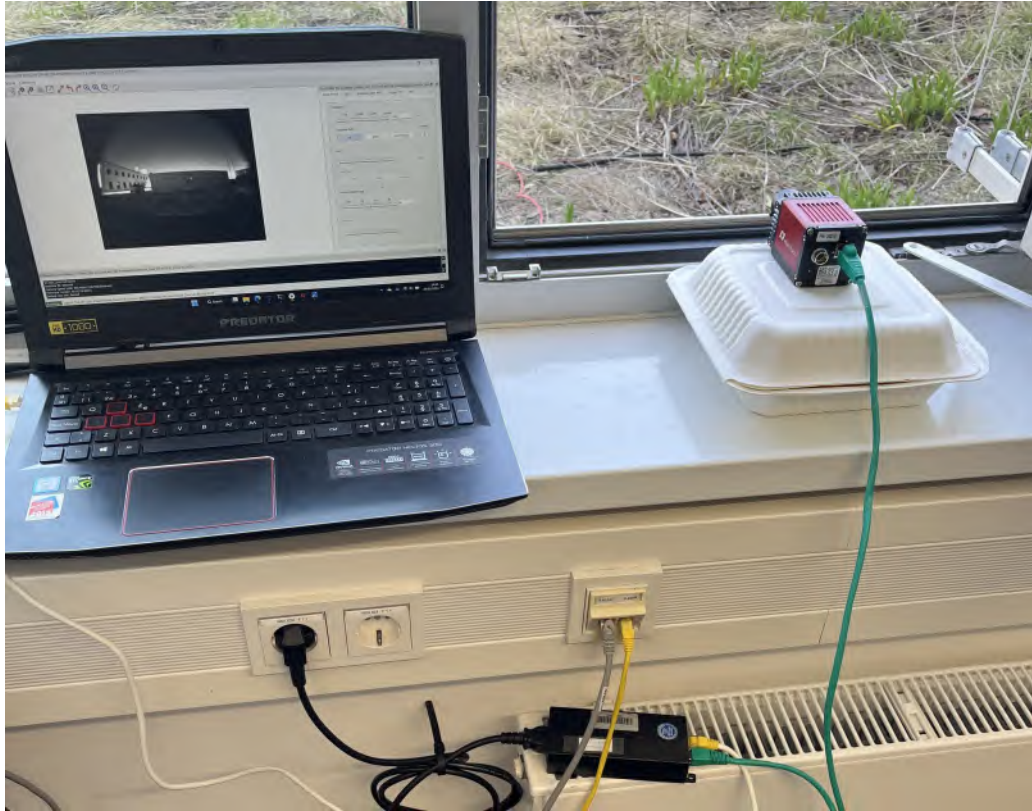


Figure 3.31: Setup of the first FOV experiment.

In the first image, the subject is positioned at 7.42 m from the camera, while in the second image, the subject is 19.32 m away from its initial position. Using basic trigonometry, the field of view of the lens can be calculated, as shown in equation (3.15):

$$FOV[^\circ] = \arctan \frac{19.32\text{m}}{7.42\text{m}} = 68.99^\circ \Rightarrow 137.98^\circ \quad (3.15)$$

To confirm these results, we used a Pan-Tilt-Unit (PTU). By selecting a reference point in the center of the frame and panning the PTU along the x-axis until the point reaches the edge of the frame, we precisely determine the camera's field of view, as illustrated in Fig. 3.32.



Figure 3.32: PTU pointing to 0° (left). PTU pointing to 70° (right).

Using the right edge of the sewer as a reference, as shown in Fig. 3.33, we confirm that the camera's

field of views approximately 140 degrees, as estimated.

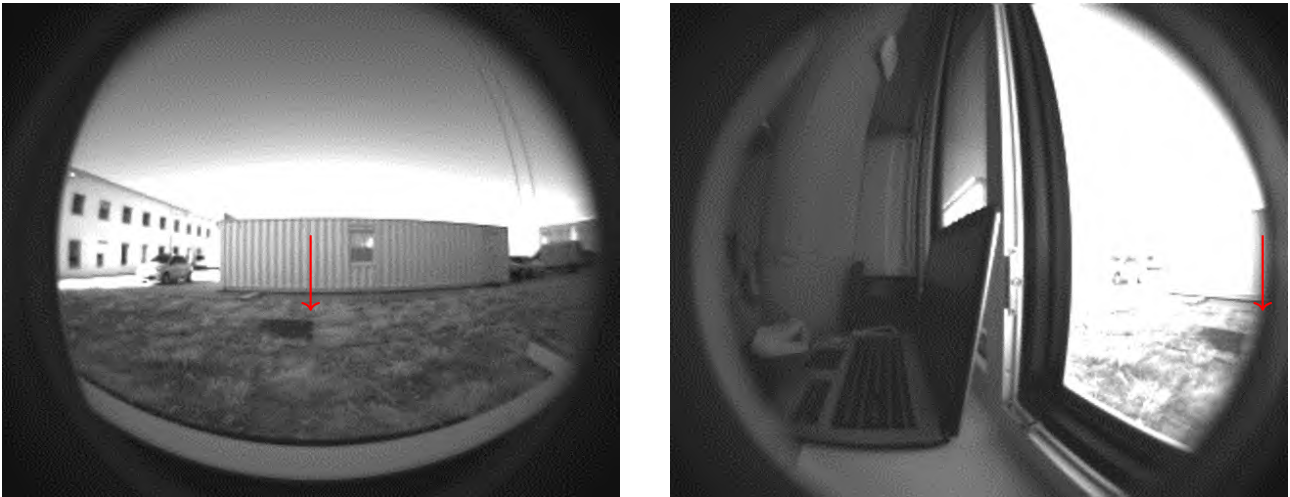


Figure 3.33: Reference point in the middle of the frame. (left). Reference point on the right edge of the frame. (right)

The primary issue with the Fujinon FE185C057HA-1, as noted in Table 3.2, is its fixed focus, which results in blurry images. This is a major drawback when attempting to evaluate laser intensity. We tried adjusting the focus using spacer rings, but it was unsuccessful as it was impossible to screw the lens in a consistent way. This led to instability and inconsistency in the focus, which rendered our results unreliable. Summed to the low transitivity of the lens made us disregard the Fujinon lens.

3.5.3 Intensity Measurement with a Coarse Wavelength Division Multiplexing Transceiver

After calculating the required minimum intensity and checking the correct functioning of the lens, we checked whether the system could detect Flying Laptop at 15-degrees of elevation, our worst-case scenario. We used a 1.6 mW Coarse Wavelength Division Multiplexing (CWDM) single-mode transceiver, centered at 1550 nm, connected to a Single Mode Fiber (SMF) patch, to simulate the laser signal. This approach provided an affordable and efficient method to validate the intensity received by the camera.

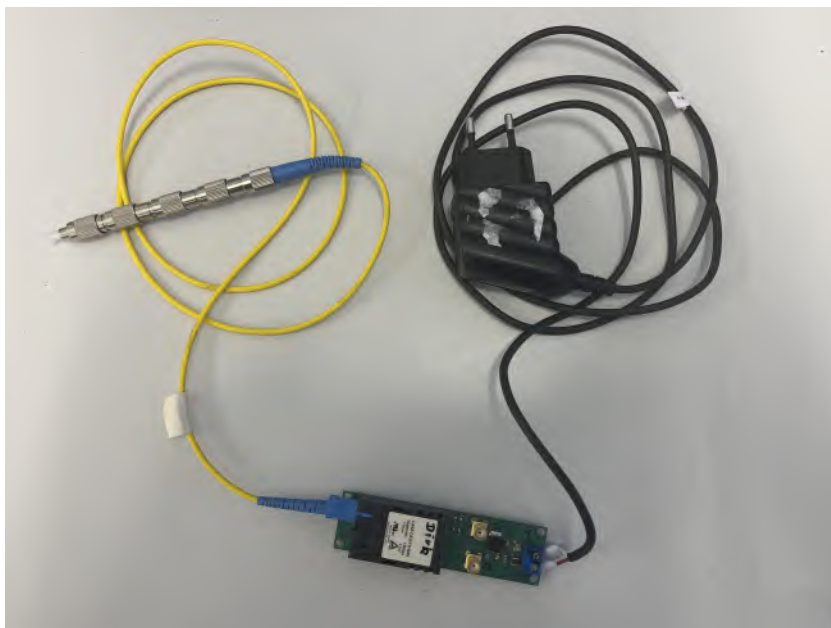


Figure 3.34: LS42-CAU-TC-N55 CWDM transceiver.

With the aforementioned transceiver, we only needed the Full Width Half Angle (FWHM) to assess the distance required to setup the laser away from the camera, so the axial intensity received replicates the one we would receive from flying laptop at 15° elevation angle.

$$I_0(L) = \frac{4 \ln 2}{\pi} \cdot \frac{P_0}{(L \cdot 1.18 \cdot \theta_{SM})^2} \quad (3.16)$$

The axial intensity does not account for atmospheric or pointing losses and assumes a Gaussian far-field beam pattern [64]. Our main unknown, θ_{SM} , is defined by equation (3.17):

$$\theta_{SM} = M^2 \frac{\lambda}{\pi w_0} \quad (3.17)$$

The divergence or acceptance angle θ_{SM} , is defined as the point with $1/e^2$ times the maximum intensity of a Gaussian beam. However, in telecommunications, the full width half angle is more commonly used. This full beam divergence angle is 1.18 times the half-angle divergence [110], as shown in equation (3.17).

The full width half angle is highly dependent on the fiber used—we connected the transmitter side of the transceiver to a SMF-28 fiber patch [111]. The beam quality factor, or M^2 parameter, is defined as the ratio of the beam's divergence to that of an ideal fundamental Gaussian beam. Since the fundamental Gaussian beam has the least divergence, real beam always follow $M^2 > 1$ (1.123 for the fundamental mode LP_{01} [112]). The beam waist w_0 , described in subsection 2.4.4, can be approximated to half of the Mode Field Diameter (MFD) for single-mode fibers, as the beam profile at the fiber output is identical to that within the fiber [113], [114].

$$w_0 = \frac{MFD}{2} \quad (3.18)$$

With all necessary parameters, we calculated the required distance using equation (3.19):

$$L = \sqrt{\frac{4 \ln 2 \cdot P_0}{\pi \cdot (1.18 \cdot \theta_{SM})^2 \cdot I_0(L)}} \quad (3.19)$$

Where:

- $\theta_{SM} = 1.12 \frac{1550 \cdot 10^{-9} \text{ m}}{\pi \frac{10.5 \cdot 10^{-6} \text{ m}}{2}} = 0.1137 \text{ rad}$
- $I_0(L) = 0.17232 \text{ } \mu\text{W}/\text{m}^2$
- $P_0 = 1.6 \text{ mW} = 1600 \text{ } \mu\text{W}$

The required distance for the test is $L = 674.71 \text{ m}$, an unachievable distance, as the test was intended to be conducted in the basement of the Institute of Communications and Navigation IKN. To address this, we used different attenuators to lower the power, and therefore the distance, as illustrated in Fig. 3.35.

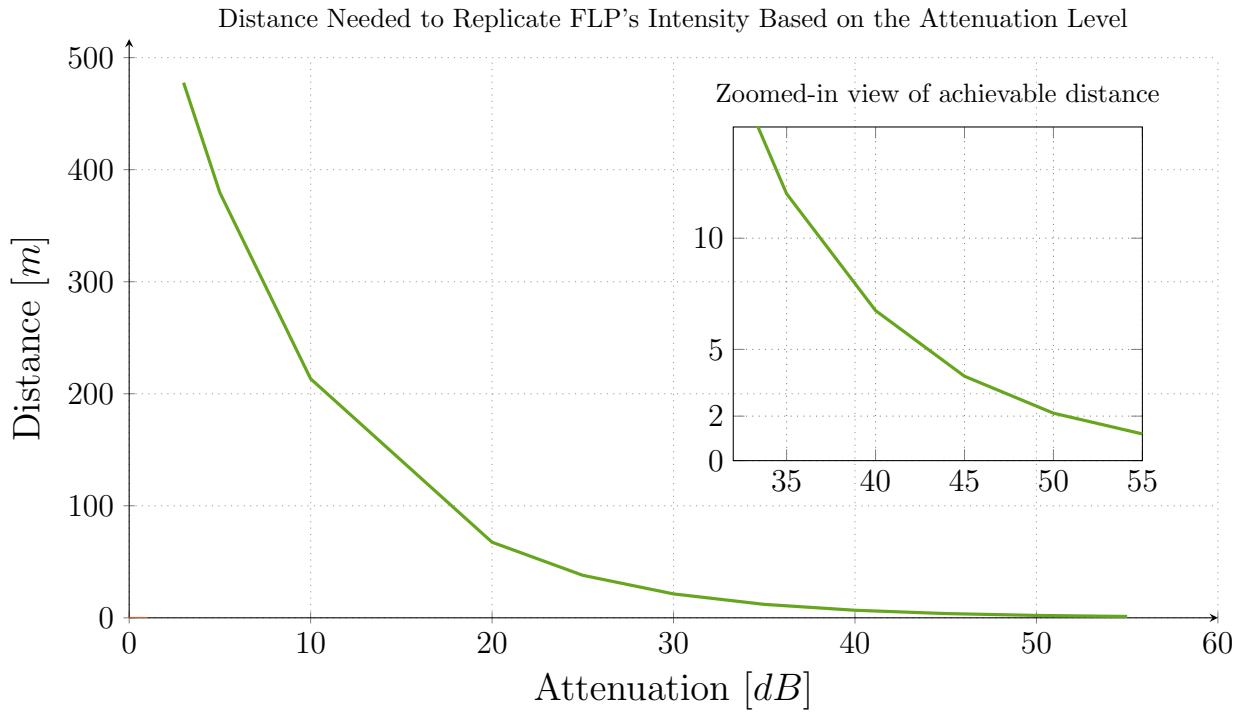


Figure 3.35: Attenuation for achievable distance.

The room used for the experiment has a length of 5 m, so we decided to use 50 dB of attenuation. The laser was positioned 2.65 meters away from the camera, farther than the 2.13 m required to achieve the target intensity. As seen in Fig 3.36, the transceiver was visible with the Thorlabs lens, meaning that the satellite would also be detectable. This was not the case with the Fujinon lens, providing another reason to discard it.

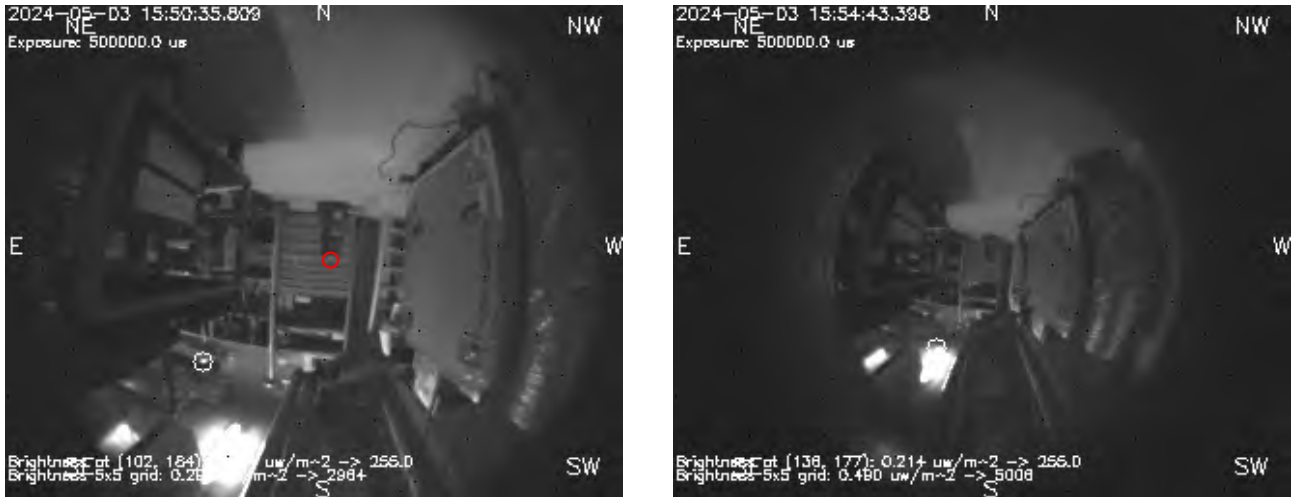


Figure 3.36: Thorlabs lens taken frame, laser not tracked as software was not ready yet. (left). Fujinon lens taken frame. (right)

We measured the power on the fiber tip using a power-meter, registering a value of $0.02 \mu W$. According to equation (3.16), this equaled to an axial intensity of $0.139 W/m^2$ at the camera. We used this value to calibrate the system—the system captures frames, which are measured by the digital number of their pixel values, to convert them to intensity we need to apply a conversion—multiplying the brightest pixel value by the obtained axial intensity, and then divided it by the curve generated from taking pictures of the spot when it was undetectable by the camera until saturation (255 pixel value),

as illustrated in Fig. 3.37.

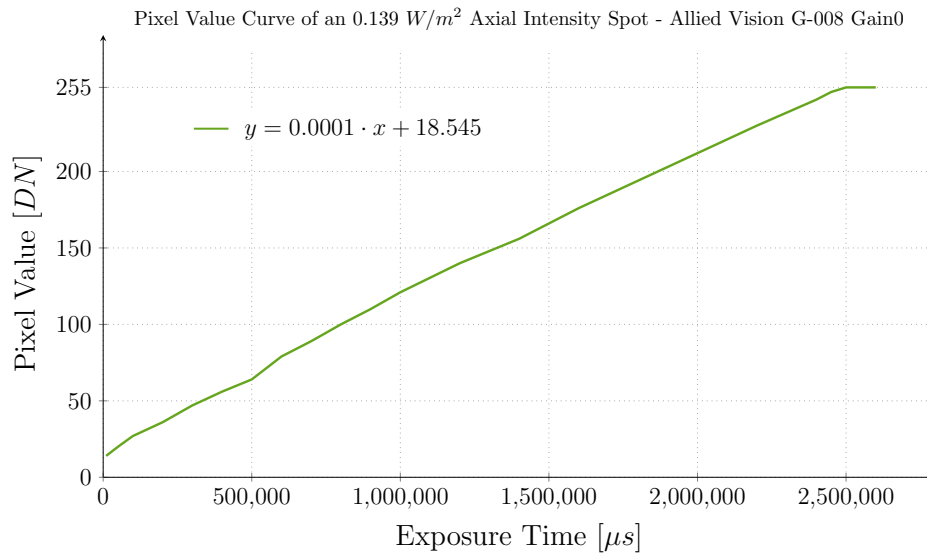


Figure 3.37: Camera's curve for an 0.139 W/m^2 axial intensity in gain 0 mode.

While this method allowed us to estimate the correct intensity regardless of the exposure time, it raised two main issues. First, we had no way to precisely point the laser to the camera, leading to losses in the detected intensity with no way to account for them. Second, the calibration factor was specific for an intensity value similar to the one used, meaning that only similar intensity values would be estimated accurately. The next experiment aimed to fix these issues.

3.5.4 Camera Calibration and Intensity Assessing with the Radio Tower

At the Deutsches Zentrum für Luft- und Raumfahrt (DLR), we have equipped a radio tower with a 2 mW , 1550 nm laser (with a minimum power output of 0.79 mW), an Erbium-Doped Fiber Amplifier (EDFA); and a Pan-Tilt Unit (PTU), all controlled via DLR servers. This setup enabled us to replicate the previous experiment, this time conducted on the IKN rooftop, aiming the laser with an angular precision of one degree. The setup is identical as the one used by a previous student at DLR [115], replacing the optical ground station focal assembly (SOFA with our camera positioned besides the OGS-OP. The presence of the Pan-Tilt unit in the setup solved the pointing problem, allowing us to precisely direct the laser. The calibration problem was harder to solve. A diagram of the experiment is shown in Fig. 3.38.

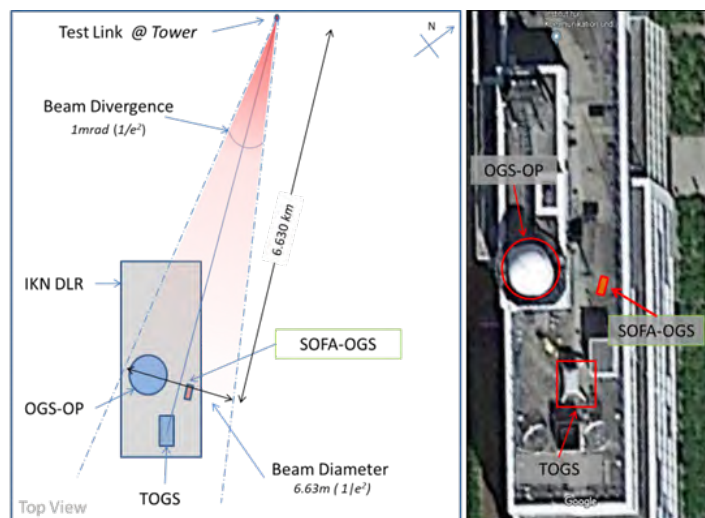


Figure 3.38: IKN rooftop experiment viewed from above

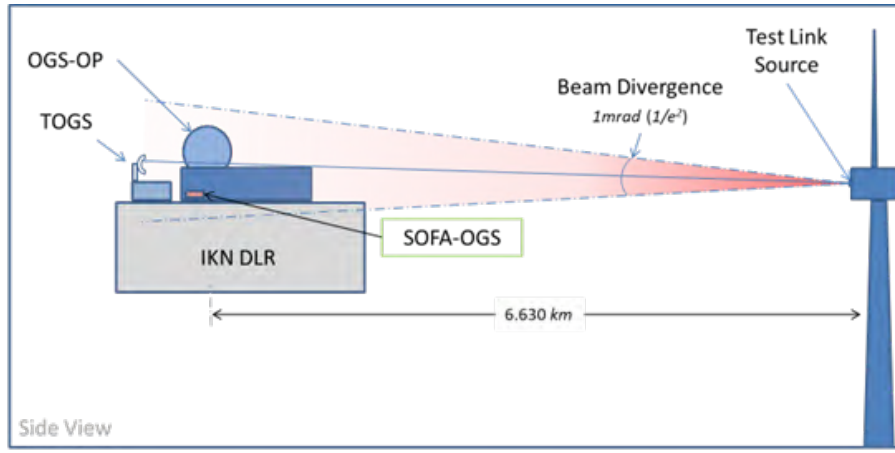


Figure 3.39: IKN rooftop experiment viewed from the side.

The tower is located 6.6 km away from the OGS-OP with a full width half angle of 1 mrad . Based on these parameters and equation (3.16), the lowest intensity generated was $15.95 \mu\text{W}/\text{m}^2$, much higher than the laser we were using in the basement. This always saturated the camera, regardless of the exposure time. While adjusting the laser's pointing was a solution, it reintroduced the original pointing problem.

We were unable to calibrate the camera using this method. The solution is either to install a filter on the radio tower or use a laser with adjustable power, fixed on a movable mount. The correct procedure for calibrating the camera is detailed in [116]. This method is similar to what we applied in subsection 3.5.3, but in this case, the exposure remains fixed, while the power is changed from undetectable levels until saturation, allowing us to obtain an accurate calibration curve for the entire exposure range, as shown in Fig. 3.40.

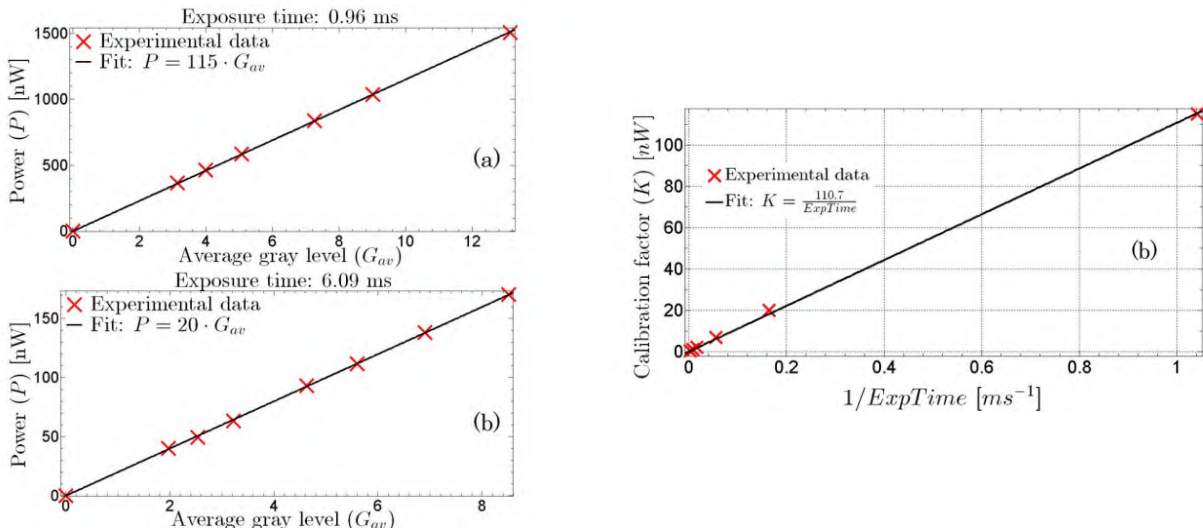


Figure 3.40: Exposure curves with moving power (left). Final exposure curve (right). Figure taken from [116].

A picture of the the saturated result are found next in Fig. 3.41. Pictures of the PTU menu and the setup of the experiment are shown in Fig. 3.42 and Fig. 3.43 and 3.44, respectively. The pathing from both the IKN and GSOC is shown in Fig. 3.45 and 3.46.

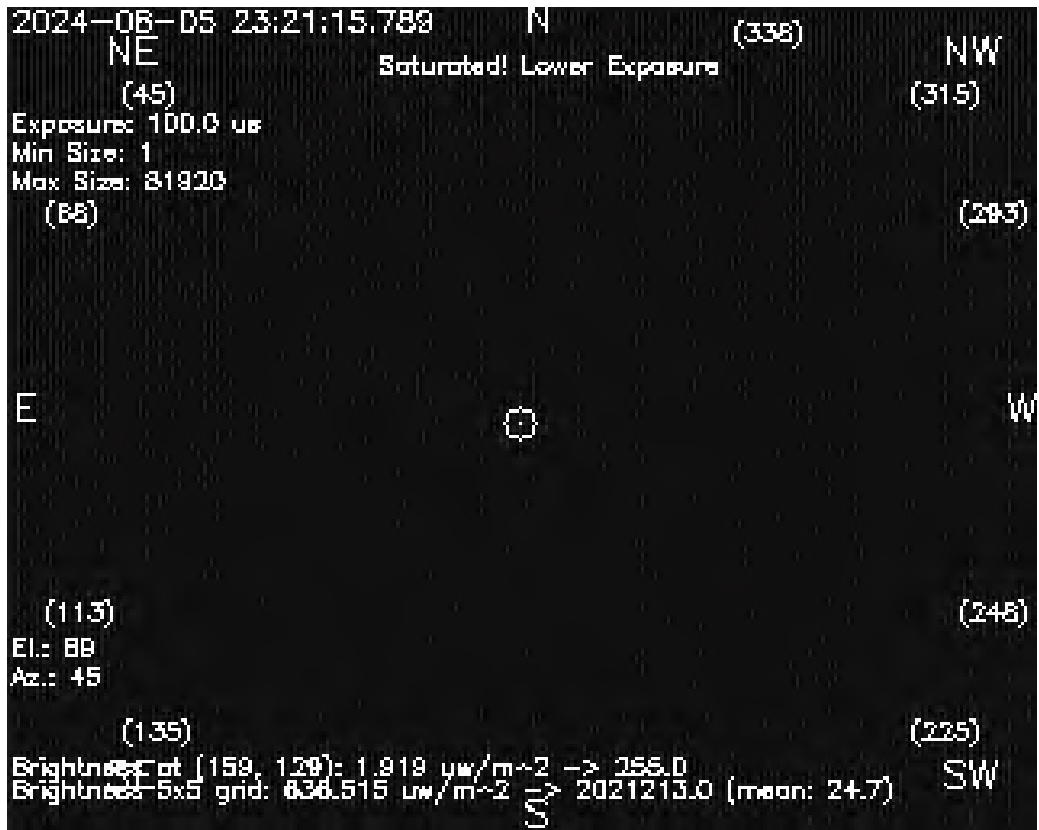


Figure 3.41: Picture of the radio tower taken by the camera using gain 1 mode at 0 dBm

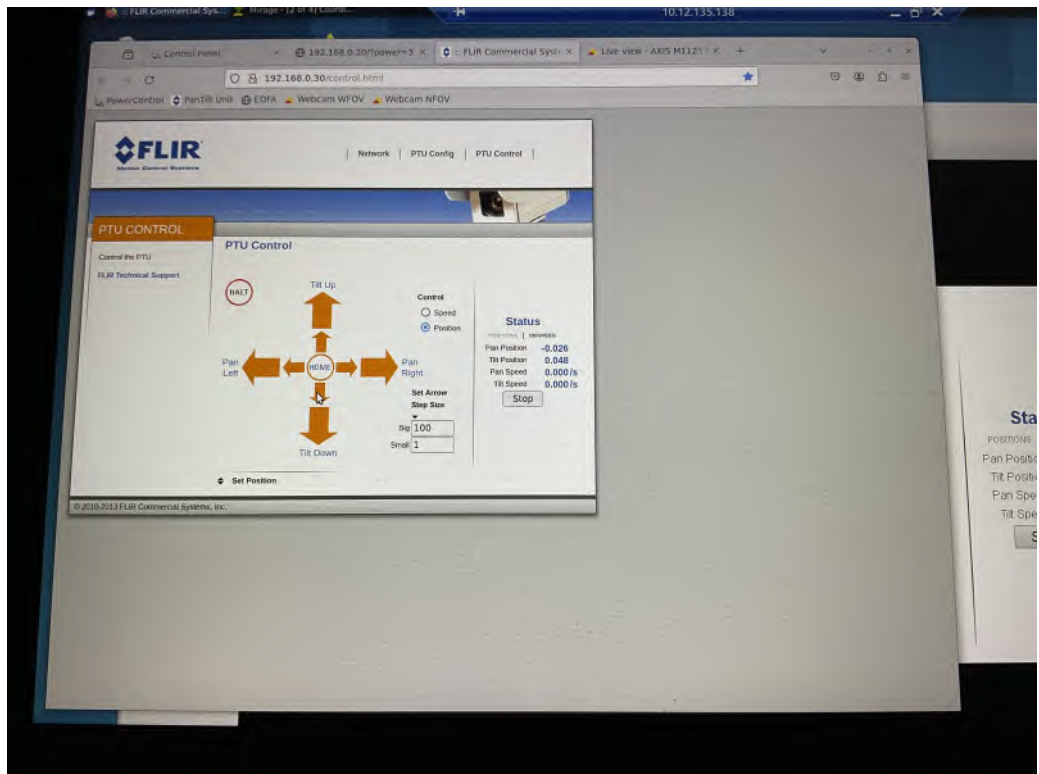


Figure 3.42: Picture of the pan-tilt unit menu

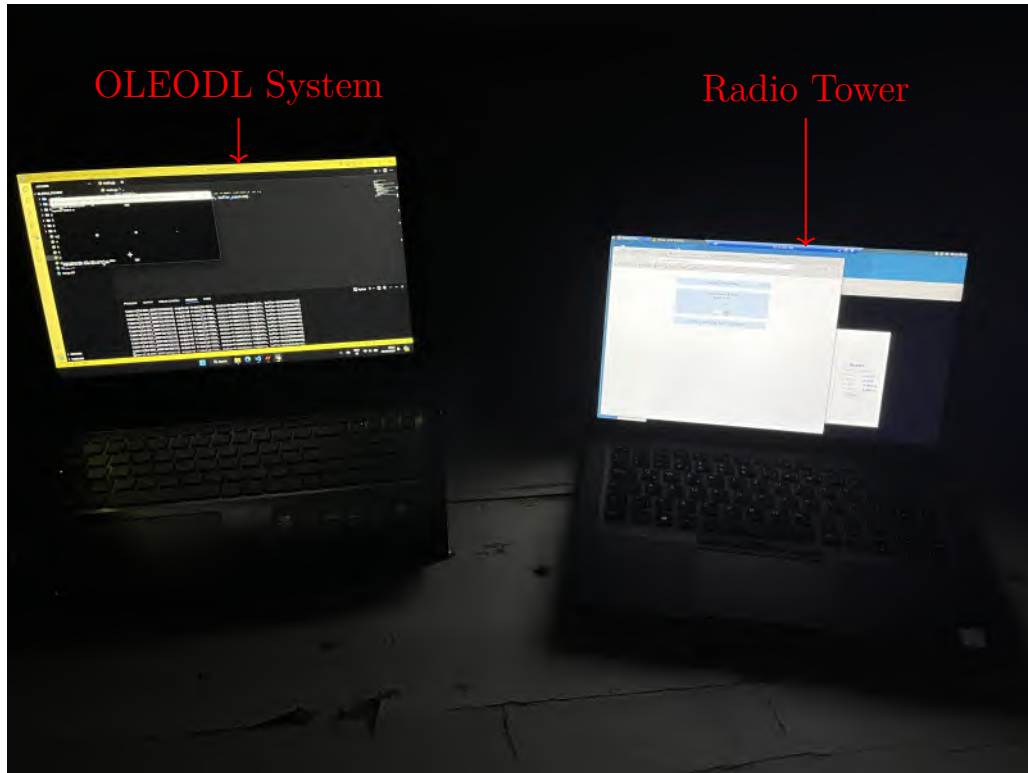


Figure 3.43: Picture of the two laptops controlling the OLEODL system (left) and the radio tower (right)



Figure 3.44: Picture of the Allied Vision G-008 camera besides the OGS-OP

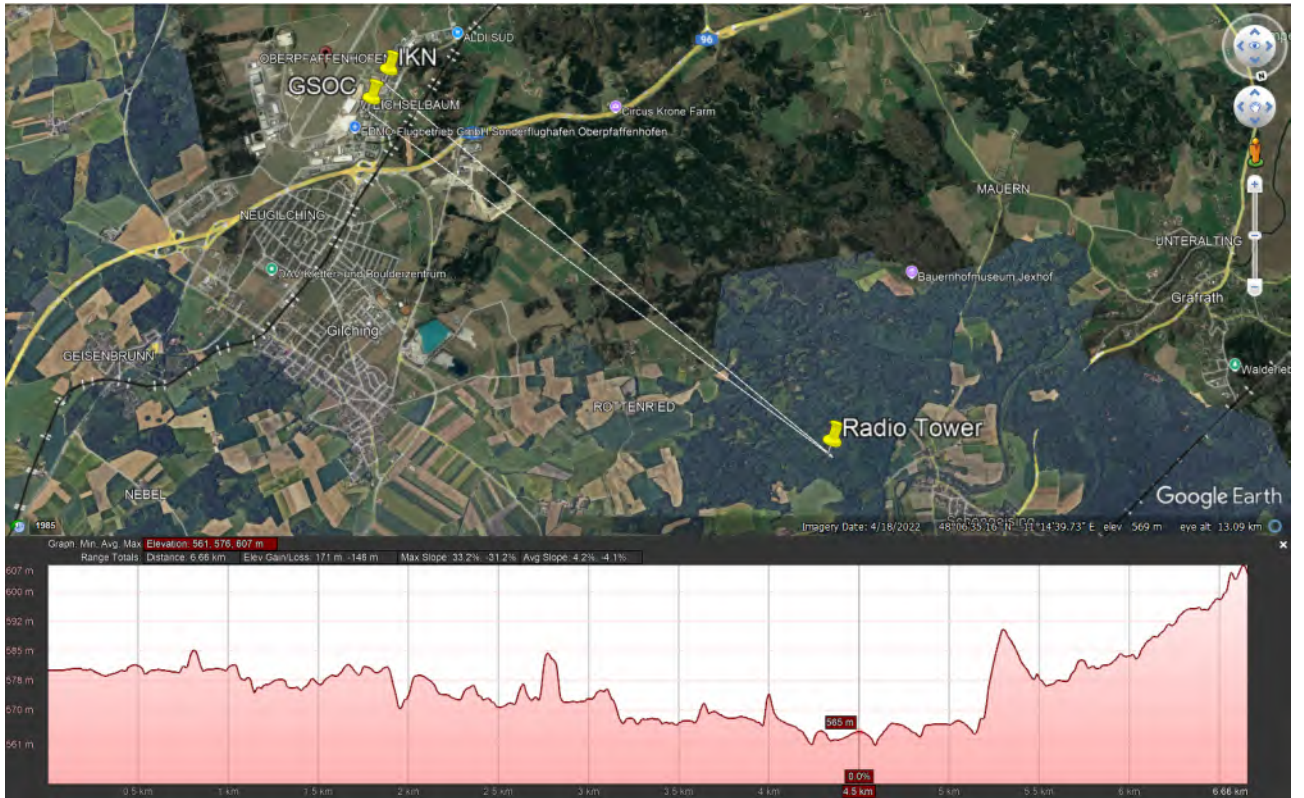


Figure 3.45: Image of the distance from the radio tower to both the IKN and GSOC. Figure taken from Google Earth Pro.

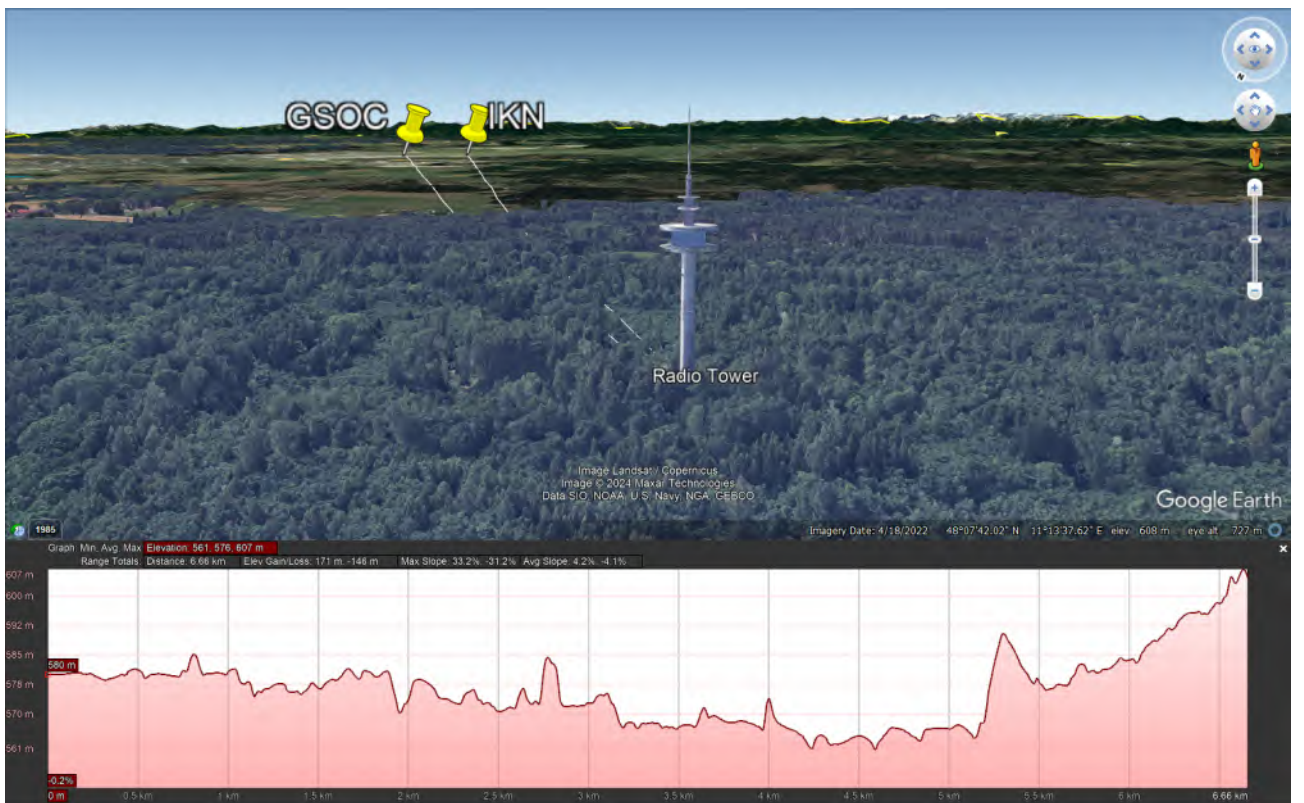


Figure 3.46: Image of the radio tower. Figure taken from Google Earth Pro.

4 Results & Discussion

We found that the device was useful, capable of detecting the satellite downlink and helping with the identification of the failure point of the system. We tested the device while this work was still in development, which means that the state of the device in the point of each measurement was usually different. This proved to be a challenging process as satellite downlinks are organized in campaigns—periods of approximately two weeks where links are conducted every two days or so. If the device was not ready for a specific campaign, we would not get any measurements until the next campaign, which are really limited, taking several months between each other.

The first campaign we participated in was the Flying Laptop (FLP) campaign in April. This campaign was unsuccessful as the software was incomplete at that time. The exposure time could not be changed during operation, and the satellite was tracked by just looking for the brightest point of the image without any filtering, thresholding or spot size filtering. Also, the visibility conditions were inadequate during the campaign, which means that we probably would have not seen the laser signal from OSIRIS on the satellite either way.

4.1 OSIRIS4CubeSat Onboard Laser CubeSat Campaign

The Laser CubeSat (CubeL) campaign took place in early July, while our software was still under development. During this campaign, the outdated image processing technique was still used, however we had already implemented the higher gain mode and the Look-Up Table (LUT) into the camera, improving our detection threshold.

We detected the OSIRIS4CubeSat laser terminal onboard CubeL during this campaign, whereas the OGS-OP did not. Initially, we considered the detection to be due to sun reflecting onto the satellite, as some links were attempted still in the visible time. However, we believe we saw the actual signal from the terminal, as sunlight reflection would have produced sudden sparks of light, rather than a continuous signal during the satellite pass.

CubeL, as explained in subsection 2.5.2, is the type of satellite that requires to receive a beacon to start the downlink. We tried to detect the satellite again when the beacon had not been sent, and did not observe it, which supports our hypothesis of seeing the signal. Although this result may seem minor, just for our camera to be able to see the laser terminal from the satellite, suggest that the Optical Ground Station (OGS) should also be able to see it. The OGS not detecting the signal indicates a potential issue with the telescope, probably related to the pointing accuracy. This was exactly one of the main goals of this work, and we managed to prove its value.

Although highly unlikely, the satellite’s orbit could be slightly off, enough to miss it. For this reason, the camera system is also designed to assess the elevation and azimuth of the satellite, and the dB lost with respect to the expected intensity received from the laser terminal at that precise elevation angle: assessing how off the satellite was from the expected values. This feature was not implemented for this campaign and still requires further testing.

A frame of the pass can be seen in Fig. 4.1. We could also present the intensity values during

the pass, but it is not really useful as the calibration of the intensity is inaccurate.



Figure 4.1: Pictures taken with the OLEODL system of the CubeL satellite

4.2 CubeCat Onboard NORSTAT-TD Campaign

We contacted the Dutch Organization for Applied Scientific Research (TNO) to establish a link with their satellite, NORSTAT-TD, fitted with the CubeCat laser terminal. This satellite operates similarly to CubeL, with the principal difference being that its downlink remains active from the horizon, using the beacon only to locate the targeted OGS, and refine its pointing accuracy. This satellite stays within visible range for approximately the first 12 degrees, before shifting to the infrared spectrum.

Conducted at the German Space Operations Center (GSOC) during the last week of August, this campaign was also unsuccessful. While the satellite downlink process worked normally for TNO in The Hague, we were unable to consistently detect the CubeCat laser terminal onboard NORSTAT-TD: nor did the GSOC-OGS, nor did I with the camera. We detected the laser terminal during the visual range on the first day, but we were unable to replicate the results the following day due to clouds.

We arranged a meeting to discuss potential causes of the issues we encountered. Two main points were identified: first, the Two-Line Elements (TLE) files we used might not have been precise enough, as TNO uses Consolidated Prediction Format (CPF) files, which they find to be more accurate. The second was the differences in our beacons; while ours is a 4 W beacon, TNO's is 6 W. Although this difference in power should not have been a problem, the divergence angle difference was significant. TNO's beacon had a divergence angle of 220 μ rad, whereas our beacon had a divergence angle of 2.1 mrad. This 10x increase could have prevented the satellite to detect our beacon, resulting in the satellite spiraling instead of sending the downlink directly to us.

The following day, we found out that the link was impeded due to problems with the orbital elements and the too low intensity of the beacon pointing to the satellite. This made sense, because even if the TLE was imprecise and the satellite was not pointing directly at us, the OLEODL system developed in this work should have detected the satellite, however it did not. After fitting a new collimator into the telescope, we tried again the same night, but nothing was seen except three or four sparks in the OLEODL system. These sparks seem to be the reflection of the downlink interacting

with the beacon of the telescope. This occurred due to humid conditions that night, which caused some fog, leading to atmospheric interactions and reflections.

The presence of these reflections indicated that the satellite was likely sending the downlink as intended. However, we were unable to assess the exact cause of our failure.



Figure 4.2: Pictures taken with the OLEODL system of the reflections from the NORSAT-TD satellite.



Figure 4.3: Picture taken of the setup for the NORSAT-TD link

5 Conclusion

5.1 Summary

Optical Low Earth Orbit DownLinks (OLEODL) are establishing themselves as an alternative to Radio Frequency (RF) links in specific scenarios due to their reduced equipment volume, lower power consumption, and avoidance of the regulatory restrictions and tariffs associated with RF.

When attempting Optical Low Earth Orbit Downlinks (OLEODL), various factors can cause a failure, such as weather conditions, visibility, performance of the Optical Ground Station (OGS), or issues with the satellite itself. Identifying the precise cause of a failure is challenging.

This work focuses on building a compact, portable, and waterproof validation tool for OLEODL links. This tool is capable of assessing the signal intensity of a laser terminal onboard a satellite, including deviations from the expected intensity as per the link budget. The azimuth and elevation angle of the satellite are also computed, evaluating the overall performance of the link. Our device is based on an Indium Gallium Arsenide (InGaAs) camera, which operates in the 900 – 1700 *nm* spectral range. The captured images are processed using a filtering-thresholding-contouring technique, for the intensity-dependent value on that precise elevation to be compared to the expected intensity on that same elevation angle.

This thesis demonstrates that the proposed proof-of-concept is feasible, and can be a valuable tool during the downlinks, capable of detecting the satellite even when the OGS did not, providing us with another tool to assess the failure point of the system. The goal is to establish this device as a commonly used tool during the OLEODL campaigns. Although the system is operational, it is still under development, with potential identified improvements and further testing needed.

The lack of consistent downlink campaigns, combined with the difficulties in establishing the link, made testing challenging. Additionally, the imprecise intensity calibration caused the recorded values to deviate from the expected values; if the values are far from our calibration factor.

5.2 Future Work

The AllSky-Camera system for Monitoring of Optical Satellite Downlinks aims to become a standard tool for optical satellite downlinks. The main improvement needed lies in the intensity calibration process, explained in subsection 3.5.4, which could not be fully accomplished due to the lack of appropriate tools (a challenge impossible to solve within our time frame).

Having proven the device's usefulness, it will be upgraded with more suitable components, replacing off-the-shelf components with custom-made ones. A custom-designed Field of View closer to 180 degrees (allowing us to see the whole hemisphere) with appropriate transitivity will be commissioned, as well as a crystal dome made of a more fitting material, such as BK7. These upgrades were initially omitted to keep the proof-of-concept within a limited budget.

A 1550 *nm* band pass filter could be implemented. The main problem with these filters is that

their performance varies, highly, depending on the incident angle, rendering them useless for our case. If we really want to implement the band pass filter, it should be placed between the sensor and the lens, where the incident angles are much lower than before the lens. The spacing between the lens and the sensor is approximately 4 *mm*, which would allow us to find a suitable filter if desired.

As a minor improvement, remote operation of the system could also be implemented in the future. The project was developed with this in mind, but the DLR firewalls prevented its deployment. An exception to the firewall is being considered, but this will take time.

In conclusion, this work successfully developed a device that will serve as an automated verification tool for any satellite downlink in the near future. The closest application of the AllSky-Camera system for Monitoring of Optical Satellite Downlinks is its deployment in Almeria, where it will operate alongside the newly developed robotic Optical Ground Station (OGS) to monitor the planned satellite downlinks.

Bibliography

- [1] N. Takato, N. Okada, G. Kosugi, M. Suganuma, A. Miyashita, and F. Uraguchi, “All-sky 10-um cloud monitor on mauna kea,” in *Large Ground-based Telescopes*, vol. 4837. SPIE, 2003, pp. 872–877.
- [2] Y. Wang, D. Liu, W. Xie, M. Yang, Z. Gao, X. Ling, Y. Huang, C. Li, Y. Liu, and Y. Xia, “Day and night clouds detection using a thermal-infrared all-sky-view camera,” *Remote Sensing*, vol. 13, no. 9, p. 1852, 2021.
- [3] P. Crispel and G. Roberts, “All-sky photogrammetry techniques to georeference a cloud field,” *Atmospheric measurement techniques*, vol. 11, no. 1, pp. 593–609, 2018.
- [4] E. Kerr, B. D. C. López, N. Maric, J. N. Torres, G. Falco, N. Sánchez Ortiz, C. Dorn, and S. Eves, “Design and prototyping of a low-cost leo optical surveillance sensor,” in *Proceedings of the 8th European Conference on Space Debris, Darmstadt, Germany, 2021*, pp. 20–23.
- [5] M. N. Sarvi, D. Abbasi-Moghadam, M. Abolghasemi, and H. Hoseini, “Design and implementation of a star-tracker for leo satellite,” *Optik*, vol. 208, p. 164343, 2020.
- [6] K. Riesing, H. Yoon, and K. Cahoy, “A portable optical ground station for low-earth orbit satellite communications,” in *2017 IEEE International Conference on Space Optical Systems and Applications (ICSOS)*. IEEE, 2017, pp. 108–114.
- [7] N. Estell, D. Ma, and P. Seitzer, “Daylight imaging of leo satellites using cots hardware,” in *Proc. AMOS*, 2019.
- [8] H. Kaushal, V. Jain, and S. Kar, *Free space optical communication*. Springer, 2017, vol. 60.
- [9] A. G. Bell, “Apparatus for signaling and communicating, called photophone,” U.S. Patent No. 235,199, Dec. 7, 1880.
- [10] G. Marconi, “Improvements in transmitting electrical impulses and signals and in apparatus there-for,” British Patent No. 12,039, Jul. 7, 1897.
- [11] A. G. Bell, “The photophone,” *Science*, no. 11, pp. 130–134, 1880.
- [12] D. Giggenbach, “Optimierung der optischen freiraumkommunikation durch die turbulente atmosphäre-focal array receiver,” Ph.D. dissertation, Shaker-Verlag, 2005.
- [13] M. M. Hassan and G. Rather, “Free space optics (fso): a promising solution to first and last mile connectivity (flmc) in the communication networks,” *IJ Wireless and Microwave Technologies*, vol. 4, no. 1, p. 1, 2020.
- [14] M. N. Sadiku, S. M. Musa, and S. R. Nelatury, “Free space optical communications: an overview,” *European scientific journal*, vol. 12, no. 9, pp. 55–68, 2016.
- [15] K. A. Sebastian. ”UCS Satellite Database”. Union of Concerned Scientist. Accessed: Aug. 9, 2024. [Online]. Available: <https://www.ucsusa.org/resources/satellite-database>
- [16] P.-H. Chen and R. L.-T. Cho, “The technological trajectory of leo satellites: Perspectives from main path analysis,” *IEEE Transactions on Engineering Management*, 2023.

- [17] V. Pesce, A. Colagrossi, and S. Silvestrini, “Chapter four - orbital dynamics,” in *Modern spacecraft guidance, navigation, and control: from system modeling to AI and innovative applications*. Elsevier, 2022, pp. 131–206.
- [18] H. Riebeek. ”Catalog of Earth Satellite Orbits”. NASA Earth Observatory. Accessed: Aug. 9, 2024. [Online]. Available: <https://earthobservatory.nasa.gov/features/OrbitsCatalog>
- [19] “Syncom II Summary Report,” NASA - Hughes Aircraft Co. SSD 3128R, Culver City, CA, USA, Sum. Rep. N66-23589, 1963, Accessed: Aug. 9, 2024. [Online]. Available: <https://ntrs.nasa.gov/api/citations/19660014300/downloads/19660014300.pdf>.
- [20] P. Dickson, *Sputnik: The shock of the century*. Bloomsbury Publishing USA, 2001.
- [21] K. Maine, C. Devieux, and P. Swan, “Overview of iridium satellite network,” in *Proceedings of WESCON’95*. IEEE, 1995, p. 483.
- [22] J. Puig-Suari, J. Schoos, C. Turner, T. Wagner, R. Connolly, and R. P. Block, “Cubesat developments at cal poly: the standard deployer and polysat,” in *Small Payloads in Space*, vol. 4136. SPIE, 2000, pp. 72–78.
- [23] C. Kitts, J. Hines, E. Agasid, A. Ricco, B. Yost, K. Ronzano, and J. Puig-Suari, “The genesat-1 microsatellite mission challenge in small satellite design,” 2006.
- [24] F. Michel, M. Trevisan, D. Giordano, and O. Bonaventure, “A first look at starlink performance,” in *Proceedings of the 22nd ACM Internet Measurement Conference*, 2022, pp. 130–136.
- [25] C. Pardini and L. Anselmo, “Environmental sustainability of large satellite constellations in low earth orbit,” *Acta Astronautica*, vol. 170, pp. 27–36, 2020.
- [26] J. N. Pelton, “The space debris threat and the kessler syndrome,” in *Space Debris and Other Threats from Outer Space*. Springer, 2013, pp. 17–23.
- [27] “ESA’S Annual Space Environment Report,” ESA Space Debris Office, Darmstadt, Germany, Ann. Rep., 2024. Accessed: Aug. 10, 2024. [Online]. Available: https://www.sdo.esoc.esa.int/environment_report/Space_Environment_Report_latest.pdf.
- [28] “International Space Station Deorbit Analysis Summary,” NASA, Washington, DC, USA, White Paper, 2024. Accessed: Aug. 10, 2024. [Online]. Available: <https://www.nasa.gov/wp-content/uploads/2024/06/iss-deorbit-analysis-summary.pdf>.
- [29] A. Carrasco-Casado and R. Mata-Calvo, “Space optical links for communication networks,” in *Springer Handbook of Optical Networks*. Springer, 2020, pp. 1057–1103.
- [30] Z. Sodnik, J. P. Armengol, R. H. Czichy, and R. Meyer, “Adaptive optics and esa’s optical ground station,” in *Free-Space Laser Communications IX*, vol. 7464. SPIE, 2009, pp. 47–55.
- [31] J. Crass, “The adaptive optics lucky imager: combining adaptive optics and lucky imaging,” Ph.D. dissertation, 2014.
- [32] C. Fuchs, D. Giggenbach, R. M. Calvo, and W. Rosenkranz, “Optical transmitter diversity with phase-division in bit-time,” in *2022 IEEE International Conference on Space Optical Systems and Applications (ICSOS)*. IEEE, 2022, pp. 1–4.
- [33] R. M. Calvo, P. Becker, D. Giggenbach, F. Moll, M. Schwarzer, M. Hinz, and Z. Sodnik, “Transmitter diversity verification on artemis geostationary satellite,” in *Free-space laser communication and atmospheric propagation xxvi*, vol. 8971. SPIE, 2014, pp. 24–37.
- [34] D. Giggenbach, F. Moll, C. Schmidt, C. Fuchs, and A. Shrestha, “Optical on-off keying data links for low earth orbit downlink applications,” *Satellite Communications in the 5G Era*, vol. 79, pp. 307–339, 2018.

- [35] A. Mustafa, D. Giggenbach, J. Poliak, A. Shrestha, R. Mata-Calvo, and C. Fuchs, "Lab implementation of 10 gbps/channel optical transmitter diversity scheme for geostationary satellite feeder links," in *Photonic Networks; 16. ITG Symposium*. VDE, 2015, pp. 1–3.
- [36] R. Kaushik, V. Khandelwal, and R. C. Jain, "Effect of aperture averaging and spatial diversity on capacity of optical wireless communication systems over lognormal channels," *Radioelectronics and Communications Systems*, vol. 59, pp. 527–535, 2016.
- [37] A. Mustafa, "Spectrally efficient transmitter diversity scheme for optical satellite feeder links," Ph.D. dissertation, Universität Stuttgart, 2024.
- [38] M. R. Garcia-Talavera, J. A. Rodriguez, T. Viera, H. Moreno-Arce, J. L. Rasilla, F. Gago, L. F. Rodriguez, P. Gomez, and E. B. Ramirez, "Design and performance of the esa optical ground station," in *Free-Space Laser Communication Technologies XIV*, vol. 4635. SPIE, 2002, pp. 248–261.
- [39] A. Alonso, M. Reyes, and Z. Sodnik, "Performance of satellite-to-ground communications link between artemis and the optical ground station," in *Optics in Atmospheric Propagation and Adaptive Systems VII*, vol. 5572. SPIE, 2004, pp. 372–383.
- [40] K. Saucke, C. Seiter, F. Heine, M. Gregory, D. Tröndle, E. Fischer, T. Berkefeld, M. Feriencik, M. Feriencik, I. Richter *et al.*, "The tesat transportable adaptive optical ground station," in *Free-Space Laser Communication and Atmospheric Propagation XXVIII*, vol. 9739. SPIE, 2016, pp. 37–47.
- [41] IQOQI Vienna, Austrian Academy of Sciences. "Laser from Optical Ground Station on Tenerife". ESA. Accessed: Aug. 12, 2024. [Online]. Available: https://www.esa.int/ESA_Multimedia/Images/2012/09/Laser_from_Optical_Ground_Station_on_Tenerife
- [42] E. Fischer, T. Berkefeld, M. Feriencik, M. Feriencik, V. Kaltenbach, D. Soltau, B. Wandernoth, R. Czichy, J. Kunde, K. Saucke *et al.*, "Development, integration and test of a transportable adaptive optical ground station," in *2015 IEEE International Conference on Space Optical Systems and Applications (ICSOS)*. IEEE, 2015, pp. 1–6.
- [43] N. Perlot, M. Knapek, D. Giggenbach, J. Horwath, M. Brechtelsbauer, Y. Takayama, and T. Jono, "Results of the optical downlink experiment kiodo from oicets satellite to optical ground station oberpfaffenhofen (ogs-op)," in *Free-Space Laser Communication Technologies XIX and Atmospheric Propagation of Electromagnetic Waves*, vol. 6457. SPIE, 2007, pp. 28–35.
- [44] J. Prell, A. Dului, R. Andrew, I. Hristovski, S. Amita, F. Moll, and C. Fuchs, "Optical ground station oberpfaffenhofen next generation: first satellite link tests with 80 cm telescope and ao system," in *2023 IEEE International Conference on Space Optical Systems and Applications (ICSOS)*. IEEE, 2023, pp. 42–48.
- [45] I. R. Hristovski, A. R. Campelo, B. Femenía-Castella, E. Doensdorf-Sternal, A. O. Dului, S. Haeusler, J. F. Holzman, K. Klemich, D. J. Laidlaw, T. Marynowski *et al.*, "Pre-distortion adaptive optics: experimental results from bi-directional tracking links between dlr's optical ground station and alphasat's tdp-1 terminal," in *Free-Space Laser Communications XXXVI*, vol. 12877. SPIE, 2024, pp. 328–336.
- [46] G. E. Stillman, "Optoelectronics," in *Reference data for engineers: radio, electronics, computers and communications*. Elsevier, 2002, pp. 21–1–21–31.
- [47] B. Rödiger, D. Ginhör, J. P. Labrador, J. Ramirez, C. Schmidt, and C. Fuchs, "Demonstration of an fso/rf hybrid-communication system on aeronautical and space applications," in *Laser Communication and Propagation through the Atmosphere and Oceans IX*, vol. 11506. SPIE, 2020, p. 1150603.

- [48] K. E. Wilson, J. R. Lesh, and T.-Y. Yan, “Gopex: a laser uplink to the galileo spacecraft on its way to jupiter,” in *Free-Space Laser Communication Technologies V*, vol. 1866. SPIE, 1993, pp. 138–146.
- [49] K. Araki, Y. Arimoto, M. Shikatani, M. Toyoda, M. Toyoshima, T. Takahashi, S. Kanda, and K. Shiratama, “Performance evaluation of laser communication equipment onboard the ets-vi satellite,” in *Free-Space Laser Communication Technologies VIII*, vol. 2699. SPIE, 1996, pp. 52–59.
- [50] G. Fletcher, T. Hicks, and B. Laurent, “The silex optical interorbit link experiment,” *Electronics & communication engineering journal*, vol. 3, no. 6, pp. 273–279, 1991.
- [51] J. Horwath, N. Perlot, M. Knappek, and F. Moll, “Experimental verification of optical backhaul links for high-altitude platform networks: Atmospheric turbulence and downlink availability,” *International Journal of Satellite Communications and Networking*, vol. 25, no. 5, pp. 501–528, 2007.
- [52] M. Toyoshima, H. Takenaka, Y. Shoji, Y. Takayama, Y. Koyama, and H. Kunimori, “Results of kirari optical communication demonstration experiments with nict optical ground station (koden) aiming for future classical and quantum communications in space,” *Acta Astronautica*, vol. 74, pp. 40–49, 2012.
- [53] R. Fields, C. Lunde, R. Wong, J. Wicker, D. Kozlowski, J. Jordan, B. Hansen, G. Muehlnikel, W. Scheel, U. Sterr *et al.*, “Nfire-to-terrasar-x laser communication results: satellite pointing, disturbances, and other attributes consistent with successful performance,” in *Sensors and Systems for Space Applications III*, vol. 7330. SPIE, 2009, pp. 211–225.
- [54] D. M. Boroson, B. S. Robinson, D. V. Murphy, D. A. Burianek, F. Khatri, J. M. Kovalik, Z. Sodnik, and D. M. Cornwell, “Overview and results of the lunar laser communication demonstration,” in *Free-Space Laser Communication and Atmospheric Propagation XXVI*, vol. 8971. SPIE, 2014, pp. 213–223.
- [55] A. Carrasco-Casado, H. Takenaka, D. Kolev, Y. Munemasa, H. Kunimori, K. Suzuki, T. Fuse, T. Kubo-Oka, M. Akioka, Y. Koyama *et al.*, “Leo-to-ground optical communications using sota (small optical transponder)–payload verification results and experiments on space quantum communications,” *Acta Astronautica*, vol. 139, pp. 377–384, 2017.
- [56] D. Giggenbach, J. Poliak, R. Mata-Calvo, C. Fuchs, N. Perlot, R. Freund, and T. Richter, “Preliminary results of terabit-per-second long-range free-space optical transmission experiment thrust,” in *Unmanned/Unattended Sensors and Sensor Networks XI; and Advanced Free-Space Optical Communication Techniques and Applications*, vol. 9647. SPIE, 2015, pp. 61–73.
- [57] J. Yin, Y. Cao, Y.-H. Li, S.-K. Liao, L. Zhang, J.-G. Ren, W.-Q. Cai, W.-Y. Liu, B. Li, H. Dai *et al.*, “Satellite-based entanglement distribution over 1200 kilometers,” *Science*, vol. 356, no. 6343, pp. 1140–1144, 2017.
- [58] D. Calzolaio, F. Curreli, J. Duncan, A. Moorhouse, G. Perez, and S. Voegt, “Edrs-c—the second node of the european data relay system is in orbit,” *Acta Astronautica*, vol. 177, pp. 537–544, 2020.
- [59] D. J. Israel, B. L. Edwards, R. L. Butler, J. D. Moores, S. Piazzolla, N. Du Toit, and L. Braatz, “Early results from nasa’s laser communications relay demonstration (lcrd) experiment program,” in *Free-Space Laser Communications XXXV*, vol. 12413. SPIE, 2023, pp. 10–24.
- [60] D. Rieländer, A. Di Mira, D. Alaluf, R. Daddato, S. Mejri, J. Piris, J. Alves, D. Antsos, A. Biswas, N. Karafolas *et al.*, “Esa ground infrastructure for the nasa/jpl psyche deep-space optical communication demonstration,” in *International Conference on Space Optics—ICSO 2022*, vol. 12777. SPIE, 2023, pp. 159–169.

- [61] D. Giggenbach, A. Shrestha, C. Fuchs, C. Schmidt, and F. Moll, “System aspects of optical leo-to-ground links,” in *International Conference on Space Optics—ICSO 2016*, vol. 10562. SPIE, 2017, pp. 1635–1643.
- [62] D. Giggenbach and F. Moll, “Scintillation loss in optical low earth orbit data downlinks with avalanche photodiode receivers,” in *2017 IEEE International Conference on Space Optical Systems and Applications (ICSOS)*. IEEE, 2017, pp. 115–122.
- [63] D. Giggenbach, F. Moll, C. Fuchs, T. de Cola, and R. Mata-Calvo, “Space communications protocols for future optical satellite-downlinks,” 2011.
- [64] D. Giggenbach, M. T. Knopp, and C. Fuchs, “Link budget calculation in optical leo satellite downlinks with on/off-keying and large signal divergence: A simplified methodology,” *International Journal of Satellite Communications and Networking*, vol. 41, no. 5, pp. 460–476, 2023.
- [65] A. Carrillo-Flores, D. Giggenbach, M. Knopp, D. Orsucci, and A. Shrestha, “Effects of pointing errors on intensity losses in the optical leo uplink,” in *International Conference on Space Optics—ICSO 2022*, vol. 12777. SPIE, 2023, pp. 2476–2491.
- [66] EDMUND OPTICS. “Gaussian Beam Propagation”. EDMUND OPTICS. Accessed: Feb. 27, 2024. [Online]. Available: <https://www.edmundoptics.com/knowledge-center/application-notes/lasers/gaussian-beam-propagation/>
- [67] D. Giggenbach and A. Shrestha, “Atmospheric absorption and scattering impact on optical satellite-ground links,” *International Journal of Satellite Communications and Networking*, vol. 40, no. 2, pp. 157–176, 2022.
- [68] H. Hemmati, “Near-earth laser communications,” in *Near-Earth Laser Communications, Second Edition*. CRC press, 2020, pp. 1–40.
- [69] A. Tunick, “The refractive index structure parameter/atmospheric optical turbulence model: Cn2 (no. arl-tr-1615),” *ARMY RESEARCH LABORATORY ADELPHI MD*, 1998.
- [70] Y. K. Chahine, S. A. Tedder, B. E. Vyhnalek, and A. C. Wroblewski, “Beam propagation through atmospheric turbulence using an altitude-dependent structure profile with non-uniformly distributed phase screens,” in *Free-Space Laser Communications XXXII*, vol. 11272. SPIE, 2020, pp. 263–277.
- [71] E. Aristidi, A. Ziad, J. Chabé, Y. Fantéi-Caujolle, C. Renaud, and C. Giordano, “A generalized differential image motion monitor,” *Monthly Notices of the Royal Astronomical Society*, vol. 486, no. 1, pp. 915–925, 2019.
- [72] F. Moll and M. Knapek, “Wavelength selection criteria and link availability due to cloud coverage statistics and attenuation affecting satellite, aerial, and downlink scenarios,” in *Free-Space Laser Communications VII*, vol. 6709. SPIE, 2007, pp. 347–358.
- [73] J. P. Jakobs, A. Köhler, M. T. Knopp, and A. Ohndorf, “Development of an optical ground station (ogs) network in germany and europe,” 2023.
- [74] D. Giggenbach and H. Henniger, “Fading-loss assessment in atmospheric free-space optical communication links with on-off keying,” *Optical Engineering*, vol. 47, no. 4, pp. 046 001–046 001, 2008.
- [75] F. Moll, D. Giggenbach, C. Schmidt, and C. Fuchs, “Analysis of power scintillation and fading margin in the leo-ground downlink with the osirisv1 laser terminal on flying laptop and the dlr optical ground station oberpfaffenhofen,” in *Environmental Effects on Light Propagation and Adaptive Systems V*, vol. 12266. SPIE, 2022, pp. 75–82.

- [76] J. Keim, S. Gaißer, P. Hagel, M. Böttcher, M. Lengowski, M. Graß, D. Giggenbach, C. Fuchs, C. Schmidt, S. Klinkner *et al.*, “Commissioning of the optical communication downlink system osirisv1 on the university small satellite “flying laptop”,” in *70th International Astronautical Congress (IAC), Washington*, 2019.
- [77] D. Giggenbach, C. Fuchs, C. Schmidt, B. Rödiger, S. Gaißer, S. Klinkner, D.-H. Phung, J. Chabé, C. Courde, N. Maurice *et al.*, “Downlink communication experiments with osirisv1 laser terminal onboard flying laptop satellite,” *Applied optics*, vol. 61, no. 8, pp. 1938–1946, 2022.
- [78] D. Giggenbach, P. Karafillis, J. Rittershofer, A. Immerz, A. Spoerl, S. Gaisser, S. Klinkner, and M. Knopp, “Transmitter beam bias verification for optical satellite data downlinks with open-loop pointing—the 3-ogs-experiment,” in *International Conference on Space Optics—ICSO 2022*, vol. 12777. SPIE, 2023, pp. 398–412.
- [79] C. Fuchs, F. Moll, D. Giggenbach, C. Schmidt, J. Keim, and S. Gaisser, “Osirisv1 on flying laptop: Measurement results and outlook,” in *2019 IEEE International Conference on Space Optical Systems and Applications (ICSOS)*. IEEE, 2019, pp. 1–5.
- [80] B. Rödiger and C. Schmidt, “In-orbit demonstration of the world’s smallest laser communication terminal-osiris4cubesat/cubelet,” in *Small Satellites Systems and Services-The 4S Symposium 2024*, 2024.
- [81] B. Rödiger, C. Menninger, C. Fuchs, L. Grillmayer, S. Arnold, C. Rochow, P. Wertz, and C. Schmidt, “High data-rate optical communication payload for cubesats,” in *Laser Communication and Propagation through the Atmosphere and Oceans IX*, vol. 11506. SPIE, 2020, pp. 12–24.
- [82] DLR Institute of Communications and Navigation. “OSIRIS4CubeSat / CubeLCT”. DLR. Accessed: Aug. 14, 2024. [Online]. Available: <https://www.dlr.de/en/kn/research-transfer/projects/osiris-optical-communication-in-space/cube4cubesat-cubelet>
- [83] B. Rödiger, L. R. Rodeck, M.-T. Hahn, and C. Schmidt, “Transformation of dlr’s laser communication terminals for cubesats towards new application scenarios,” in *Small Satellites Systems and Services-The 4S Symposium 2024*, 2024.
- [84] DLR Institute of Communications and Navigation. “OSIRIS - Optical Communication in Space”. DLR. Accessed: Aug. 14, 2024. [Online]. Available: <https://www.dlr.de/en/kn/research-transfer/projects/osiris-optical-communication-in-space>
- [85] SONY. “Short-Wavelength InfraRed Image Sensor Technology SenSWIR™”. SONY. Accessed: Jan. 18, 2024. [Online]. Available: <https://www.sony-semicon.com/en/technology/industry/senswir.html>
- [86] IDS Imaging Development Systems GmbH. “Sensor sizes”. IDS. Accessed: Jan. 21, 2024. [Online]. Available: <https://www.1stvision.com/cameras/IDS/IDS-manuals/en/basics-sensor-size.html>
- [87] Allied Vision. “Goldeye G-008 TEC1”. Allied Vision. Accessed: Feb. 13, 2024. [Online]. Available: <https://www.alliedvision.com/en/camera-selector/detail/goldeye/g-008-tec1/>
- [88] ——. “Goldeye G-130 TEC1”. Allied Vision. Accessed: Feb. 13, 2024. [Online]. Available: <https://www.alliedvision.com/en/camera-selector/detail/goldeye/g-130-tec1/>
- [89] Exosens. “Bobcat 320 Series”. Exosens. Accessed: Feb. 22, 2024. [Online]. Available: <https://www.exosens.com/products/bobcat-320-series>
- [90] NAVITAR. “SWIR/Hyperspectral Lenses - SWIR-8”. NAVITAR. Accessed: Aug. 16, 2024. [Online]. Available: <https://www.navitar.com/-/media/project/oneweb/oneweb/navitar/navitar-product/swir/swir-catalog-page-navitar.pdf?la=en&revision=6d4f2a19-1a0b-49c9-8719-d26a6d921765>

- [91] KOWA. "LM100JC1MS | 2/3" 100mm 2MP C-Mount Lens". KOWA. Accessed: Mar. 12, 2024. [Online]. Available: <https://www.kowa-lenses.com/en/lm100jc1ms-2mp-industrial-lens-c-mount>
- [92] THORLABS. "MVL4WA - 3.5 mm EFL, f/1.4, for 1/2" C-Mount Format Cameras, with Lock". THORLABS. Accessed: Mar. 12, 2024. [Online]. Available: <https://www.thorlabs.de/thorproduct.cfm?partnumber=MVL4WA>
- [93] FUJIFILM. "FE185 Series". FUJIFILM. Accessed: Mar. 12, 2024. [Online]. Available: <https://www.fujifilm.com/de/en/business/optical-devices/mvlens/fe185>
- [94] KOWA. "LM100JC1MS(100mmF2.8) Transmission". KOWA. Accessed: Mar. 12, 2024. [Online]. Available: https://www.kowa-lenses.com/media/pdf/34/d4/83/LM100JC1MS_Transmission_03_2020.pdf
- [95] THORLABS. "MVL4WA - Machine Vision Lens Transmission". THORLABS. Accessed: Mar. 12, 2024. [Online]. Available: <https://view.officeapps.live.com/op/view.aspx?src=https%3A%2F%2Fwww.thorlabs.de%2Fimages%2Ftabimages%2FMVL4WA.xlsx&wdOrigin=BROWSELINK>
- [96] ——. "Camera Lenses for Machine Vision". THORLABS. Accessed: Mar. 12, 2024. [Online]. Available: https://www.thorlabs.de/newgrouppage9.cfm?objectgroup_id=1822
- [97] EDMUND OPTICS. "The Correct Material for Infrared (IR) Applications". EDMUND OPTICS. Accessed: Mar. 27, 2024. [Online]. Available: <https://www.edmundoptics.de/knowledge-center/application-notes/optics/the-correct-material-for-infrared-applications/#:~:text=Index%20of%20Refraction%20%E2%80%93%20IR,N%20DSF11%2C%20BOROFLOAT%20AE%20etc.>
- [98] KOFFERMARKT. "Max Koffer MAX540H245 Outdoor Case 2 Rollen leer schwarz". KOFFERMARKT. Accessed: Jun. 20, 2024. [Online]. Available: <https://www.koffermarkt.com/max-koffer-max540h245-outdoor-case-2-rollen/>
- [99] Iker Aldasoro. "AllSkyCam4OLEODL package". READ THE DOCS. Accessed: Aug. 22, 2024. [Online]. Available: <https://allskycam4oleodl.readthedocs.io/en/latest/AllSkyCam4OLEODL.html>
- [100] ALLIED VISION. "VmbPy repository". GITHUB. Accessed: Aug. 22, 2024. [Online]. Available: <https://github.com/alliedvision/VmbPy>
- [101] Iker Aldasoro. "AllSkyCam4OLEODL repository". GITHUB. Accessed: Aug. 22, 2024. [Online]. Available: <https://github.com/Ikerald/AllSkyCam4OLEODL>
- [102] ALLIED VISION. "Python API Manual". READ THE DOCS. Accessed: Aug. 22, 2024. [Online]. Available: https://docs.alliedvision.com/Vimba_X/Vimba_X_DeveloperGuide/pythonAPIManual.html
- [103] "Linearity Goldeye G/CL-008," Allied Vision, Osnabrueck, Germany, Tech. Rep., May. 2024.
- [104] S. Paris, P. Kornprobst, J. Tumblin, F. Durand *et al.*, "Bilateral filtering: Theory and applications," *Foundations and Trends® in Computer Graphics and Vision*, vol. 4, no. 1, pp. 1–73, 2009.
- [105] F. Durand and J. Dorsey, "Fast bilateral filtering for the display of high-dynamic-range images," in *Proceedings of the 29th annual conference on Computer graphics and interactive techniques*, 2002, pp. 257–266.
- [106] N. Otsu *et al.*, "A threshold selection method from gray-level histograms," *Automatica*, vol. 11, no. 285-296, pp. 23–27, 1975.
- [107] A. Nabil, M. Abdelfatah, A. Mousa, and G. El-Fiky, "A new model for reduction of azimuth asymmetry biases of tropospheric delay," *NRIAG Journal of Astronomy and Geophysics*, vol. 8, no. 1, pp. 97–102, 2019.

- [108] PANOTOOLS. "Fisheye Projection". PANOTOOLS. Accessed: Apr. 16, 2024. [Online]. Available: https://wiki.panotools.org/Fisheye_Projection
- [109] K. Miller. "Python API Manual". MATHEMATICS STACK EXCHANGE. Accessed: Aug. 22, 2024. [Online]. Available: <https://math.stackexchange.com/questions/1596513/find-the-bearing-angle-between-two-points-in-a-2d-space>
- [110] R. Paschotta. "Beam Divergence". RP Photonics AG. Accessed: Mar. 7, 2024. [Online]. Available: https://www.rp-photonics.com/beam_divergence.html#:~:text=For%20a%20diffraction,beam%20waist.
- [111] CORNING. "https://math.stackexchange.com/questions/1596513/find-the-bearing-angle-between-two-points-in-a-2d-space". CORNING. Accessed: Mar. 7, 2024. [Online]. Available: <https://www.corning.com/media/worldwide/coc/documents/Fiber/SMF-28%20ULL.pdf>
- [112] H. Yoda, P. Polynkin, and M. Mansuripur, "Beam quality factor of higher order modes in a step-index fiber," *Journal of lightwave technology*, vol. 24, no. 3, pp. 1350–1355, 2006.
- [113] R. Paschotta. "Mode Radius". RP Photonics AG. Accessed: Mar. 7, 2024. [Online]. Available: https://www.rp-photonics.com/mode_radius.html
- [114] ——. "Beam Radius". RP Photonics AG. Accessed: Mar. 7, 2024. [Online]. Available: https://www.rp-photonics.com/beam_radius.html
- [115] R. Jaiswal, "Design and implementation of an integrated optical signal sensor device for telescopes for optical satellite data reception and measurements of signal variations," Master's thesis, Technische Universität Berlin (TUB) - Institute for Aeronautics and Astronautics, 2020.
- [116] S. T. Popescu, P. S. Gheorghe, and A. Petris, "Measuring very low optical powers with a common camera," *Applied Optics*, vol. 53, no. 24, pp. 5460–5464, 2014.

Appendix A

A.1 Main.py

```
1  """Main fuction of the project where everything is called.
2
3  Python version:      3.12.2.
4  Numpy version:      2.0.0.
5  Scipy version:      1.14.0.
6  Matplotlib version: 3.9.1.
7  Mplcursors version: 0.5.3.
8  Tkinter version:    0.1.0.
9  Pytz version:       2024.1.
10 OpenCV version:     4.10.0.84.
11
12
13 Author:
14     Iker Aldasoro - 19.04.2024
15 """
16
17 # C:\Users\alda_ik\Documents\04_PROGRAMMING\02_FINAL_PROJECT\constants.py
18
19 from tkinter import ttk
20 from datetime import datetime
21 from typing import Tuple
22 import time
23 import matplotlib.pyplot as plt
24 import os
25
26 import AllSkyCam40LEODL
27
28
29 def create_graph(
30     elevation_in, payload
31 ) -> Tuple[plt.figure, plt.axes, plt.hlines, list, list]:
32     """Creates the live graph displayed in the GUI:
33
34     1. Creates the plot with an specific size, position, title and labels.
35
36     2. If a payload with full elevation range has been chosen, the graph will be smaller
37     ↪
38     to acomodate the link budget graph.
39
40     3. Initializes the data for the graph.
41
42     Args:
```

```

42     elevation_in (tk.StringVar): Container of the elevation mode (Individual or
43     ↪ Full).
44     payload (tk.StringVar): Container of the payload used (None, K1000, OsirisV1,
45     ↪ Osiris4CubeSat, CubeCat).
46
47 Returns:
48     tuple[plt.figure, plt.axes, plt.hlines, list, list]: fig (plt.figure): Figure of
49     ↪ the created plot.
50
51     ax (plt.axes): Axes of the created plot.
52
53     line (plt.hlines): Lines of the created plot.
54
55     xdata (list): X-axis data from the created plot.
56
57     ydata (list): Y-axis data from the created plot.
58 """
59 # Create figure and axis objects
60 fig, ax = plt.subplots()
61 if elevation_in.get() == "Full" and payload.get() != "None":
62     # Size and position of the intensity graph.
63     fig.set_size_inches(5.38, 3.3)
64     fig.canvas.manager.window.wm_geometry("+5+290")
65     fig.subplots_adjust(left=0.11, right=0.95, top=0.92, bottom=0.13)
66 else:
67     fig.set_size_inches(8.9, 3.3)
68     fig.canvas.manager.window.wm_geometry("+5+290")
69     fig.subplots_adjust(left=0.08, right=0.97, top=0.92, bottom=0.13)
70
71 (line,) = ax.plot([], [], lw=2)
72
73 ax.set_ylim(0, 255)
74 ax.grid()
75 if payload.get() != "None":
76     ax.set_title(
77         f"{payload.get()} downlink on {datetime.now().strftime('%Y-%m-%d')}"
78     )
79 else:
80     ax.set_title(f"Downlink on {datetime.now().strftime('%Y-%m-%d')}")
81 ax.set_xlabel("Time [UTC]")
82 ax.set_ylabel("Brightness")
83
84 # Initialize empty data
85 xdata, ydata = [], []
86
87 return fig, ax, line, xdata, ydata
88
89 def main():
90     AllSkyCam40LEODL.print_preamble()
91     cam_id = AllSkyCam40LEODL.parse_args()
92
93     with AllSkyCam40LEODL.VmbSystem.get_instance():
94         with AllSkyCam40LEODL.get_camera(cam_id) as cam:
95             AllSkyCam40LEODL.print_preamble_settings()
96
97             (
98                 gain_in,
99                 check_in,
100                light_in,

```

```

99         payload_in,
100         h_ogs_in,
101         zenith_in,
102         elevation_in,
103         elevation_angle_in,
104         exposure_in,
105         exposure_time_in,
106         iso_in,
107         root,
108         exposure_time_entry,
109         elevation_angle_entry,
110     ) = AllSkyCam4OLEODL.create_menu()
111
112     def start_streaming():
113         # Validate inputs
114         (
115             elevation_angle,
116             exposure_time_value,
117             zenith,
118             h_ogs,
119         ) = AllSkyCam4OLEODL.checks(
120             elevation_in,
121             elevation_angle_in,
122             exposure_in,
123             exposure_time_in,
124             zenith_in,
125             h_ogs_in,
126         )
127
128         if payload_in.get() != "None":
129             AllSkyCam4OLEODL.link_budget(
130                 elevation_in, elevation_angle, payload_in, zenith, h_ogs
131             )
132
133         # Setup camera
134         AllSkyCam4OLEODL.upload_lut(
135             cam, AllSkyCam4OLEODL.LUT_INDEX, gain_in
136         )
137         AllSkyCam4OLEODL.setup_camera(
138             cam, gain_in, exposure_in, exposure_time_value, iso_in
139         )
140         AllSkyCam4OLEODL.setup_pixel_format(cam)
141         AllSkyCam4OLEODL.grab_frame(cam)
142         AllSkyCam4OLEODL.print_start_stream()
143
144         # Create graph
145         fig, ax, line, xdata, ydata = create_graph(
146             elevation_in, payload_in
147         )
148         # plt.show(block=False) # Show the plot window without blocking
149
150         handler = AllSkyCam4OLEODL.Handler(
151             cam,
152             exposure_time_value,
153             check_in,
154             light_in,
155             gain_in,
156             iso_in,
157             payload_in,
158             elevation_in,

```

```

159         fig,
160         ax,
161         line,
162         xdata,
163         ydata,
164     )
165     handler.create_camera_control_slider(root)
166     plt.ion() # Turn on interactive mode
167     plt.show()
168
169     try:
170         cam.start_streaming(handler=handler, buffer_count=10)
171         while not handler.shutdown_event.is_set():
172             root.update()
173             time.sleep(
174                 0.01
175             ) # Small delay to prevent high CPU usage
176     finally:
177         cam.stop_streaming()
178         AllSkyCam4OLEODL.print_end_stream()
179         handler.save_plot() # Save the plot when streaming stops
180         root.quit()
181         root.destroy()
182         if os.path.isfile(AllSkyCam4OLEODL.BACKGROUND_FRAME_DIR):
183             os.remove(AllSkyCam4OLEODL.BACKGROUND_FRAME_DIR)
184
185     start_button = ttk.Button(
186         root, text="Start Capture", command=start_streaming, width=60
187     )
188     # start_button.grid(row=13, column=0, columnspan=2, pady=10)
189     start_button.grid(
190         row=13, column=0, columnspan=2, pady=10, sticky=""
191     )
192
193     # Initial call to set the correct state of the exposure and elevation
194     AllSkyCam4OLEODL.update_entry(exposure_in, exposure_time_entry)
195     AllSkyCam4OLEODL.update_entry(elevation_in, elevation_angle_entry)
196
197     root.mainloop()
198
199
200 if __name__ == "__main__":
201     main()

```

A.2 AllSkyCam4OLEODL Package

A.2.1 `__init__.py`

```

1 # __init__.py
2
3 from .api import *
4 from .constants import *
5 from .gui import *
6 from .image_processing import *
7 from .input_checks import *

```

```
8 from .link_budget import *
9 from .printer import *
```

A.2.2 api.py

```
1 """This module contains the API of the Allied Vision Goldeye Camera.
2
3 It has been modified in order to allow both streaming and recording. It
4 allows processing of the frames without the need of writting them first.
5 """
6
7 # C:\Users\alda_ik\Documents\O4_PROGRAMMING\O2_FINAL_PROJECT\api.py
8
9 from vmbpy import * # noqa: F403
10
11 from typing import Optional
12 from datetime import datetime, timedelta
13 from tkinter import ttk
14 from matplotlib import dates as mdates
15 import sys
16 import os
17 import threading
18 import cv2
19 import math
20 import pytz
21 import tkinter as tk
22 import matplotlib.pyplot as plt
23 import matplotlib.animation as animation
24
25 from . import image_processing as im
26 from . import constants as const
27 from . import printer as pri
28
29 # All frames will either be recorded in this format, or transformed to it before being
30 ↪ displayed
31 opencv_display_format = PixelFormat.Bgr8 # noqa: F405
32
33 def feature_changed_handler(feature) -> None:
34     """API proprietary printing fuction to indicate a changed of value of a feature.
35
36     Args:
37         feature (_type_): Feature to be changed.
38     """
39     msg = "Feature '{}' changed value to '{}'"
40     print(msg.format(str(feature.get_name()), str(feature.get())), flush=True)
41
42
43 def abort(reason: str, return_code: int = 1, usage: bool = False) -> None:
44     """API proprietary exiting fuction and indicate an error.
45
46     Args:
47         reason (str): Reason to abort operation.
48         return_code (int, optional): Error code raised. Defaults to 1.
49         usage (bool, optional): Bool to check if an argument has been parsed. Defaults
50         ↪ to False.
51     """
51     print(reason + "\n")
```

```

52
53     if usage:
54         pri.print_usage()
55
56     sys.exit(return_code)
57
58
59 def parse_args() -> Optional[str]:
60     """API proprietary fuction to parse an argument.
61
62     Returns:
63         Optional[str]: Parsed argument.
64     """
65     args = sys.argv[1:]
66     argc = len(args)
67
68     for arg in args:
69         if arg in ("/h", "-h"):
70             pri.print_usage()
71             sys.exit(0)
72
73     if argc > 1:
74         abort(
75             reason="Invalid number of arguments. Abort.",
76             return_code=2,
77             usage=True,
78         )
79
80     return None if argc == 0 else args[0]
81
82
83 def get_camera(camera_id: Optional[str]) -> Camera: # noqa: F405
84     """API proprietary fuction to obtain the camera.
85
86     Args:
87         camera_id (Optional[str]): Specific camera we want to connect to.
88
89     Returns:
90         Camera: Camera we have connected to.
91     """
92     with VmbSystem.get_instance() as vmb: # noqa: F405
93         # ip = vmb.GevDeviceForceIPAddress.get()
94         if camera_id:
95             try:
96                 return vmb.get_camera_by_id(camera_id)
97
98             except VmbCameraError: # noqa: F405
99                 abort("Failed to access Camera '{}'. Abort.".format(camera_id))
100
101         else:
102             cams = vmb.get_all_cameras()
103             if not cams:
104                 abort("No Cameras accessible. Abort.")
105
106             return cams[0]
107
108
109 def setup_camera(
110     cam: Camera, # noqa: F405
111     gain: tk.StringVar,

```

```

112     exposure: tk.StringVar,
113     exposure_time_value: int,
114     iso: tk.StringVar,
115 ) -> None:
116     """Configures the camera based on user inputs:
117
118     1. Checks camera mode, if the own camera's background is chosen, it needs be
119     ↪ enabled.
120
121     2. Sets the gain mode, either 0dB or 18dB.
122
123     3. Selects the exposure mode, Auto or Manual. If Manual, sets the exposure value.
124
125     4. Enables white balancing if camera supports it.
126
127     5. Adjusts GeV packet size (just for PoE camera).
128
129     Args:
130     cam (Camera): Camera object from the VMBPY API module.
131     gain (tk.StringVar): Container of the gain mode (0 [0 dB] or 1 [18 dB]).
132     exposure (tk.StringVar): Container of the exposure mode (Manual or Auto).
133     exposure_time_value (int): Specified exposure value for Manual mode.
134     iso (tk.StringVar): Container of the camera mode: Normal, Hot-pixel
135     ↪ subtraction, Subtraction or Camera's BC.
136     """
137
138     with cam:
139         # print(cam.LUTEnable)
140         # lut = cam.LUTEnable.get()
141         # print(cam.LUTEnable.get())
142         # # lut = True
143         # lut = True
144         # print(cam.LUTEnable)
145         # print(lut)
146         # cam.LUTEnable.set(lut)
147         # print(cam.LUTEnable)
148         # print(cam.LUTEnable)
149         # cam.LUTEnable.value(True)
150         # print(cam.LUTEnable)
151
152         # Default settings
153         cam.BCMode.set("Off")
154         cam.IntegrationMode.set("IntegrateWhileRead")
155         # cam.IntegrationMode.set("IntegrateThenRead")
156         print(cam.IntegrationMode)
157
158         # Background Correction settings
159         if iso.get() == "Camera's BC":
160             cam.BCMode.set("On")
161             cam.BCIntegrationStart.run()
162             print(cam.BCMode)
163
164         # lut_enable = cam.LUTEnable
165         # print(lut_enable)
166         # lut_enable.set(True)
167         # print(lut_enable)
168
169         # Gain settings
170         if gain.get() == "1 [18 dB]":
171             try:
172                 cam.SensorGain.set("Gain1")

```

```

170         except (AttributeError, VmbFeatureError): # noqa: F405
171             pass
172     else:
173         try:
174             cam.SensorGain.set("Gain0")
175         except (AttributeError, VmbFeatureError): # noqa: F405
176             pass
177     print(cam.SensorGain)
178
179     # Exposure settings
180     if exposure.get() == "Manual":
181         try:
182             cam.ExposureAuto.set("Off")
183             exposure_time = cam.ExposureTime
184             exposure_time.set(exposure_time_value)
185         except (AttributeError, VmbFeatureError): # noqa: F405
186             pass
187     else:
188         try:
189             cam.ExposureAuto.set("Continuous")
190         except (AttributeError, VmbFeatureError): # noqa: F405
191             pass
192
193     # White balancing settings
194     try:
195         cam.BalanceWhiteAuto.set("Continuous")
196     except (AttributeError, VmbFeatureError): # noqa: F405
197         pass
198
199     # GeV packet size settings (only available for GigE Cameras)
200     try:
201         stream = cam.get_streams()[0]
202         stream.GVSPAdjustPacketSize.run()
203         while not stream.GVSPAdjustPacketSize.is_done():
204             pass
205     except (AttributeError, VmbFeatureError): # noqa: F405
206         pass
207
208
209 def setup_pixel_format(cam: Camera) -> None: # noqa: F405
210     """Configures the camera's pixel format:
211
212     1. Retrieves all the camera's compatible color pixel formats.
213
214     2. Filters out formats not compatible with OpenCV.
215
216     3. Retrieves all the camera's compatible monochrome pixel formats.
217
218     4. Filters out formats not compatible with OpenCV.
219
220     5. Selects the OpenCV-compatible color pixel format. If none exist, attempts
221     to convert an incompatible format to be compatible. If conversion is not possible,
222     selects an OpenCV-compatible monochrome pixel format.
223
224     Args:
225         cam (Camera): Camera object from the VMBPY API module.
226     """
227     # Available color pixel formats. Prefer color formats over monochrome formats
228     cam_formats = cam.get_pixel_formats()
229     cam_color_formats = intersect_pixel_formats( # noqa: F405

```



```

230     cam_formats,
231     COLOR_PIXEL_FORMATS, # noqa: F405
232 )
233 convertible_color_formats = tuple(
234     f
235     for f in cam_color_formats
236     if opencv_display_format in f.get_convertible_formats()
237 )
238
239 cam_mono_formats = intersect_pixel_formats(cam_formats, MONO_PIXEL_FORMATS) # noqa:
    ↪ F405
240 convertible_mono_formats = tuple(
241     f
242     for f in cam_mono_formats
243     if opencv_display_format in f.get_convertible_formats()
244 )
245
246 # Use OpenCV color format
247 if opencv_display_format in cam_formats:
248     cam.set_pixel_format(opencv_display_format)
249
250 # Else convert color to OpenCV format
251 elif convertible_color_formats:
252     cam.set_pixel_format(convertible_color_formats[0])
253
254 # Else use OpenCV monochrome format
255 elif convertible_mono_formats:
256     cam.set_pixel_format(convertible_mono_formats[0])
257
258 else:
259     abort("Camera does not support an OpenCV compatible format. Abort.")
260
261
262 def upload_lut(
263     cam: Camera, # noqa: F405
264     lut_dataset_selector_index: int,
265     gain: tk.StringVar,
266 ) -> None: # noqa: F405
267     """Uploads and enables the LUT:
268
269     1. Checks the gain to select the correct LUT path.
270
271     2. Opens the LUT file, loads it into the camera and runs it.
272
273     3. Prints the directory and selected LUT.
274
275     Args:
276         cam (Camera): Camera object from the VMBPY API module.
277         lut_dataset_selector_index (int): Index of the selected LUT.
278         gain (tk.StringVar): Container of the gain mode for choosing the LUT (0 [0 dB]
    ↪ or 1 [18 dB]).
279     """
280     # Set directory
281     if gain.get() == "1 [18 dB]":
282         dir = const.LUT_DIR1
283     else:
284         dir = const.LUT_DIR0
285
286     # Read LUT, upload to camera
287     with cam:

```

```

288     with open(dir, mode="rb") as file:
289         fileContent = file.read()
290
291         cam.LUTDatasetSelector.set(lut_dataset_selector_index)
292         cam.LUTValueAll.set(fileContent)
293
294         cam.LUTDatasetSave.run()
295
296     print(
297         f"LUT from file {dir} loaded into LUT Nr.{lut_dataset_selector_index}."
298     )
299
300
301 def grab_frame(cam: Camera) -> None: # noqa: F405
302     """Captures a frame to be used as a temporal frame:
303
304     1. Grabs a frame from the camera.
305
306     2. Saves the frame in the specified directory.
307
308     Args:
309         cam (Camera): Camera object from the VMBPY API module.
310     """
311     frame = cam.get_frame()
312     cv2.imwrite(const.BACKGROUND_FRAME_DIR, frame.as_opencv_image())
313
314
315 class Handler:
316     """Handles the majority of the camera operation.
317
318     Methods:
319
320         __init__:           Initializes the Handler class.
321
322         update:            Updates the live graph of the GUI.
323
324         save_plot:        Saves the plot stored in the instance.
325
326         create_camera_control_slider: Creates an slider, saves it in the instance.
327
328         set_exposure:     Updates the exposure value.
329
330         set_min_max_value: Updates the minimum or maximum spot size value.
331
332         __call__:        Between each frame, sends the frame for
333                         processing, prepares for the next one, and checks if the program has stopped.
334     """
335
336     def __init__(
337         self,
338         cam: Camera, # noqa: F405
339         exposure_time_value: int,
340         check: tk.StringVar,
341         light: tk.StringVar,
342         gain: tk.StringVar,
343         iso: tk.StringVar,
344         payload: tk.StringVar,
345         elevation_in: tk.StringVar,
346         fig: plt.figure,
347         ax: plt.axes,

```

```

348     line: plt.hlines,
349     xdata: list,
350     ydata: list,
351 ):
352     """Initializes the Handler class with the specified camera and plotting
353     parameters, and creates a directory for storing the frames:
354
355     1. Sets up all necessary instances based on the chosen settings.
356
357     2. Creates the directory for saving frames according to the specified settings
358     (will be saves in the data directory on the root folder of the project,
359     inside a folder called tracking_images).
360
361     Args:
362         self (Instance): Current instance, provides access to attributes and
363         ↪ methods.
364         cam (Camera): Camera object from the VMBPY API module.
365         exposure_time_value (int): Specified exposure value for Manual mode.
366         check (tk.StringVar): Container of the streaming mode.
367         light (tk.StringVar): Container of the time of day.
368         gain (tk.StringVar): Container of the gain mode (0 [0 dB] or 1 [18 dB]).
369         iso (tk.StringVar): Container of the camera mode: Normal, Hot-pixel
370         ↪ subtraction, Subtraction or Camera's BC.
371         payload (tk.StringVar): Container of the payload.
372         elevation_in (tk.StringVar): Container of the elevation mode.
373         fig (plt.figure): Figure for the GUI plot.
374         ax (plt.axes): Axes for the GUI plot.
375         line (plt.hlines): Lines for the GUI plot
376         xdata (list): Data for the x-axis for the GUI plot
377         ydata (list): Data for the y-axis for the GUI plot
378
379     :no-index:
380     """
381     # Setting up instances
382     self.shutdown_event = threading.Event()
383     self.cam = cam
384     self.exposure_slider = None
385     self.min_value = 1
386     self.max_value = const.H_SENSOR_SIZE * const.V_SENSOR_SIZE
387     self.root = None
388
389     # Input instances
390     self.gain = 1
391     self.counter = 0
392     self.background = 0
393     self.mode = 0
394     self.cond = 0
395
396     # Graph instances
397     self.fig = fig
398     self.ax = ax
399     self.line = line
400     self.xdata = xdata
401     self.ydata = ydata
402
403     # Graph's update
404     self.ani = animation.FuncAnimation(
405         self.fig,
406         self.update_graph,
407         interval=100,

```

```

406         blit=False,
407         cache_frame_data=False,
408     )
409
410     # Directory where the tracking frames get saved: directory of script.
411     d = r".\data"
412
413     self.payload = payload.get()
414     # self.elevation_mode = elevation_in.get()
415     if gain.get() == "1 [18 dB]":
416         self.gain = 1
417     else:
418         self.gain = 0
419
420     if iso.get() == "Normal":
421         self.background = 0
422     elif iso.get() == "Subtraction":
423         self.background = 1
424     elif iso.get() == "Camera's BC":
425         self.background = 2
426     else:
427         self.background = 3
428
429     if light.get() == "Daytime":
430         self.cond = 0
431     else:
432         self.cond = 1
433
434     if check.get() == "Record":
435         # Directory creation
436         self.mode = 1
437         now = datetime.now()
438         if exposure_time_value == 1:
439             foldername_NP = (
440                 f"tc_{now.strftime('%Y')}{now.strftime('%m')}{now.strftime('%d')}_-"
441                 f"{now.strftime('%H')}{now.strftime('%m')}{now.strftime('%S')}_-"
442                 f"exp_AUTO_GAIN{self.gain}_NP"
443             )
444         if self.background == 0:
445             foldername = (
446                 f"tc_{now.strftime('%Y')}{now.strftime('%m')}{now.}
447                 ↪ strftime('%d')}_-"
448                 f"{now.strftime('%H')}{now.strftime('%m')}{now.strftime('%S')}"
449                 f"_exp_AUTO_GAIN{self.gain}"
450             )
451         elif self.background == 1:
452             foldername = (
453                 f"tc_{now.strftime('%Y')}{now.strftime('%m')}{now.}
454                 ↪ strftime('%d')}_-"
455                 f"{now.strftime('%H')}{now.strftime('%m')}{now.strftime('%S')}_-"
456                 f"exp_AUTO_GAIN{self.gain}_IS"
457             )
458         elif self.background == 2:
459             foldername = (
460                 f"tc_{now.strftime('%Y')}{now.strftime('%m')}{now.}
461                 ↪ strftime('%d')}_-"
462                 f"{now.strftime('%H')}{now.strftime('%m')}{now.strftime('%S')}_-"
463                 f"exp_AUTO_GAIN{self.gain}_CAMERA_BC"
464             )
465         else:

```

```

463         foldername = (
464             f"tc_{now.strftime('%Y')}{now.strftime('%m')}{now.}
             ↪ strftime('%d')}_ "
465             f"{now.strftime('%H')}{now.strftime('%m')}{now.strftime('%S')}_ "
466             f"exp_AUTO_GAIN{self.gain}_HP"
467         )
468     else:
469         foldername_NP = (
470             f"tc_{now.strftime('%Y')}{now.strftime('%m')}{now.strftime('%d')}_ "
471             f"{now.strftime('%H')}{now.strftime('%m')}{now.strftime('%S')}_ "
472             f"exp_{exposure_time_value}us_GAIN{self.gain}_NP"
473         )
474     if self.background == 0:
475         foldername = (
476             f"tc_{now.strftime('%Y')}{now.strftime('%m')}{now.}
             ↪ strftime('%d')}_ "
477             f"{now.strftime('%H')}{now.strftime('%m')}{now.strftime('%S')}_ "
478             f"exp_{exposure_time_value}us_GAIN{self.gain}"
479         )
480     if self.background == 1:
481         foldername = (
482             f"tc_{now.strftime('%Y')}{now.strftime('%m')}{now.}
             ↪ strftime('%d')}_ "
483             f"{now.strftime('%H')}{now.strftime('%m')}{now.strftime('%S')}_ "
484             f"exp_{exposure_time_value}us_GAIN{self.gain}_IS"
485         )
486     if self.background == 2:
487         foldername = (
488             f"tc_{now.strftime('%Y')}{now.strftime('%m')}{now.}
             ↪ strftime('%d')}_ "
489             f"{now.strftime('%H')}{now.strftime('%m')}{now.strftime('%S')}_ "
490             f"exp_{exposure_time_value}us_GAIN{self.gain}_CAMERA_BC"
491         )
492     else:
493         foldername = (
494             f"tc_{now.strftime('%Y')}{now.strftime('%m')}{now.}
             ↪ strftime('%d')}_ "
495             f"{now.strftime('%H')}{now.strftime('%m')}{now.strftime('%S')}_ "
496             f"exp_{exposure_time_value}us_GAIN{self.gain}_HP"
497         )
498
499     if elevation_in.get() == "Full" and self.payload != "None":
500         foldername = foldername + "_" + self.payload
501         foldername_NP = foldername_NP + "_" + self.payload
502
503     self.pnp = os.path.join(d, "tracking_images", foldername_NP)
504     self.p = os.path.join(d, "tracking_images", foldername)
505
506     os.makedirs(self.p)
507     os.makedirs(self.pnp)
508
509     def update_graph(self, frame: Frame) -> plt.hlines: # noqa: F405
510         """Updates the live graph of the GUI with new data stored in the current
             ↪ instance (self):
511
512         1. If data is available, plots it on the graph.
513
514         2. Adjusts the graph's horizontal and vertical limits, extends the x-axis by 60
             ↪ seconds, and increase the y-axis limit by 10% of the maximum value.
515
516

```

```

517     3. Updates the graph's format as needed.
518
519     4. Plots the new data on the graph.
520
521     Args:
522         self (Instance): Current instance, provides access to attributes and
                    ↪ methods.
523         frame (Frame): Frame object from the VMBPY API module.
524
525     Returns:
526         plt.Hlines: Updated graph instance.
527
528     :no-index:
529     """
530     if not self.xdata: # If no data, just return
531         return (self.line,)
532
533     # Ensure xdata is in UTC
534     self.xdata = [x.astimezone(pytz.UTC) for x in self.xdata]
535
536     self.line.set_data(self.xdata, self.ydata)
537     ax = self.ax
538
539     # Update axis limits
540     ax.set_xlim(
541         self.xdata[0],
542         max(self.xdata[-1], self.xdata[0] + timedelta(seconds=60)),
543     )
544
545     if self.ydata:
546         ax.set_ylim(0, max(255, max(self.ydata) * 1.1))
547
548     # Update the formatter to show appropriate range
549     locator = mdates.AutoDateLocator()
550     # formatter = mdates.AutoDateFormatter(locator)
551     formatter = mdates.DateFormatter("%H:%M:%S", tz=mdates.UTC)
552     ax.xaxis.set_major_locator(locator)
553     ax.xaxis.set_major_formatter(formatter)
554
555     self.fig.canvas.draw()
556     return (self.line,)
557
558     def save_plot(self) -> None:
559         """Saves the plot stored in the current instance (self):
560
561         1. If recording mode is selected, sets the plot size, data, title, and labels.
562
563         2. Adjust the format of the time as H:M:S.
564
565         3. If a payload is chosen, its name will be added to the plot's title.
566
567         4. Saves the plot in the same directory as the recorded frames (stored in the
568            instance).
569
570         Args:
571             self (Instance): Current instance, provides access to attributes and
                    ↪ methods.
572
573         :no-index:
574         """

```

```

575     if self.mode != 0: # Only save if in recording mode
576         plt.figure(figsize=(20, 8))
577         plt.plot(self.xdata, self.ydata)
578
579         # Enable the grid
580         plt.grid(True)
581
582         # Format the x-axis ticks
583         time_format = mdates.DateFormatter("%H:%M:%S")
584         plt.gca().xaxis.set_major_formatter(time_format)
585
586         plt.xlabel("Time [UTC]")
587         plt.ylabel("Brightness")
588         plt.gcf().autofmt_xdate() # Rotate and align the tick labels
589         # Adjust layout manually for a tighter fit, but not as tight as
590         # plt.tight_layout()
591         plt.subplots_adjust(left=0.05, right=0.95, top=0.95, bottom=0.1)
592         # plt.tight_layout()
593         if self.payload != "None":
594             plt.title(
595                 f"{self.payload} downlink on {datetime.now().strftime('%Y-%m-%d')}")
596             plt.savefig(
597                 f"{self.p}/{datetime.now().strftime('%Y-%m-%d')}__{self.}
598                 ↪ payload}_DL_plot.png"
599             )
600         else:
601             plt.title(f"Downlink on {datetime.now().strftime('%Y-%m-%d')}")
602             plt.savefig(
603                 f"{self.p}/{datetime.now().strftime('%Y-%m-%d')}_DL_plot.png"
604             )
605         plt.close()
606
607 def create_camera_control_slider(self, root: tk.Tk) -> None:
608     """Creates a slider, saves it in the current instance (self) and sets its
609     initial values:
610
611     1. Creates a slider within the current instance using the CameraControlSlider
612     class.
613
614     2. Sets the initial values of the minimum and maximum spot size and the
615     exposure with set_initial_values().
616
617     Args:
618         self (Instance): Current instance, provides access to attributes and
619         ↪ methods.
620         root (tk.Tk): Main window of the GUI menu.
621
622     :no-index:
623     """
624     self.camera_control_slider = CameraControlSlider(root, self)
625     current_exposure = self.cam.ExposureTime.get()
626     self.camera_control_slider.set_initial_values(
627         current_exposure, self.min_value, self.max_value
628     )
629
630 def set_exposure(self, exposure_time: int) -> None:
631     """Updates the exposure value stored in the current instance (self).

```

```

632         self (Instance): Current instance, provides access to attributes and
        ↪ methods.
633         exposure_time (int): Exposure time value.
634 :no-index:
635 """
636 try: # Tries to update the exposure time
637     self.cam.ExposureTime.set(exposure_time)
638 except (AttributeError, VmbFeatureError): # noqa: F405
639     print("Failed to set exposure time")
640
641 def set_min_max_value(self, value: int, siz: int) -> None:
642     """Updates the minimum or maximum spot size value stored in the current
643     instance (self).
644
645     Args:
646         self (Instance): Current instance, provides access to attributes and
        ↪ methods.
647         value (int): Final minimum or maximum spot size value.
648         siz (int): Integer to diferenciare if we want to change the minimum or the
        ↪ maximum spot size value,
649         1 for the maximum, 0 for minimum.
650
651     :no-index:
652     """
653     if siz == 1: # Max value
654         self.max_value = value
655         print(f"Max value set to: {value}")
656     else:
657         self.min_value = value
658         print(f"Min value set to: {value}")
659
660 def __call__(self, cam: Camera, stream: Stream, frame: Frame) -> None: # noqa:
    ↪ F405
661     """Between each frame, sends the current frame for processing, prepares for
662     the next one, and checks if the program has stopped:
663
664     1. If program shutdown is activated, exits the fuction.
665
666     2. If a frame has been grabbed, increments the counter and starts image
667     processing.
668
669     3. Prepares for the next frame and checks if program is stopped (by
670     pressing q / Q)
671
672     Args:
673         self (Instance): Current instance, provides access to attributes and
        ↪ methods.
674         cam (Camera): Camera object from the VMBPY API module.
675         stream (Stream): Stream object from the VMBPY API module.
676         frame (Frame): Frame object from the VMBPY API module.
677
678     :no-index:
679     """
680     if self.shutdown_event.is_set():
681         return
682
683     if frame.get_status() == FrameStatus.Complete: # noqa: F405
684         self.counter += 1
685         # Image Processing fuction
686         im.frame_processing(self, cam, frame)

```



```

687
688     cam.queue_frame(frame)
689
690     # Check for 'q' key press to stop recording
691     if cv2.waitKey(1) & 0xFF == ord("q") or cv2.waitKey(1) & 0xFF == ord(
692         "Q"
693     ):
694         self.shutdown_event.set()
695         if self.root:
696             self.root.quit()
697
698
699 class CameraControlSlider(tk.Toplevel):
700     """Handles the sliders of the GUI menu.
701
702     Methods:
703
704         __init__: Initializes the CameraControlSlider class.
705
706         setup_exposure_slider: Creates the exposure slider.
707
708         setup_min_value_slider: Creates the minimum spot size value slider.
709
710         setup_max_value_slider: Creates the maximum spot size value slider
711
712         update_exposure: Updates the exposure value.
713
714         update_min_value: Updates the minimum spot size value.
715
716         update_max_value: Updates the maximum spot size value.
717
718         update_from_exposure_entry: Updates the exposure value parsed through the
719         ↪ button.
720
721         update_from_min_entry: Updates the minimum spot size value parsed through the
722         ↪ button.
723
724         update_from_max_entry: Updates the maximum spot size value parsed through the
725         ↪ button.
726
727         set_initial_values: Sets the intial values for all the varibales of the sliders.
728
729     Args:
730         tk (tk.Toplevel): Window where the slider should be created.
731     """
732
733     def __init__(self, master: tk.Tk, camera_control: Handler):
734         """Initializes the CameraControlSlider class with the specified
735         GUI parameters, and creates the sliders:
736
737         1. Sets up all necessary instances for the slider elements in the menu.
738
739         2. Configures exposure, minimum, and maximum spot size using the appropriate
740         ↪ functions.
741
742     Args:
743         self (Instance): Current instance, provides access to attributes and
744         ↪ methods.
745         master (tk.Tk): Tinker GUI window.
746         camera_control (Handler): Parsed through handler.

```

```

742     """
743     # Allows the child class to invoke the constructor of its parent class.
744     super().__init__(master)
745     self.camera_control = camera_control
746     self.title("Camera Control Sliders")
747     # Dimensions and position of the control sliders (WidthxHeight+X+Y).
748     self.geometry("370x285+900+360")
749
750     # Creates a frame to hold min and max sliders side by side
751     self.min_max_frame = ttk.Frame(self)
752     self.min_max_frame.pack(fill="x", expand=True, pady=10)
753
754     # Slider setup
755     # Exposure slider
756     self.setup_exposure_slider()
757     # Min value slider
758     self.setup_min_value_slider()
759     # Max value slider
760     self.setup_max_value_slider()
761
762     def setup_exposure_slider(self) -> None:
763         """Creates the exposure slider:
764
765         1. Initializes all slider elements and converts the exposure to a logarithmic
766            ↪ scale.
767
768         2. Sets up the displayed exposure value and its slider.
769
770         3. Configures the button to manually change the exposure value.
771
772         Args:
773             self (Instance): Current instance, provides access to attributes and
774                ↪ methods.
775         """
776         # Initial values are converted to a logarithmic scale
777         self.min_exposure = 10
778         self.max_exposure = 3000000 # 1 second
779         self.log_min_exposure = math.log10(self.min_exposure)
780         self.log_max_exposure = math.log10(self.max_exposure)
781
782         self.current_exposure = tk.DoubleVar(value=self.log_min_exposure)
783         ttk.Label(self, text="Exposure Control").pack(pady=(10, 0))
784
785         self.exposure_label = ttk.Label(
786             self, text=f"Exposure: {self.min_exposure:.2f} μs"
787         )
788         self.exposure_label.pack(pady=(0, 5))
789
790         # Exposure slider settings
791         self.exposure_slider = ttk.Scale(
792             self,
793             from_=0,
794             to=1000,
795             orient="horizontal",
796             length=600,
797             command=self.update_exposure, # Calls the function on each value change
798             variable=self.current_exposure,
799         )
800         self.exposure_slider.pack(pady=5, padx=20, fill="x")

```

```

800     self.exposure_entry = ttk.Entry(self, width=10)
801     self.exposure_entry.pack(pady=5)
802     self.exposure_entry.bind("<Return>", self.update_from_exposure_entry)
803
804     self.exposure_set_button = ttk.Button(
805         self, text="Set Exposure", command=self.update_from_exposure_entry
806     )
807     self.exposure_set_button.pack(pady=5)
808
809 def setup_min_value_slider(self) -> None:
810     """Creates the minimum spot size value slider:
811
812     1. Initializes all slider elements and converts the minimum spot size value to a
813     ↪ logarithmic scale.
814
815     2. Sets up the displayed minimum value and its slider.
816
817     3. Configures the button to manually change the minimum spot size value.
818
819     Args:
820     self (Instance): Current instance, provides access to attributes and
821     ↪ methods.
822     """
823
824     self.min_value = 1
825     self.max_value = const.H_SENSOR_SIZE * const.V_SENSOR_SIZE
826     self.log_min_value = math.log10(self.min_value)
827     self.log_max_value = math.log10(self.max_value)
828
829     self.current_min = tk.DoubleVar(value=self.log_min_value)
830
831     min_frame = ttk.Frame(self.min_max_frame)
832     min_frame.pack(side="left", expand=True, fill="x", padx=10)
833
834     ttk.Label(min_frame, text="Minimum Value Control").pack()
835     self.min_label = ttk.Label(
836         min_frame, text=f"Min. Beam Spot Size: {self.min_value:.0f}"
837     )
838     self.min_label.pack()
839
840     self.min_slider = ttk.Scale(
841         min_frame,
842         from_=0,
843         to=1000,
844         orient="horizontal",
845         command=self.update_min_value,
846         variable=self.current_min,
847     )
848     self.min_slider.pack(fill="x")
849
850     self.min_entry = ttk.Entry(min_frame, width=10)
851     self.min_entry.pack()
852     self.min_entry.bind("<Return>", self.update_from_min_entry)
853
854     self.min_set_button = ttk.Button(
855         min_frame, text="Set Min", command=self.update_from_min_entry
856     )
857     self.min_set_button.pack()
858
859 def setup_max_value_slider(self) -> None:
860     """Creates the maximum spot size value slider:

```

```

858
859     1. Initializes all slider elements and converts the maximum spot size value to a
      ↪ logarithmic scale.
860
861     2. Sets up the displayed maximum value and its slider.
862
863     3. Configures the button to manually change the maximum spot size value.
864
865     Args:
866         self (Instance): Current instance, provides access to attributes and
      ↪ methods.
867     """
868     self.current_max = tk.DoubleVar(value=self.log_max_value)
869
870     max_frame = ttk.Frame(self.min_max_frame)
871     max_frame.pack(side="right", expand=True, fill="x", padx=10)
872
873     ttk.Label(max_frame, text="Maximum Value Control").pack()
874     self.max_label = ttk.Label(
875         max_frame, text=f"Max Beam Spot Size: {self.max_value:.0f}"
876     )
877     self.max_label.pack()
878
879     self.max_slider = ttk.Scale(
880         max_frame,
881         from_=0,
882         to=1000,
883         orient="horizontal",
884         command=self.update_max_value,
885         variable=self.current_max,
886     )
887     self.max_slider.pack(fill="x")
888
889     self.max_entry = ttk.Entry(max_frame, width=10)
890     self.max_entry.pack()
891     self.max_entry.bind("<Return>", self.update_from_max_entry)
892
893     self.max_set_button = ttk.Button(
894         max_frame, text="Set Max", command=self.update_from_max_entry
895     )
896     self.max_set_button.pack()
897
898     def update_exposure(self, event=None) -> None:
899         """Updates the exposure value parsed through the slider:
900
901         1. Gets the exposure from the slider and converts it to a logarithmic scale.
902
903         2. Sends the updated exposure value to the camera.
904
905         Args:
906             self (Instance): Current instance, provides access to attributes and
      ↪ methods.
907             event (_type_, optional): Nothing, just compatibility purposes. Defaults to
      ↪ None.
908         """
909         log_value = (
910             self.exposure_slider.get()
911             / 1000
912             * (self.log_max_exposure - self.log_min_exposure)
913             + self.log_min_exposure

```

```

914     )
915     print(f"the log_value in update_exposure is {log_value}")
916     print(
917         f"the self.exposure_slider.get() in update_exposure is
          ↪ {self.exposure_slider.get()}"
918     )
919     print(
920         f"the self.log_max_exposure in update_exposure is {self.log_max_exposure}"
921     )
922     print(
923         f"the self.log_min_exposure in update_exposure is {self.log_min_exposure}"
924     )
925     exposure = round(10**log_value)
926     self.exposure_label.config(text=f"Exposure: {exposure:.2f} µs")
927     self.camera_control.set_exposure(exposure)
928     self.exposure_entry.delete(0, tk.END)
929     self.exposure_entry.insert(0, str(exposure))
930
931     def update_min_value(self, event=None) -> None:
932         """Updates the minimum spot size value parsed through the slider:
933
934         1. Gets the minimum spot size value from the slider and converts it to a
          ↪ logarithmic scale.
935
936         2. If the minimum selected spot size value is bigger than the maximum
          spot size value, the maximum spot size value is selected as the minimum
          spot size value. If a negative value is selected, it will be converted to 0.
937
938         Args:
939
940         self (Instance): Current instance, provides access to attributes and
          ↪ methods.
941         event (_type_, optional): Nothing, just compatibility purposes. Defaults to
          ↪ None.
942
943         """
944         log_value = (
945             self.min_slider.get()
946             / 1000
947             * (self.log_max_value - self.log_min_value)
948             + self.log_min_value
949         )
950         min_value = round(10**log_value)
951         self.min_value = max(0, min(self.max_value - 1, min_value))
952         self.min_label.config(text=f"Min Value: {self.min_value:.2f}")
953         # Updates min value
954         self.camera_control.set_min_max_value(self.min_value, 0)
955         self.min_entry.delete(0, tk.END)
956         self.min_entry.insert(0, str(self.min_value))
957
958     def update_max_value(self, event=None) -> None:
959         """Updates the maximum spot size value parsed through the slider:
960
961         1. Gets the maximum spot size value from the slider and converts it to a
          ↪ logarithmic scale.
962
963         2. The maximum selected spot size value will be the maximum value between
          the minimum spot size value and the smaller value between the maximum spot
          size value selected from the slider and whole dimensions of the image.
964
965         Args:
966
967         self (Instance): Current instance, provides access to attributes and
          ↪ methods.
968

```

```

969         event (_type_, optional): Nothing, just compatibility purposes. Defaults to
970         ↪ None.
971     """
972     log_value = (
973         self.max_slider.get()
974         / 1000
975         * (self.log_max_value - self.log_min_value)
976         + self.log_min_value
977     )
978     max_value = round(10**log_value)
979     self.max_value = max(
980         self.min_value,
981         min((const.H_SENSOR_SIZE * const.V_SENSOR_SIZE), max_value),
982     )
983     self.max_label.config(text=f"Max Value: {self.max_value:.2f}")
984     self.camera_control.set_min_max_value(self.max_value, 1)
985     self.max_entry.delete(0, tk.END)
986     self.max_entry.insert(0, str(self.max_value))
987
988 def update_from_exposure_entry(self, event=None) -> None:
989     """Updates the exposure value parsed through the button:
990
991     1. Gets the exposure value and converts it to a logarithmic scale if it
992     is in the correct range. If not, it raises an error.
993
994     2. Updates the exposure value calling the update_exposure() function.
995
996     Args:
997     self (Instance): Current instance, provides access to attributes and
998     ↪ methods.
999     event (_type_, optional): Nothing, just compatibility purposes. Defaults to
1000     ↪ None.
1001
1002     Raises:
1003     ValueError: Exposure time inputed in the text-box is either bigger than the
1004     maximum exposure time or smaller than the smallest exposure time.
1005     """
1006     try:
1007         exposure = float(self.exposure_entry.get())
1008         if self.min_exposure <= exposure <= self.max_exposure:
1009             log_value = (
1010                 (math.log10(exposure) - self.log_min_exposure)
1011                 / (self.log_max_exposure - self.log_min_exposure)
1012                 * 1000
1013             )
1014             self.exposure_slider.set(log_value)
1015             # Updates the exposure value
1016             self.update_exposure(None)
1017         else:
1018             raise ValueError
1019     except ValueError:
1020         self.exposure_entry.delete(0, tk.END)
1021         self.exposure_entry.insert(
1022             0, str(round(10 ** self.current_exposure.get()))
1023         )
1024
1025 def update_from_min_entry(self, event=None) -> None:
1026     """Updates the minimum spot size value parsed through the button:
1027
1028     1. Gets the minimum spot size value and converts it to a logarithmic scale if

```

```

1026         it is bigger than zero but smaller than the maximum value.
1027
1028     2. Updates the minimum spot size value calling the update_min_value() function.
1029
1030     Args:
1031         self (Instance): Current instance, provides access to attributes and
1032             ↪ methods.
1033         event (_type_, optional): Nothing, just compatibility purposes. Defaults to
1034             ↪ None.
1035
1036     Raises:
1037         ValueError: Minimum spot size value is either smaller than zero or bigger
1038             than the maximum spot size value.
1039     """
1040     try:
1041         min_value = int(self.min_entry.get())
1042         if 0 <= min_value < self.max_value:
1043             self.min_value = min_value
1044             log_value = (
1045                 (math.log10(max(1, min_value)) - self.log_min_value)
1046                 / (self.log_max_value - self.log_min_value)
1047                 * 1000
1048             )
1049             self.min_slider.set(log_value)
1050             # Updates the min spot value
1051             self.update_min_value(None)
1052         else:
1053             raise ValueError
1054     except ValueError:
1055         self.min_entry.delete(0, tk.END)
1056         self.min_entry.insert(0, str(self.min_value))
1057
1058     def update_from_max_entry(self, event=None) -> None:
1059         """Updates the maximum spot size value parsed through the button:
1060
1061         1. Gets the maximum spot size value and converts it to a logarithmic scale
1062             if it is bigger or equal to the minimum spot size values and smaller or equal
1063             than the full image.
1064
1065         2. Updates the maximum spot size value calling the update_max_value() function.
1066
1067     Args:
1068         self (Instance): Current instance, provides access to attributes and
1069             ↪ methods.
1070         event (_type_, optional): Nothing, just compatibility purposes. Defaults to
1071             ↪ None.
1072
1073     Raises:
1074         ValueError: Maximum spot size value is either bigger than the dimensions of
1075             the whole frame or smaller than the minimum spot size value.
1076     """
1077     try:
1078         max_value = int(self.max_entry.get())
1079         if max_value >= self.min_value and max_value <= (
1080             const.H_SENSOR_SIZE * const.V_SENSOR_SIZE
1081         ):
1082             self.max_value = max_value
1083             log_value = (
1084                 (math.log10(max_value) - self.log_min_value)
1085                 / (self.log_max_value - self.log_min_value)

```

```

1082         * 1000
1083     )
1084     self.max_slider.set(log_value)
1085     # Updates the max spot value
1086     self.update_max_value(None)
1087     else:
1088         raise ValueError
1089 except ValueError:
1090     self.max_entry.delete(0, tk.END)
1091     self.max_entry.insert(0, str(self.max_value))
1092
1093 def set_initial_values(
1094     self, exposure: float, min_value: int, max_value: int
1095 ) -> None:
1096     """Sets the initial values for all the variables of the sliders.
1097
1098     1. Gets the maximum and minimum spot size and exposure values and converts them
1099     ↪ to a logarithmic scale.
1100
1101     2. Sets initial values of the sliders.
1102
1103     3. Calls the update functions to set an initial value for the variables.
1104
1105     Args:
1106         self (Instance): Current instance, provides access to attributes and
1107         ↪ methods.
1108         exposure (float): Initial exposure time.
1109         min_value (int): Initial minimum spot size value.
1110         max_value (int): Initial maximum spot size value.
1111     """
1112     log_exposure = (
1113         (
1114             math.log10(
1115                 max(self.min_exposure, min(self.max_exposure, exposure))
1116             )
1117             - self.log_min_exposure
1118         )
1119         / (self.log_max_exposure - self.log_min_exposure)
1120         * 1000
1121     )
1122     self.min_value = min_value
1123     self.max_value = max_value
1124     log_min_value = (
1125         (math.log10(max(1, self.min_value)) - self.log_min_value)
1126         / (self.log_max_value - self.log_min_value)
1127         * 1000
1128     )
1129     log_max_value = (
1130         (math.log10(self.max_value) - self.log_min_value)
1131         / (self.log_max_value - self.log_min_value)
1132         * 1000
1133     )
1134     # Sets initial values of the sliders
1135     self.exposure_slider.set(log_exposure)
1136     self.min_slider.set(log_min_value)
1137     self.max_slider.set(log_max_value)
1138     # Sets initial values
1139     self.update_exposure(None)
1140     self.update_min_value(None)

```


A.2.3 constants.py

```

1  """This module contains all the constants needed to allow the project to work
   ↪ correctly."""
2
3  # C:\Users\alda_ik\Documents\04_PROGRAMMING\02_FINAL_PROJECT\constants.py
4
5  import numpy as np
6
7  # Directories
8  HOT_PIXEL0_DIR: str = r".\data\references\gain0\hot_500000.tiff"
9  HOT_PIXEL1_DIR: str = r".\data\references\gain1\hot_50000.tiff"
10 BACKGROUND_FRAME_DIR: str = r".\temp.tiff"
11 TEMP_FRAME_DIR: str = r".\temp.tiff"
12
13 LUT_DIR0: str = r".\data\lut\Goldeye-G-CL-008_LinLUT_Gain0.bin"
14 LUT_DIR1: str = r".\data\lut\Goldeye-G-CL-008_LinLUT_Gain1.bin"
15
16 HOT_PIXEL0_THRES_VAL: int = 45
17 LUT_INDEX: int = 4
18
19 # Calibration factors
20 # CALIBRATION_THOR: float = 0.139602768 / 166
21 # CALIBRATION_THOR_GRID: float = 0.139602768 / 1426
22 # CALIBRATION_EDMU: float = 0.139602768 / 166
23 # MIN_BEAM_SIZE = 1
24 # MAX_BEAM_SIZE = 10
25
26 GRID_RADIUS: int = 2
27
28 # Lens parameters
29 LENS_FOCAL_LENGTH: float = 3.5 # mm
30 V_SENSOR_SIZE: int = 256 # Pixels
31 H_SENSOR_SIZE: int = 320 # Pixels
32 PIXEL_SIZE: float = 0.03 # mm (30um)
33
34 FISH_CENTER = [161, 131]
35
36 K = np.array(
37     [
38         [123.48774151225143, 0.0, 160.36138044001243],
39         [0.0, 123.21716405041697, 130.60363126947752],
40         [0.0, 0.0, 1.0],
41     ]
42 )
43 D = np.array(
44     [
45         [-0.04444806603723004],
46         [0.0036746704759666278],
47         [0.0030634545076764002],
48         [-0.0019588697364114325],
49     ]
50 )
51
52
53 ##### LINK BUDGET #####

```

```

54 # Fixed constants
55 C = 3e8 # m/s - speed of light
56 H = 6.626e-34 # m2-kg/s - Planck's constant
57 R_E = 6370e3 # m - Earth's radius
58
59 # Environment constants
60 PSI = 0.3
61 # PSI = 0 # a change according to el is not yet regarded
62 # PSI = 0.1
63 # PSI = 1E-8
64 P_THR = 0.1 # loss_fraction for ScintiLoss
65
66 # Satellite constants
67 # el = 15 # ° - Elevation of the satellite
68 # P_tx = 30 # dBm - Transmitted power
69 # 1W mean was used in FLP-OSIRISv1 experiments with OCAM
70 # 100mW or 50mW mean we expect in KIODO, since the 20dBm mentioned in the book might be
   ↪ peak-power

```

A.2.4 gui.py

```

1  """This module manages the GUI settings menu that appears when the program is first
   ↪ run."""
2
3  # C:\Users\alda_ik\Documents\04_PROGRAMMING\02_FINAL_PROJECT\gui.py
4
5  from tkinter import ttk
6  from typing import Tuple
7  import tkinter as tk
8
9
10 def update_entry(variable: tk.StringVar, entry: tk.ttk.Entry) -> None:
11     """Checks for the parsed state of a variable to enable
12     or disable its text box.
13
14     Args:
15         variable (tk.StringVar): Container of the variable to check.
16         entry (tk.ttk.Entry): Container of the value and its state.
17     """
18     if variable.get() == "Auto" or variable.get() == "Full":
19         # If exposure is automatic, the button will be greyed-out
20         entry.config(state="disabled")
21     else:
22         entry.config(state="normal")
23
24
25 def create_menu() -> (
26     Tuple[
27         tk.StringVar,
28         tk.StringVar,
29         tk.StringVar,
30         tk.StringVar,
31         tk.StringVar,
32         tk.StringVar,
33         tk.StringVar,
34         tk.StringVar,
35         tk.StringVar,
36         tk.StringVar,

```

```

37     tk.StringVar,
38     tk.Tk,
39     tk.ttk.Entry,
40     tk.ttk.Entry,
41 ]
42 ):
43     """Creates the GUI menu to configure the initial settings:
44
45     1. Creates the variables windows with an specific size and position.
46
47     2. Creates varibales to store the inputs.
48
49     3. Creates dropdown menus with default values.
50
51     4. Defines a lambda function to parse the exposure and elevation varibales to
    ↪ update_time_entry().
52
53 Returns:
54     tuple: gain_var (tk.StringVar): Container of the gain mode (0 [0 dB] or 1 [18
    ↪ dB]).
55
56     check_var (tk.StringVar): Container of the streaming mode (Stream or Record).
57
58     light_var (tk.StringVar): Container of the time of the day (Daytime or
    ↪ Nighttime).
59
60     payload_var (tk.StringVar): Container of the payload used (None, KIODO,
61     OsirisV1, Osiris4CubeSat or CubeCat).
62
63     h_ogs_var (tk.StringVar): Container of the height of the OGS used (IKN-OP or
    ↪ GSOC-OP).
64
65     zenith_var (tk.StringVar): Container of the zenith attenuation (Bad
66     1550nm [0.891], Good 1550nm [0.986], Bad 850nm [0.705], Good 850nm
67     [0.950] or CubeCat 20240822 [0.963])
68
69     elevation_var (tk.StringVar): Container of the elevation mode (Individual or
    ↪ Full).
70
71     elevation_angle_var (tk.StringVar): Container of the elevation angle (if
    ↪ manual).
72
73     exposure_var (tk.StringVar): Container of the exposure mode (Auto or Manual).
74
75     exposure_time_var (tk.StringVar): Container of the exposure value (if manual).
76
77     iso_var (tk.StringVar): Container of the main camera mode (Normal, Hot-pixel
78     substraction, Subtraction ormCamera's BC).
79
80     root (tk.Tk): Main window of the GUI menu.
81
82     exposure_time_entry (tk.ttk.Entry): Value of the exposure.
83
84     elevation_angle_entry (tk.ttk.Entry): Value of the elevation.
85     """
86     root = tk.Tk()
87     root.title("IR Camera for Satellite Tracking")
88     # Dimensions and position of the settings menu (WidthxHeight+X+Y).
89     root.geometry("370x320+900+5")
90

```

```

91  # Variables
92  gain_var = tk.StringVar(value="1")
93  check_var = tk.StringVar(value="S")
94  light_var = tk.StringVar(value="D")
95  payload_var = tk.StringVar(value="")
96  h_ogs_var = tk.StringVar(value="IKN-OP")
97  zenith_var = tk.StringVar(value="B_1")
98  elevation_var = tk.StringVar(value="F")
99  elevation_angle_var = tk.StringVar(value="")
100 exposure_var = tk.StringVar(value="M")
101 exposure_time_var = tk.StringVar(value="")
102 iso_var = tk.StringVar(value="N")
103
104 # Camera title
105 ttk.Label(text="Camera settings", font=(14)).grid(
106     row=0, column=0, pady=5, sticky=""
107 )
108 # LB title
109 ttk.Label(text="LB Settings", font=(14)).grid(
110     row=0, column=1, columnspan=1, pady=5
111 )
112
113 # Dropdown menus
114 ttk.Label(text="Gain:").grid(row=1, column=0, sticky="")
115 gain_combo = ttk.Combobox(
116     textvariable=gain_var, values=["0 [0 dB]", "1 [18 dB]"]
117 )
118 gain_combo.grid(row=2, column=0)
119 gain_combo.set("1 [18 dB]")
120
121 ttk.Label(text="Payload:").grid(row=1, column=1, sticky="")
122 payload_combo = ttk.Combobox(
123     textvariable=payload_var,
124     values=[
125         "None",
126         "KIODO",
127         "OsirisV1",
128         "Osiris4CubeSat",
129         "CubeCat",
130     ],
131 )
132 payload_combo.grid(row=2, column=1)
133 payload_combo.set("None")
134
135 ttk.Label(text="Capture Mode:").grid(row=3, column=0, sticky="")
136 check_combo = ttk.Combobox(
137     textvariable=check_var, values=["Stream", "Record"]
138 )
139 check_combo.grid(row=4, column=0)
140 check_combo.set("Stream")
141
142 ttk.Label(text="OGS:").grid(row=3, column=1, sticky="")
143 h_ogs_combo = ttk.Combobox(
144     textvariable=h_ogs_var, values=["IKN-OP", "GSOC-OP"]
145 )
146 h_ogs_combo.grid(row=4, column=1)
147 h_ogs_combo.set("IKN-OP")
148
149 ttk.Label(text="Zenith-attenuation:").grid(row=5, column=1, sticky="")
150 zenith_combo = ttk.Combobox(

```

```

151     textvariable=zenith_var,
152     values=[
153         "Bad 1550nm [0.891]",
154         "Good 1550nm [0.986]",
155         "Bad 850nm [0.705]",
156         "Good 850nm [0.950]",
157         "CubeCat 20240822 [0.963]",
158     ],
159 )
160 zenith_combo.grid(row=6, column=1)
161 zenith_combo.set("Bad 1550nm [0.891]")
162
163 ttk.Label(text="Time of the day:").grid(row=5, column=0, sticky="")
164 light_combo = ttk.Combobox(
165     textvariable=light_var, values=["Daytime", "Nighttime"])
166 )
167 light_combo.grid(row=6, column=0)
168 light_combo.set("Daytime")
169
170 ttk.Label(text="Elevation:").grid(row=7, column=1, sticky="")
171 elevation_combo = ttk.Combobox(
172     textvariable=elevation_var, values=["Full", "Individual"])
173 )
174 elevation_combo.grid(row=8, column=1)
175 elevation_combo.set("Full")
176
177 ttk.Label(text="Elevation Angle (°):").grid(row=9, column=1, sticky="")
178 elevation_angle_entry = ttk.Entry(textvariable=elevation_angle_var)
179 elevation_angle_entry.grid(row=10, column=1)
180
181 ttk.Label(text="Exposure:").grid(row=7, column=0, sticky="")
182 exposure_combo = ttk.Combobox(
183     textvariable=exposure_var, values=["Auto", "Manual"])
184 )
185 exposure_combo.grid(row=8, column=0)
186 exposure_combo.set("Manual")
187
188 ttk.Label(text="Exposure Time (µs):").grid(row=9, column=0, sticky="")
189 exposure_time_entry = ttk.Entry(textvariable=exposure_time_var)
190 exposure_time_entry.grid(row=10, column=0)
191
192 ttk.Label(text="Technique Used:").grid(row=11, column=0, sticky="")
193 iso_combo = ttk.Combobox(
194     textvariable=iso_var,
195     values=[
196         "Normal",
197         "Hot-pixel subtraction",
198         "Subtraction",
199         "Camera's BC",
200     ],
201 )
202 iso_combo.grid(row=12, column=0)
203 iso_combo.set("Normal")
204
205 # lambda to parse exposure and elevation states
206 exposure_var.trace_add(
207     "write",
208     lambda *args: update_entry(exposure_var, exposure_time_entry),
209 )
210

```

```

211     elevation_var.trace_add(
212         "write",
213         lambda *args: update_entry(elevation_var, elevation_angle_entry),
214     )
215
216     return (
217         gain_var,
218         check_var,
219         light_var,
220         payload_var,
221         h_ogs_var,
222         zenith_var,
223         elevation_var,
224         elevation_angle_var,
225         exposure_var,
226         exposure_time_var,
227         iso_var,
228         root,
229         exposure_time_entry,
230         elevation_angle_entry,
231     )

```

A.2.5 image_processing.py

```

1  """This module manages the processing of the frames taken by the camera."""
2
3  # C:\Users\alda_ik\Documents\04_PROGRAMMING\02_FINAL_PROJECT\image_processing.py
4
5  from datetime import datetime
6  from typing import Tuple
7  import cv2
8  import os
9  import csv
10 import math
11 import numpy as np
12
13 from . import constants as const
14
15
16 def dark_frame_setup(frame: np.array) -> np.array:
17     """Prepares a frame for processing:
18
19     1. A threshold of 45 is applied to a previously recorded image of the camera's hot
20     ↪ pixels.
21
22     2. The resulting thresholded image is normalized, resulting in an image with values
23     ↪ [0, 1].
24
25     3. Finally the normalized image is scaled, obtaining an image with values [0, 255].
26
27     Args:
28     frame (np.array): Frame with the hot pixels present.
29
30     Returns:
31     np.array: Image after normalization, thresholding and scaling.
32     """
33     # Apply threshold to create a binary image
34     _, thresh = cv2.threshold(

```

```

33     frame, const.HOT_PIXEL0_THRES_VAL, 255, cv2.THRESH_BINARY
34 )
35
36 # Normalize the binary image
37 normalized = cv2.normalize(
38     thresh, None, 0, 1.0, cv2.NORM_MINMAX, dtype=cv2.CV_32F
39 )
40 # Scale the image to [0, 255]
41 normalized = normalized * 255
42 normalized = normalized.astype(np.uint8)
43
44 return normalized
45
46
47 def subtract_frames(frame: np.array, frame_subtracted: np.array) -> np.array:
48     """Subtracts one frame from another using OpenCV:
49
50     1. Checks if both frames have the same dimensions and format.
51
52     2. Subtracts both of the frames.
53
54     Args:
55         frame (np.array): Original frame.
56         frame_subtracted (np.array): Frame to subtract.
57
58     Returns:
59         np.array: Image obtained after frame subtraction.
60     """
61     # Ensure images are the same size and format
62     assert (
63         frame.shape == frame_subtracted.shape
64     ), "Both image frames must have the same dimensions"
65     assert (
66         frame.dtype == frame_subtracted.dtype
67     ), "Both image frames must have the same data type"
68
69     # Subtract the dark frame using OpenCV
70     subtracted_image = cv2.subtract(frame, frame_subtracted)
71
72     return subtracted_image
73
74
75 def write_csv(
76     self,
77     frame_mean_pixel_value: int,
78     frame_number: str,
79     time: str,
80     exposure: float,
81     r: float,
82     elevation: float,
83     azimuth: float,
84     fov: float,
85     location: Tuple,
86     pvalue: float,
87     pvalue_grid: np.uint32,
88     intensity: float,
89     intensity_grid: np.float64,
90 ) -> None:
91     """Writes a csv file with all the parameters needed to perform the analysis of the
92     → final satellite pass:

```

```

92
93     1. Creates the dictionaries and fields.
94
95     2. Writes the csv file.
96
97     Args:
98         self (Instance): Parsed instance from Handler in the api module, provides access
99             ↪ to attributes and methods.
100         frame_mean_pixel_value (int): Mean Pixel Value of the entire frame.
101         frame_number (str): Frame number.
102         time (str): Current time where the frame as been recorded.
103         exposure (float): Exposure time used for that particular frame.
104         r (float): Radial position of the brightest point.
105         elevation (float): Elevation of the brightest point
106         azimuth (float): Azimuth of the brightest point.
107         fov (float): Field Of View of the camera, in degrees, at the brightest point
108         location (tuple): Location of the brightest point: [0] = x-axis, [1] = y-axis.
109         pvalue (float): Pixel Value of the brightest point [0-255].
110         pvalue_grid (np.uint32): Pixel Value of the whole brightest contour.
111         intensity (float): Intensity value of the brightest point.
112         intensity_grid (np.float64): Intensity value of the whole brightest contour.
113     """
114     if self.gain == 1:
115         gain = "Gain 1 [18dB]"
116     else:
117         gain = "Gain 0 [0dB]"
118     exposure = exposure.get()
119     mydict = [
120         {
121             "Frame": frame_number,
122             "Gain Mode": gain,
123             "Time [CEST]": time,
124             "Exposure [us]": exposure,
125             "Location [x, y]": location,
126             "Elevation [°]": elevation,
127             "Azimuth [°]": azimuth,
128             "FOV": fov,
129             "R": r,
130             "Mean Pixel Value [DN]": frame_mean_pixel_value,
131             "Brightest Pixel Value [DN]": pvalue,
132             "Grid Brightest Pixel Value [DN]": pvalue_grid,
133             "Intensity [uW/m-2]": intensity,
134             "Grid Intensity[uW/m-2]": intensity_grid,
135         }
136     ]
137     fields = [
138         "Frame",
139         "Gain Mode",
140         "Time [CEST]",
141         "Exposure [us]",
142         "Location [x, y]",
143         "Elevation [°]",
144         "Azimuth [°]",
145         "FOV",
146         "R",
147         "Mean Pixel Value [DN]",
148         "Brightest Pixel Value [DN]",
149         "Grid Brightest Pixel Value [DN]",
150         "Intensity [uW/m-2]",

```



```

151     "Grid Intensity[uW/m-2]",
152 ]
153
154 if self.payload != "None":
155     filename =
156         ↪ f"{self.p}/{datetime.now().strftime('%Y-%m-%d')}_self.payload_DL_csv.csv"
157 else:
158     filename = f"{self.p}/{datetime.now().strftime('%Y-%m-%d')}_DL_csv.csv"
159 file_exists = os.path.isfile(filename)
160
161 # Write csv
162 with open(filename, "a", newline="") as csvfile:
163     writer = csv.DictWriter(csvfile, fieldnames=fields)
164     if not file_exists:
165         writer.writeheader()
166         writer.writerow(mydict)
167
168 def brightest_V2(
169     self,
170     frame: np.array,
171     exposure: float,
172 ) -> Tuple[Tuple, float, float, float, float, float]:
173     """Calculates the brightest point of the frame based on an specified minimum and
174     ↪ maximum spot size.
175
176     1. Setups the calibration factor.
177
178     2. Depending if the daylight or nighttime is selcted a different process will be
179     ↪ applied:
180
181         In case of Daytime: Bilateral filter 3 200x200 -> OTSU Thresholding.
182
183         In case of Nighttime: Gaussian blur 3x3 -> Threshold based on black values.
184
185     3. Finds the contours of the figure (zones of the fram with similar pixel values).
186
187     4. Bounds the contours and filters them based on the minimum and maximum spot sizes
188     ↪ values.
189
190     5. Select the contour with the highest mean pixel value.
191
192     6. Obtains the brightest pixel and the sum of all the values from the brightest
193     ↪ contour.
194
195     7. Converts pixel value to intensity using the correction factor.
196
197     Args:
198     self (Instance): Current instance, provides access to attributes and methods.
199     frame (np.array): Frame from where the brightest point will be obtained.
200     exposure (float): Exposure time used for that particular frame.
201
202     Returns:
203     tuple[tuple, float, float, float, float, float]: max_loc (tuple):Location of the
204     ↪ brightest point:
205     [0] = x-axis, [1] = y-axis.
206
207     max_val (float): Pixel value of the brightest point [0-255].
208
209     intensity_brightest (float): Intensity value of the brightest point.

```

```

205
206     max_mean_pixel_value (float): Mean pixel value of the whole brightest contour.
207
208     sum_max_mean_pixel_value[0] (float): Summed pixel value of the whole brightest
209     ↪ contour.
210
211     intensity_brightest_grid (float): Summed intensity value of the whole brightest
212     ↪ contour.
211     """
212     max_mean_pixel_value = 0
213     max_val = 0
214     max_loc = [0, 0]
215     intensity_brightest = 0
216     intensity_brightest_grid = 0
217     sum_max_mean_pixel_value = [0, 0, 0]
218     # sum_max_mean_pixel_value[0]
219
220     exposure = exposure.get() # Exposure in us
221
222     # Calibration factors
223     calibration_THOR = 0.139602768 / (0.0001 * exposure + 18.545)
224     calibration_THOR_grid = 0.139602768 / (0.0008 * exposure + 443.22)
225     if self.gain == 1:
226         calibration_THOR_gain = 0.139602768 / (1.4788 * exposure - 82.62)
227     else:
228         calibration_THOR_gain = 0.139602768 / (0.2427 * exposure + 1.67)
229
230     gray = cv2.cvtColor(frame, cv2.COLOR_BGR2GRAY)
231     if self.cond == 0:
232         # Processing for Daytime - Bilateral filter and otsu thresholding
233         # filter = cv2.bilateralFilter(gray, 3, 100, 100)
234         filter = cv2.bilateralFilter(gray, 3, 200, 200)
235         # filter = cv2.GaussianBlur(gray, (5, 5), 0)
236         # filter = cv2.GaussianBlur(gray, (3, 3), 0)
237
238         _, th = cv2.threshold(
239             filter, 0, 255, cv2.THRESH_BINARY + cv2.THRESH_OTSU
240         )
241     else:
242         # Processing for Nighttime - Gaussian filter and thresholding based on dark
243         # ↪ pixels pixel value
244         thresh_val = 0.0004 * exposure + 13.113
245
246         filter = cv2.GaussianBlur(gray, (3, 3), 0)
247         _, th = cv2.threshold(filter, thresh_val, 255, cv2.THRESH_BINARY)
248
249     contours, _ = cv2.findContours(th, cv2.RETR_TREE, cv2.CHAIN_APPROX_SIMPLE)
250
251     min_size = self.min_value
252     max_size = self.max_value
253
254     for contour in contours:
255         _, _, w, h = cv2.boundingRect(contour)
256         # Filter contours based on min and max spot size
257         if min_size <= w * h and max_size >= w * h:
258             mask = np.zeros(gray.shape, np.uint8)
259             cv2.drawContours(mask, [contour], 0, 255, -1)
260
261             mean_pixel_value = cv2.mean(gray, mask=mask)[0]

```

```

262         # Compares current contour with the brightest one
263         if mean_pixel_value > max_mean_pixel_value:
264             max_mean_pixel_value = mean_pixel_value
265
266         # Obtain brightest point and full brightness of the contour
267         masked_gray = cv2.bitwise_and(gray, gray, mask=mask)
268         sum_max_mean_pixel_value = cv2.sumElems(masked_gray)
269         _, max_val, _, max_loc = cv2.minMaxLoc(masked_gray)
270
271         # Convert to intensity
272         intensity_brightest = max_val * calibration_THOR
273         intensity_brightest_grid = (
274             sum_max_mean_pixel_value[0] * calibration_THOR_grid
275         )
276
277     return (
278         max_loc,
279         max_val,
280         intensity_brightest,
281         max_mean_pixel_value,
282         sum_max_mean_pixel_value[0],
283         intensity_brightest_grid,
284     )
285
286
287 def calculate_el_azi(max_loc: Tuple) -> Tuple[float, float, float, float]:
288     """Calculates the elevation and azimuth of the brightest point of the frame,
289     making use of the fisheye projections. Equidistant, equisolid and stereographic
290     can be selected.
291
292     1. Calculates the distance from the center of the image to the brightest point.
293
294     2. Applies the projection to obtain the fov of the lens in the brightest point.
295
296     3. Obtains the elevation based on the fov.
297
298     4. Calculates the azimuth based on the center of the lens.
299
300     Args:
301         max_loc (tuple): Location of the brightest point: [0] = x-axis, [1] = y-axis.
302
303     Returns:
304         tuple[float, float, float, float]: elevation (float): Elevation of the brightest
305         ↪ point.
306
307         fov (float): Field Of View of the camera, in degrees, at the brightest point.
308
309         r (float): Radial position of the brightest point.
310
311         azimuth (float): Azimuth of the brightest point.
312     """
313     # print(max_loc)
314     # print(type(max_loc))
315     # max_loc = np.array([[max_loc[0], max_loc[1]]], dtype=np.float32)
316     # # Undistort the point
317     # undist_max_loc = cv2.fisheye.undistortPoints(max_loc, const.K, const.D, P=const.K)
318     # undist_max_loc = undist_max_loc[0][0]
319     # max_loc = (int(round(undist_max_loc[0])), int(round(undist_max_loc[1])))
320     # print(max_loc)

```

```

321 F = const.LENS_FOCAL_LENGTH
322 r = math.sqrt(
323     (max_loc[0] - const.FISH_CENTER[0]) ** 2
324     + (max_loc[1] - const.FISH_CENTER[1]) ** 2
325 )
326
327 # Lens Projections
328 # EQUIDISTANT PROJECTION
329 # fov_rad = (r * const.PIXEL_SIZE) / F # rad - FOV in radians
330 # EQUISOLID PROJECTION
331 fov_rad = 2 * math.asin((r * const.PIXEL_SIZE) / (2 * F))
332 # STEREOGRAPHIC PROJECTION
333 # fov_rad = 2 * math.atan((r * const.PIXEL_SIZE) / (2 * F))
334 # RECTILINEAR PROJECTION
335 # fov_rad = math.atan((r * const.PIXEL_SIZE) / F)
336
337 fov = (fov_rad * (180 / math.pi)) * 2 # ° - FOV in degrees
338 elevation = (180 - fov) / 2
339
340 # Azimuth at the exact center of the frame
341 if max_loc[1] == const.FISH_CENTER[1]:
342     azimuth = 0
343 else:
344     azimuth = (
345         math.atan(
346             (max_loc[0] - const.FISH_CENTER[0])
347             / (max_loc[1] - const.FISH_CENTER[1])
348         )
349     ) * (180 / math.pi)
350
351 # If point is in the upper part of the frame
352 if max_loc[1] >= const.FISH_CENTER[1]:
353     azimuth = 180 + azimuth
354 else:
355     # If point is the bottom-right part of the frame
356     if max_loc[0] >= const.FISH_CENTER[0]:
357         azimuth = 360 + azimuth
358
359 return elevation, fov, r, azimuth
360
361
362 def frame_draw(
363     frame: np.array,
364     time: str,
365     exposure: float,
366     rad: int,
367     max_bright_loc: Tuple,
368     max_bright_val: float,
369     int_bright_val: float,
370     mean_bright_grid_val: np.uint32,
371     max_bright_grid_val: np.uint32,
372     int_bright_grid_val: np.float64,
373     min_size: int,
374     max_size: int,
375     elevation: float,
376     azimuth: float,
377 ) -> None:
378     """Draws the overlays on top of the frame:
379
380     Args:

```

```

381     frame (np.array): Frame where the overlays will be drawn.
382     time (str): Actual time in that particular frame.
383     exposure (float): Exposure time used for that particular frame.
384     rad (int): Radius of the intensity grid.
385     max_bright_loc (tuple): Location of the brightest point: [0] = x-axis, [1] =
    ↪ y-axis.
386     max_bright_val (float): Pixel value of the brightest point [0-255].
387     int_bright_val (float): Intensity value of the brightest point.
388     mean_bright_grid_val (np.uint32): Mean pixel value of the whole brightest
    ↪ contour.
389     max_bright_grid_val (np.uint32): Summed pixel value of the whole brightest
    ↪ contour.
390     int_bright_grid_val (np.float64): Summed intensity value of the whole brightest
    ↪ contour.
391     min_size (int): Minimum spot size value used.
392     max_size (int): Maximum spot size value used.
393     elevation (float): Elevation of the brightest point.
394     azimuth (float): Azimuth of the brightest point.
395     """
396     # Draw the time, exposure, coordinates and crosshair on the frame
397     cv2.putText(
398         frame,
399         time,
400         (1, 7),
401         cv2.FONT_HERSHEY_SIMPLEX,
402         0.3,
403         (255, 255, 255),
404         1,
405     )
406     cv2.putText(
407         frame,
408         f"Exposure: {exposure.get()} us",
409         (1, 38),
410         cv2.FONT_HERSHEY_SIMPLEX,
411         0.25,
412         (255, 255, 255),
413         1,
414     )
415     cv2.putText(
416         frame,
417         f"Min Size: {min_size:.0f}",
418         (1, 47),
419         cv2.FONT_HERSHEY_SIMPLEX,
420         0.25,
421         (255, 255, 255),
422         1,
423     )
424     cv2.putText(
425         frame,
426         f"Max Size: {max_size:.0f}",
427         (1, 56),
428         cv2.FONT_HERSHEY_SIMPLEX,
429         0.25,
430         (255, 255, 255),
431         1,
432     )
433     cv2.putText(
434         frame,
435         f"El.: {elevation:.0f}",
436         (1, 201),

```

```

437     cv2.FONT_HERSHEY_SIMPLEX,
438     0.25,
439     (255, 255, 255),
440     1,
441 )
442 cv2.putText(
443     frame,
444     f"Az.: {azimuth:.0f}",
445     (1, 210),
446     cv2.FONT_HERSHEY_SIMPLEX,
447     0.25,
448     (255, 255, 255),
449     1,
450 )
451 cv2.putText(
452     frame,
453     f"Brightness at {max_bright_loc}: {int_bright_val:.3f} uw/m^2 ->
454     ↪ {max_bright_val}",
455     (1, 238),
456     cv2.FONT_HERSHEY_SIMPLEX,
457     0.25,
458     (255, 255, 255),
459     1,
460 )
461 if max_bright_val == 255:
462     cv2.putText(
463         frame,
464         "Saturated! Lower Exposure",
465         (115, 20),
466         cv2.FONT_HERSHEY_SIMPLEX,
467         0.25,
468         (255, 255, 255),
469         1,
470 )
471 cv2.putText(
472     frame,
473     f"Brightness {rad*2+1}x{rad*2+1} grid: {int_bright_grid_val:.3f} uw/m^2 "
474     f"-> {max_bright_grid_val} (mean: {mean_bright_grid_val:.1f})",
475     (1, 245),
476     cv2.FONT_HERSHEY_SIMPLEX,
477     0.25,
478     (255, 255, 255),
479     1,
480 )
481 cv2.putText(
482     frame,
483     "N",
484     (160, 7),
485     cv2.FONT_HERSHEY_SIMPLEX,
486     0.4,
487     (255, 255, 255),
488     1,
489 )
490 cv2.putText(
491     frame,
492     "S",
493     (160, 254),
494     cv2.FONT_HERSHEY_SIMPLEX,
495     0.4,
496     (255, 255, 255),

```

```

496     1,
497 )
498 cv2.putText(
499     frame,
500     "E",
501     (1, 128),
502     cv2.FONT_HERSHEY_SIMPLEX,
503     0.4,
504     (255, 255, 255),
505     1,
506 )
507 cv2.putText(
508     frame,
509     "W",
510     (310, 128),
511     cv2.FONT_HERSHEY_SIMPLEX,
512     0.4,
513     (255, 255, 255),
514     1,
515 )
516 cv2.putText(
517     frame,
518     "SW",
519     (290, 242),
520     cv2.FONT_HERSHEY_SIMPLEX,
521     0.4,
522     (255, 255, 255),
523     1,
524 )
525 cv2.putText(
526     frame,
527     "(225)",
528     (280, 227),
529     cv2.FONT_HERSHEY_SIMPLEX,
530     0.25,
531     (255, 255, 255),
532     1,
533 )
534 cv2.putText(
535     frame,
536     "(248)",
537     (295, 190),
538     cv2.FONT_HERSHEY_SIMPLEX,
539     0.25,
540     (255, 255, 255),
541     1,
542 )
543 cv2.putText(
544     frame,
545     "NW",
546     (290, 17),
547     cv2.FONT_HERSHEY_SIMPLEX,
548     0.4,
549     (255, 255, 255),
550     1,
551 )
552 cv2.putText(
553     frame,
554     "(338)",
555     (225, 10),

```

```

556         cv2.FONT_HERSHEY_SIMPLEX,
557         0.25,
558         (255, 255, 255),
559         1,
560     )
561     cv2.putText(
562         frame,
563         "(315)",
564         (280, 29),
565         cv2.FONT_HERSHEY_SIMPLEX,
566         0.25,
567         (255, 255, 255),
568         1,
569     )
570     cv2.putText(
571         frame,
572         "(293)",
573         (295, 66),
574         cv2.FONT_HERSHEY_SIMPLEX,
575         0.25,
576         (255, 255, 255),
577         1,
578     )
579     cv2.putText(
580         frame,
581         "SE",
582         (30, 242),
583         cv2.FONT_HERSHEY_SIMPLEX,
584         0.4,
585         (255, 255, 255),
586         1,
587     )
588     cv2.putText(
589         frame,
590         "(135)",
591         (35, 227),
592         cv2.FONT_HERSHEY_SIMPLEX,
593         0.25,
594         (255, 255, 255),
595         1,
596     )
597     cv2.putText(
598         frame,
599         "(113)",
600         (11, 190),
601         cv2.FONT_HERSHEY_SIMPLEX,
602         0.25,
603         (255, 255, 255),
604         1,
605     )
606     cv2.putText(
607         frame,
608         "NE",
609         (30, 17),
610         cv2.FONT_HERSHEY_SIMPLEX,
611         0.4,
612         (255, 255, 255),
613         1,
614     )
615     cv2.putText(

```



```

616         frame,
617         "(45)",
618         (35, 29),
619         cv2.FONT_HERSHEY_SIMPLEX,
620         0.25,
621         (255, 255, 255),
622         1,
623     )
624     cv2.putText(
625         frame,
626         "(68)",
627         (11, 66),
628         cv2.FONT_HERSHEY_SIMPLEX,
629         0.25,
630         (255, 255, 255),
631         1,
632     )
633
634     # Circle for the brightest point
635     cv2.circle(frame, max_bright_loc, 5, (255, 255, 255), 1)
636
637     # Crosshair
638     # cv2.line(frame, (159, 128), (161, 128), (255, 255, 255), 1)
639     # cv2.line(frame, (160, 127), (160, 129), (255, 255, 255), 1)
640
641
642     def frame_processing(self, cam, frame) -> None:
643         """Processes the frame.
644
645         1. Grabs a temporal frame.
646
647         2. Depending on the selected mode by the user:
648
649         - Hot-pixel removal.
650             A frame with the hot pixels will threshold and normalized by the
651             dark_frame_setup() fuction and then subtracted to the the taken frame
652             with the subtract_frames() function.
653
654         - Own background correction.
655             Subtracts the temporal frame to the next grabbed frame. The
656             subtract_frames() fuction is applied for subtracting the temporal frame,
657             just grabbed, with the next frame.
658
659         - Normal operation.
660             The temporal frame will be used directly.
661
662         - Camera's own background correction.
663             The temporal frame will be used directly.
664
665         3. Obtains the brightest point thanks to the brightest_V2() function.
666
667         4. Obtains the elevation and azimuth of the brightest pixel with the
668             → calculate_el_azi() fuction.
669
670         5. Draws all the desired values on top of the frame using the frame_draw() fuction.
671
672         6. Just in case the Record mode is being used, both the processed and unprocessed
673             → frames,
674             besides the csv file, will all be saved.

```

```

674 7- Finally the frames will be display and the first temporal frame will be removed.
675
676 Args:
677     self (Instance): Current instance, provides access to attributes and methods.
678     cam (Camera): Camera object from the VMBPY API module.
679     frame (Frame): Frame object from the VMBPY API module.
680     """
681 # Get the current time with ms.
682 now = datetime.now()
683 current_time = datetime.now().strftime("%Y-%m-%d %H:%M:%S.%f")[:-3]
684 exposure_time = cam.ExposureTime
685 msg = "Stream from '{}'. Press <q> to stop stream."
686
687 print("{} acquired {}".format(cam, frame), flush=True)
688
689 # Create a temporal frame where the proccessing will be made.
690 cv2.imwrite(const.TEMP_FRAME_DIR, frame.as_opencv_image())
691 frame_temp = cv2.imread(const.TEMP_FRAME_DIR)
692
693 # Hot-pixel removal
694 if self.background == 3:
695     # Setup of the hot pixels of the wanted exposure.
696     hot = cv2.imread(const.HOT_PIXEL0_DIR)
697     normalized = dark_frame_setup(hot)
698     # Removal of the dark pixels from the taken frame.
699     frame_subs = subtract_frames(frame_temp, normalized)
700 # Background substraction.
701 elif self.background == 1:
702     normalized = cv2.imread(const.BACKGROUND_FRAME_DIR)
703     # background = background.astype(np.uint8)
704     frame_subs = subtract_frames(frame_temp, normalized)
705     # frame_subs = subtract_frames(normalized, frame_temp) # Chroma effect
706 # Normal operation or Background correction mode
707 else:
708     frame_subs = cv2.imread(const.TEMP_FRAME_DIR)
709
710 # Calculate the brightest point, elevation and azimuth
711 mean_val_grid = 0
712 (
713     max_loc,
714     max_val,
715     intensity_brightest,
716     mean_val_grid,
717     max_val_grid,
718     intensity_brightest_grid,
719 ) = brightest_V2(self, frame_subs, exposure_time)
720
721 elevation, fov, r, azimuth = calculate_el_azimuth(max_loc)
722
723 # Append data for update the live graph of the GUI
724 self.xdata.append(now)
725 self.ydata.append(max_val)
726
727 # Draw on-top of the frame
728 frame_draw(
729     frame_subs,
730     current_time,
731     exposure_time,
732     const.GRID_RADIUS,
733     max_loc,

```

```

734     max_val,
735     intensity_brightest,
736     mean_val_grid,
737     max_val_grid,
738     intensity_brightest_grid,
739     self.min_value,
740     self.max_value,
741     elevation,
742     azimuth,
743 )
744
745 # We only write the frame if the mode selected is Record.
746 if self.mode != 0:
747     cv2.imwrite(
748         f"{self.p}/{"now.strftime('%Y')}{"now.strftime('%m')}{"now.}
749         ↪ strftime('%d')}_{"now.strftime('%H')}"}"
750         f"{now.strftime('%M')}{"now.strftime('%S')}_frame_{str(self.counter)}.tiff",
751         frame_subs,
752     )
753     cv2.imwrite(
754         f"{self.pnp}/{"now.strftime('%Y')}{"now.strftime('%m')}{"now.}
755         ↪ strftime('%d')}_{"now.strftime('%H')}"}"
756         f"{now.strftime('%M')}{"now.strftime('%S')}_frame_{str(self.counter)}.tiff",
757         frame_temp,
758     )
759
760 # Calculate mean pixel value of the frame and generate csv
761 frame_mpv = frame_subs.mean()
762 frame_num = f"frame_{str(self.counter)}"
763 write_csv(
764     self,
765     frame_mpv,
766     frame_num,
767     current_time,
768     exposure_time,
769     r,
770     elevation,
771     azimuth,
772     fov,
773     max_loc,
774     max_val,
775     max_val_grid,
776     intensity_brightest,
777     intensity_brightest_grid,
778 )
779
780 # Create the window for the frames
781 window = np.concatenate((frame_subs, frame_temp), axis=1)
782 winname = msg.format(cam.get_name())
783 cv2.namedWindow(winname)
784 cv2.moveWindow(winname, 70, 5)
785 cv2.imshow(winname, window) # Show the frame
786
787 if os.path.isfile(const.TEMP_FRAME_DIR):
788     os.remove(const.TEMP_FRAME_DIR)

```

A.2.6 input_checks.py

```
1 """This module manages the checking and validation of the user inputs."""
2
3 # C:\Users\alda_ik\Documents\04_PROGRAMMING\02_FINAL_PROJECT\input_checks.py
4
5 from typing import Tuple
6
7 def checks(
8     elevation_in,
9     elevation_angle_in,
10    exposure_in,
11    exposure_time_in,
12    zenith,
13    h_ogs,
14 ) -> Tuple[int, int, float, int]:
15     """Based on the selected values in the GUI it prepares the exposure, elevation and
16     zenith attenuation we will finally use.
17
18     1. If manual exposure mode is selected, retrieves the exposure time, ensuring that
19     the value is non-negative.
20
21     2. If individual elevation mode is selected, retrieves the elevation angle, ensuring
22     ↪ that the selected value is between 0 and 90 degrees of elevation.
23
24     3. Selects the value of the atmospheric zenith attenuation.
25
26     Args:
27     elevation_in (tk.StringVar): Container of the chosen elevation mode.
28     elevation_angle_in (tk.StringVar): Container of the chosen elevation angle (if
29     ↪ manual).
30     exposure_in (tk.StringVar): Container of the chosen exposure mode.
31     exposure_time_in (tk.StringVar): Container of the chosen exposure value (if
32     ↪ manual).
33     zenith (tk.StringVar): Container of the atmospheric zenith attenuation.
34     h_ogs (tk.StringVar): Container of the height of the OGS used.
35
36     Raises:
37     ValueError: Exposure time value is a lower than zero.
38     ValueError: Elevation angle is lower than 0 or bigger than 90.
39
40     Returns:
41     tuple[int, int, float, int]: elevation_angle (int): Final selected elevation
42     ↪ angle (if individual).
43
44     exposure_time_value (int): Final selected exposure value (if manual).
45
46     zenith (float): Final selected zenith attenuation value.
47
48     h_ogs (int): Final height of the selected OGS.
49     """
50     # Validate exposure time
51     if exposure_in.get() == "Manual":
52         try:
53             exposure_time_value = int(exposure_time_in.get())
54             if exposure_time_value <= 0:
55                 raise ValueError
56             # Error validation
57         except ValueError:
```

```

55         print("[ERROR] Invalid exposure time. Must be a positive integer.")
56         return
57     else:
58         exposure_time_value = 1 # Default value for Auto mode
59
60     # Validate elevation
61     if elevation_in.get() == "Individual":
62         try:
63             elevation_angle = int(elevation_angle_in.get())
64             print(elevation_angle)
65             if elevation_angle <= 0 or elevation_angle >= 90:
66                 raise ValueError
67             # Error validation
68         except ValueError:
69             print(
70                 "[ERROR] Invalid elevation angle. Must be a whole angle between 1 and 89
71                 ↪ degrees."
72             )
73         return
74     else:
75         elevation_angle = 15 # Default value for Auto mode
76
77     if zenith.get() == "Bad 1550nm [0.891]":
78         zenith = 0.891
79     elif zenith.get() == "Good 1550nm [0.986]":
80         zenith = 0.986
81     elif zenith.get() == "Bad 850nm [0.705]":
82         zenith = 0.705
83     elif zenith.get() == "Good 850nm [0.950]":
84         zenith = 0.950
85     else:
86         zenith = 0.963
87
88     if h_ogs.get() == "IKN-OP":
89         h_ogs = 650
90     else:
91         h_ogs = 600
92
93     return (
94         elevation_angle,
95         exposure_time_value,
96         zenith,
97         h_ogs,
98     )

```

A.2.7 link_budget.py

```

1  """This modules manages the creation and display of the link budget."""
2
3  # C:\Users\alda_ik\Documents\04_PROGRAMMING\03_SCRIPTS\05_LINK_BUDGET\link_budget.py
4
5  from typing import Union
6  from scipy.special import erfinv
7
8  import numpy as np
9  import mplcursors
10 import matplotlib.pyplot as plt
11

```

```

12 import math
13
14 from . import constants as const
15
16
17 def printer_lb(
18     el: Union[np.ndarray, int],
19     elevation_mode,
20     sat,
21     a_tx: int,
22     p_tx: int,
23     ppb: int,
24     teta_tx: float,
25     a_rx: int,
26     leng: Union[np.ndarray, float],
27     g_tx: float,
28     a_fsl: Union[np.ndarray, float],
29     i_axial: Union[np.ndarray, float],
30     area_rx: float,
31     a_atm: Union[np.ndarray, float],
32     a_bw: int,
33     g_rx: float,
34     p_rx: Union[np.ndarray, float],
35     int_ogs_lin: Union[np.ndarray, float],
36     int_ogs_lin_loss: Union[np.ndarray, float],
37     p_ogs_mean: Union[np.ndarray, float],
38     p_ogs_mean_loss: Union[np.ndarray, float],
39     p_rx_lin: Union[np.ndarray, float],
40     wl: float,
41     p_rfe_lin: float,
42     a_sci: int,
43 ) -> None:
44     """Prints the graph or the results and summary of the link budget.
45
46     1. If the elevation mode is "Full" it will just print the graph, if not
47     it will print the result of the link budget.
48
49     Args:
50         el (np.ndarray | int): Elevation of the satellite
51         elevation_mode (tk.StringVar): Container of the elevation mode.
52         sat (tk.StringVar): Container of the payload used.
53         a_tx (int): Transmitter optical loss.
54         p_tx (int): Transmitter power.
55         ppb (int): Photons/bit.
56         teta_tx (float): Transmitter divergence.
57         a_rx (int): Receiver optical loss onto RFE.
58         leng (np.ndarray | float): Length of the link.
59         g_tx (float): Transmitter antenna gain.
60         a_fsl (np.ndarray | float): Free-space loss.
61         i_axial (np.ndarray | float): Axial intensity at OGS-distance.
62         area_rx (float): Receiver antenna area.
63         a_atm (np.ndarray | float): Atmospheric attenuation loss.
64         a_bw (int): Mean BeamWander loss.
65         g_rx (float): Reveiver antenna gain.
66         p_rx (np.ndarray | float): Received power.
67         int_ogs_lin (np.ndarray | float): Intensity onto OGS-apertue exc. losses.
68         int_ogs_lin_loss (np.ndarray | float): Intensity onto OGS-apertue inc. losses.
69         p_ogs_mean (np.ndarray | float): Power into the OGS-apertue - no additional
70         ↪ RX-losses.
71         p_ogs_mean_loss (np.ndarray | float): Power into the OGS-apertue including
72         ↪ RX-losses.

```

```

71     p_rx_lin (np.ndarray | float): R $\times$ Power onto RFE-detector incl all losses.
72     wl (float): Wavelength.
73     p_rfe_lin (float): RFE-sensitivity for an specific Photons/bit.
74     a_sci (int): Scintillation loss.
75     """
76     if elevation_mode.get() == "Full":
77         print(int_ogs_lin_loss)
78         el = np.arange(5, 90)
79         print(el)
80         plt.figure()
81
82         plt.plot(el, int_ogs_lin_loss * 1e6, "-", color="r", linewidth=2)
83         plt.ylabel("Intensity onto Camera-apertue /  $\mu\text{W}/\text{m}^2$ ")
84         plt.xlabel("Elevation /  $1^\circ$ ")
85         plt.subplots_adjust(left=0.17, right=0.95, top=0.92, bottom=0.13)
86         plt.title(f"{sat.get()} intensity Link Budget")
87         plt.grid(True)
88
89         fig_manager = plt.get_current_fig_manager()
90
91         # Dimensions and position of the link budget window (Width $\times$ Height+X+Y)
92         fig_manager.window.wm_geometry("355x372+545+290")
93
94         mplcursors.cursor()
95         plt.show(block=False)
96     else:
97         print("////////////////////////////////////")
98         print()
99         print(f"Transmit-power = {p_tx} dBm")
100        print(f"Divergence = {((teta_tx*1E6*10)/10)}  $\mu\text{rad}$ ")
101        print(f"Optical loss Tx = {a_tx} dB")
102
103        print(
104            f"Optical loss onto RFE (incl. splitting) = {a_rx} dB - We are not "
105            f"taking into account optical loss as the receiver is a camera"
106        )
107        # if sat == "OsirisV1":
108        #     print(
109        #         f"Optical loss onto RFE (incl. splitting) = {a_rx} dB - in OSIRISv1
110        #          $\rightarrow$  from FLP -7,5dB were measured in 30cm telescope towards PowerSensor"
111        #     )
112        #     print(f"Optical loss Rx (incl. splitting) = {a_rx} dB - in KIODO only 4% of
113        #      $\rightarrow$  Rx-light was on RFE-APD")
114
115        print()
116        print(f"Link-distance = {(leng/100)*.1} km")
117        print(f"Tx-antenna gain = + {g_tx} dB")
118        print(f"Freespace Loss = {a_fsl} dB")
119        print(
120            f" # axial Intensity a OGS-distance = {i_axial*1E6}  $\mu\text{W}/\text{m}^2$ , after "
121            f"only distance and Tx-internal losses"
122        )
123        print(f" # Area of Rx-antenna = {area_rx}  $\text{m}^2$ ")
124        print(
125            f" # power into Rx-aperture [no a_atmo nor a_pointing, only a_Tx, "
126            f"a_fsl, g_Rx] = {1E6*i_axial * area_rx}  $\mu\text{W}$ "
127        )
128        print()
129        print(f"atmosph. atten. = {a_atm} dB")
130        print(

```

```

129         f"mean BeamWander loss = {a_bw} dB - Being the receiver a camera, we are "
130         f"not taking into account BeamWander losses"
131     )
132
133     print(
134         f"scinti-loss      = {a_sci} dB - Once again we suppose Scintillation loss as
           ↪ zero"
135     )
136
137     print()
138     print(f"Rx-antenna gain = + {g_rx} dB")
139     print(f"optical loss Rx = {a_rx} dB, includes splitting for Tracking")
140     print(f"RxPower on RFE with all losses = {p_rx} dBm")
141     print(
142         f" # intensity onto OGS-apertue incl atmosphere but excl. "
143         f"Rx-losses = {int_ogs_lin *1E6} μW/m^2"
144     )
145     print(
146         f" # intensity onto OGS-apertue incl atmosphere including "
147         f"Rx-losses = {int_ogs_lin_loss *1E6} μW/m^2"
148     )
149     print(
150         f" # power into the OGS-apertue - no additional RX-losses"
151         f"= {(10**(p_ogs_mean/10)/1000)*1E6} μW"
152     )
153     print(
154         f" # power into the OGS-apertue including RX-losses = "
155         f"{(10**(p_ogs_mean_loss/10)/1000)*1E6} μW"
156     )
157     print(
158         f"RxPower onto RFE-detector incl all losses = {p_rx_lin*1E9} nW, "
159         f"sufficient for {(p_rx_lin/ppb/(const.H*const.C/wl))/1E9} Gbps at {ppb}
           ↪ Photons/bit"
160     )
161     print(
162         f"RFE-sensitivity for {ppb} Ppb = {p_rfe_lin*1E9} nW or "
163         f"{math.log10(p_rfe_lin*1000)*10} dBm"
164     )
165     print()
166     print(f"Link Margin: {p_rx - math.log10(p_rfe_lin*1000)*10 } dBm")
167     print()
168
169     print("//////////////////// Summary //////////////////////////////////////")
170     if elevation_mode.get() == "Individual":
171         print(f"mean source power  +{p_tx} dBm")
172         print(f"Tx-internal losses {a_tx} dBm")
173         print(f"Tx-antenna gain    +{g_tx} dB")
174         print(f"pointing loss      {a_bw} dB")
175         print(f"Distance           {leng/1000} km")
176         print(f"freespace loss     {a_fsl} dB")
177         print(f"Atmospheric loss   {a_atm} dB")
178         print(f"scintillation loss {a_sci} dB")
179         print(f"Rx-antenna gain    +{g_rx} dB")
180         print(f"Power into Rx-Aper {p_ogs_mean} dBm")
181         print(f"Rx-internal losses {a_rx} dB")
182         p_rx_ = (
183             p_tx + a_tx + g_tx + a_bw + a_fsl + a_atm + a_sci + g_rx + a_rx
184         )
185         print(f"Power onto detectr {p_rx_} dBm")
186         print(

```



```

187         f"Sensitivity of RFE {10*math.log10(p_rfe_lin*1000)} dBm /
188         ↪ {p_rfe_lin*1E9} nW"
189     )
190     print(
191         f"Link Margin          {p_rx_ - 10*math.log10(p_rfe_lin*1000)} dB"
192     )
193     print()
194     print("//////////////////// Intensity //////////////////////")
195     print(
196         f"Axial Intensity at OGS-distance = {i_axial*1E6} μW/m^2, after only "
197         f"distance and Tx-internal losses"
198     )
199     print(
200         f"Intensity onto OGS-apertue incl atmosphere but excl. Rx-losses = "
201         f"{int_ogs_lin *1E6} μW/m^2"
202     )
203     print(
204         f"Intensity onto OGS-apertue incl atmosphere including Rx-losses = "
205         f"{int_ogs_lin_loss *1E6} μW/m^2"
206     )
207     print()
208     print("//////////////////// Power //////////////////////")
209     print(
210         f"Power into Rx-aperture [no a_atmo nor a_pointing, only a_Tx, a_fsl, "
211         f"g_Rx] = {1E6*i_axial * area_rx} μW"
212     )
213     )
214     print(
215         f"Power into the OGS-apertue - no additional RX-losses = "
216         f"{(10**(p_ogs_mean/10)/1000)*1E6} μW"
217     )
218     print(
219         f"Power into the OGS-apertue including RX-losses = "
220         f"{(10**(p_ogs_mean_loss/10)/1000)*1E6} μW"
221     )
222     )
223
224 def link_budget(elevation_mode, el: int, payload, zenith: float, h_ogs: int) -> None:
225     """Performs the link budget based on the parameters from the GUI:
226
227     1. Selects specific parameters based on the payload chosen.
228
229     2. Specifies the losses.
230
231     3. Calculates antennas dimensions.
232
233     4. If the elevation mode is "Full", the elevation angle will be converted to an
234     ↪ array from 0 to 90 degrees.
235
236     5. The rest of the parameters dependent on the elevation are calculated based on if
237     the elevation is just a point or the full range.
238
239     6. Computes the final received power at the receiver.
240
241     7. Calculates the intensity onto the receiver using its area.
242
243     Args:
244     elevation_mode (tk.StringVar): Container of the elevation mode.
245     el (int): Elevation angle.

```

```

245     payload (tk.StringVar): Container of the payload used.
246     zenith (float): Final selected zenith attenuation value.
247     h_ogs (int): Final height of the selected OGS.
248     """
249     if payload.get() == "OsirisV1":
250         h_orbit = 595 # km - Satellite height
251         wl = 1545e-9 # m - Wavelength of the downlink
252         p_tx = 30 # dBm - Transmitted power
253         teta_tx = 1e-3 # rad - OSIRISv1: 1.0E-3 oder 1.2E-3 mrad - die Dokumente sagen
254         ↪ immer 1,2 aber CF meinte frs CNES-Paper 1,0
255         a_tx = -1 # dB - Optical Transmissor losses (Tx)
256         dr = 39e6 # bps - datarate in KIODO, 39Mbps in OSIRIS-FLP for OCAM and some
257         ↪ tests to OP
258         ppb = 250 # ppb - Photons per bit required bei RFE at BER=1E-3 at first OSIRIS
259         ↪ with APD-RFE-100-OLD, 320Photons for RFE-300-NEW
260         # diese Formel muss noch durch WL ergnzt werden: D_tx=0.2; teta_tx = 100E-6 *
261         ↪ 0.01/D_tx; % estimate for near-optimum cut-gauss Tx
262     elif payload.get() == "KIODO":
263         h_orbit = 610 # km - Satellite height
264         wl = 847e-9 # m - Wavelength of the downlink
265         p_tx = 20 # dBm - Transmitted power
266         # p_tx = 16.99
267         teta_tx = 5.5e-6 # rad - OICETS-Kirari-LUCE FWHM beam divergence
268         a_tx = -1 # dB - Optical Transmissor losses (Tx)
269         dr = 39e6 # bps - datarate in KIODO, 39Mbps in OSIRIS-FLP for OCAM and some
270         ↪ tests to OP
271         ppb = 250 # ppb - Photons per bit required bei RFE at BER=1E-3 at first OSIRIS
272         ↪ with APD-RFE-100-OLD, 320Photons for RFE-300-NEW
273     elif payload.get() == "CubeCat":
274         h_orbit = 455 # km - Satellite height
275         wl = 1545e-9 # m - Wavelength of the downlink
276         p_tx = 24.7712 # dBm - Transmitted power [300 mW]
277         # p_tx = 16.99
278         teta_tx = 104E-6 # rad - collimator F220FC-1550
279         a_tx = 0 # dB - Optical Transmissor losses (Tx)
280         dr = 39e6 # bps - datarate in KIODO, 39Mbps in OSIRIS-FLP for OCAM and some
281         ↪ tests to OP
282         ppb = 250 # ppb - Photons per bit required bei RFE at BER=1E-3 at first OSIRIS
283         ↪ with APD-RFE-100-OLD, 320Photons for RFE-300-NEW
284         # diese Formel muss noch durch WL ergnzt werden: D_tx=0.2; teta_tx = 100E-6 *
285         ↪ 0.01/D_tx; % estimate for near-optimum cut-gauss Tx
286     else:
287         h_orbit = 595 # km - Satellite height
288         wl = 1545e-9 # m - Wavelength of the downlink
289         p_tx = 30 # dBm - Transmitted power
290         teta_tx = 1e-3 # mrad - OSIRISv1: 1.0E-3 oder 1.2E-3 mrad - die Dokumente sagen
291         ↪ immer 1,2 aber CF meinte frs CNES-Paper 1,0
292         a_tx = -1 # dB - Optical Transmissor losses (Tx)
293         dr = 39e6 # bps - datarate in KIODO, 39Mbps in OSIRIS-FLP for OCAM and some
294         ↪ tests to OP
295         ppb = 250 # ppb - Photons per bit required bei RFE at BER=1E-3 at first OSIRIS
296         ↪ with APD-RFE-100-OLD, 320Photons for RFE-300-NEW
297         # diese Formel muss noch durch WL ergnzt werden: D_tx=0.2; teta_tx = 100E-6 *
298         ↪ 0.01/D_tx; % estimate for near-optimum cut-gauss Tx
299
300     h_orbit_m = h_orbit * (10**3) # m - Satellite height
301     # 1W mean was used in FLP-OSIRISv1 experiments with OCAM
302     # 100mW or 50mW mean we expect in KIODO, since the 20dBm mentioned in the book might
303     ↪ be peak-power

```

```

291 sigma_jit = 0.85 * teta_tx / 2 # erzeugt dann -3dB BW-loss
292 # sigma_jit = 1E-9 # 0.85*teta_tx/2 # erzeugt dann -3dB BW-loss
293 # sigma_jit = teta_tx/4 # irrelevant when we set beta later below
294
295 beta = teta_tx**2 / sigma_jit**2 / (8 * math.log(2))
296 # beta = 8
297 # beta = 2 # produces a pointing loss of -1.7dB
298 # beta=1000 # no pointing loss for the plot in fig.10
299
300 ##### RECEIVER SETTINGS ##### -> Check standalone script for
    ↪ noncam values
301 # LOSSES
302 a_rx = 0 # dB - Optical Receiver losses (Tx) -
303 a_bw = 0 # dB - Beam Wander losses
304 a_sci = 0 # dB - Scintillation losses
305
306 ##### ANTENA'S DIMENTIONS #####
307 d_rx_o = 2.5e-3 # m - Diameter Rx-apertur in meter - Infra-FE4.41.0-17
308 # d_rx_o = 5.6e-3 # m - Diameter Rx-apertur in meter - Infra-FE5.61.0-
309 area_rx = math.pi * (d_rx_o / 2) ** 2
310 # m^2 - Area of a fisheye lens based on its aperture
311
312 # alpha = (180/math.pi) * math.asin( (const.R_E+h_ogs)/(const.R_E+h_orbit) *
    ↪ math.sin((90+el)*math.pi/180) )
313 # gamma = 90 - el - alpha;
314 # leng = math.sqrt( (const.R_E+h_ogs)**2 + (const.R_E+h_orbit_m)**2 - 2 *
    ↪ (const.R_E+h_ogs)*(const.R_E+h_orbit_m)*math.cos(gamma*math.pi/180) )
315 if elevation_mode.get() == "Individual":
316     a = math
317     grad = el * math.pi / 180
318 else:
319     el = np.arange(5, 90)
320     a = np
321     grad = np.radians(el)
322
323 leng = a.sqrt(
324     (const.R_E + h_ogs) ** 2 * a.sin(grad) ** 2
325     + 2 * (h_orbit_m - h_ogs) * (const.R_E + h_ogs)
326     + (h_orbit_m - h_ogs) ** 2
327 ) - (const.R_E + h_ogs) * a.sin(grad)
328
329 a_fsl = 10 * a.log10((wl / (4 * math.pi * leng)) ** 2)
330 # dB - Freespace losses
331
332 a_atm = 10 * a.log10(zenith ** (1.0 / a.sin(math.pi * el / 180)))
333 # dB - Atmospheric Attenuation
334 # It is using degrees now
335
336 g_tx = 10 * math.log10((3.33 / teta_tx) ** 2)
337 # dB - Gain of thetransmissor antena
338
339 # weitere Berechnung - sollte selbes rauskommen: i_axial = (0.693/pi) * 10**(
    ↪ (a_tx+p_tx) /10)/1000 / (leng*teta_tx/2)**2 # W/m^2
340 i_axial = 0.001 * 10 ** (
341     (
342     p_tx
343     + a_tx
344     + g_tx
345     + a_fsl
346     + 10 * math.log10(4 * math.pi * 1 / (wl**2))

```

```

347     )
348     / 10
349 ) # W/m2 - Axial Intensity
350
351 g_rx = 10 * math.log10(4 * math.pi * area_rx / (wl**2))
352 # dB - Gain of the receiver antenna
353 # g_rx = 0
354
355 p_rx = (
356     p_tx + a_tx + g_tx + a_fsl + a_bw + a_atm + a_sci + g_rx + a_rx
357 ) # dBm - RxPower on RFE with all losses
358
359 p_ogs_mean = p_rx - a_rx
360 # dBm - power onto OGS-aperture - no Rx-internal losses
361 p_ogs_mean_loss = p_rx
362 # dBm - power onto OGS-aperture - WITH Rx-internal losses
363 int_ogs_lin = (10 ** ((p_ogs_mean) / 10) / 1000) / area_rx
364 int_ogs_lin_loss = (10 ** ((p_ogs_mean_loss) / 10) / 1000) / area_rx
365 p_rx_lin = (10 ** (p_rx / 10)) / 1000 # W
366 p_rfe_lin = ppb * const.H * const.C * dr / wl # W
367
368 printer_lb(
369     el,
370     elevation_mode,
371     payload,
372     a_tx,
373     p_tx,
374     ppb,
375     teta_tx,
376     a_rx,
377     leng,
378     g_tx,
379     a_fsl,
380     i_axial,
381     area_rx,
382     a_atm,
383     a_bw,
384     g_rx,
385     p_rx,
386     int_ogs_lin,
387     int_ogs_lin_loss,
388     p_ogs_mean,
389     p_ogs_mean_loss,
390     p_rx_lin,
391     wl,
392     p_rfe_lin,
393     a_sci,
394 )

```

A.2.8 printer.py

```

1 """This script manages all the printing functions needed to display the results
  ↪ correctly."""
2
3 # C:\Users\alda_ik\Documents\04_PROGRAMMING\02_FINAL_PROJECT\constants.py
4
5
6 def print_preamble() -> None:

```

```

7     """Printing fuction - prints program preamble."""
8     print("////////////////////////////////////")
9     print("/// IR Camera System for Satellite Observation ///")
10    print("////////////////////////////////////\n")
11
12
13    def print_preamble_settings() -> None:
14        """Printing fuction - prints settings preamble."""
15        print("//////// Settings //////////")
16
17
18    def print_start_stream() -> None:
19        """Printing fuction - prints the start of the stream."""
20        print()
21        print("/// Stream started. Press <q> to stop stream ///")
22
23
24    def print_end_stream() -> None:
25        """Printing fuction - prints the end of the stream."""
26        print("//////// Stream ended //////////")
27        print("////////////////////////////////////\n")
28
29
30    def print_usage() -> None:
31        """Printing fuction - prints the usage."""
32        print("Usage:")
33        print("    python asynchronous_grab_opencv.py [camera_id]")
34        print("    python asynchronous_grab_opencv.py [/h] [-h]")
35        print()
36        print("Parameters:")
37        print(
38            "    camera_id    ID of the camera to use (using first camera if not specified)"
39        )
40    print()

```
